

4. Other Data Relevant to an Evaluation of Carcinogenicity and its Mechanisms

4.1 Absorption, distribution, metabolism and excretion

4.1.1 Humans

(a) *4-(Methylnitrosamino)-1-(3-pyridyl)-1-butanone (NNK) and 4-(methylnitrosamino)-1-(3-pyridyl)-1-butanol (NNAL)*

(i) *Absorption*

NNK has been detected in the saliva of snuff dippers, users of *khaini*, chewers of betel quid with tobacco and users of *toombak* (see Section 1.4.1(a)).

Absorption of NNK in smokeless tobacco users was demonstrated by the detection of its metabolites, NNAL and NNAL-Gluc, in plasma and urine and of NNAL-*N*-oxide in urine (Kresty *et al.*, 1996; Carmella *et al.*, 1997; Hecht, 2002; Hecht *et al.*, 2002). Similar results have been obtained in smokers, although only NNAL has been reported in plasma (Hecht *et al.*, 1999a; Hecht, 2002). NNAL-*N*-Gluc comprised $50 \pm 25\%$ of total NNAL-Gluc in the urine of smokers and $24 \pm 12\%$ in snuff-dippers (Carmella *et al.*, 2002). *Toombak* users excreted exceptionally high levels of NNAL and NNAL-Gluc (0.12–0.14 mg per day), which demonstrated a higher uptake of NNK by humans than of any other non-occupational carcinogen (Murphy *et al.*, 1994). Further information on NNAL and NNAL-Gluc in urine is presented in Section 4.1.1(c).

Absorption of NNK by nonsmokers exposed to secondhand cigarette smoke has been demonstrated by detection of NNAL and NNAL-Gluc in urine in several studies (Hecht, 2002).

NNAL, but not NNAL-Gluc, was detected in the amniotic fluid of mothers who smoked (Milunsky *et al.*, 2000). Both NNAL and NNAL-Gluc were detected in the urine of neonates born to mothers who smoked, but not in the urine of newborns of nonsmoking mothers (Lackmann *et al.*, 1999). These results indicate that NNK is converted to NNAL in the mother, and that NNAL crosses the placental barrier and is absorbed and metabolized to NNAL-Gluc in the late stages of fetal development.

(ii) *Distribution*

As noted above, NNAL and NNAL-Gluc have been detected in the plasma of smokeless tobacco users, and NNAL has been detected in plasma of smokers (Hecht *et al.*, 1999a, 2002). Pyridyloxobutyl-haemoglobin adducts derived from NNK and/or NNN have been detected in the blood of smokers, snuff-dippers, *toombak* users and nasal snuff users (Hecht, 1998). NNK was detected in the cervical mucus of smokers and its levels were significantly higher than those in nonsmokers (Prokopczyk *et al.*, 1997). NNK and NNAL were detected in pancreatic juice of smokers. Levels of NNK were significantly higher than in pancreatic juice from nonsmokers, and NNAL was detected more frequently in smokers than in nonsmokers (Prokopczyk *et al.*, 2002). DNA adducts of NNK and/or NNN have been detected in the lung tissue of smokers (Hecht, 1998). Haemoglobin and DNA adducts are discussed in more detail in Section 4.1.1(c).

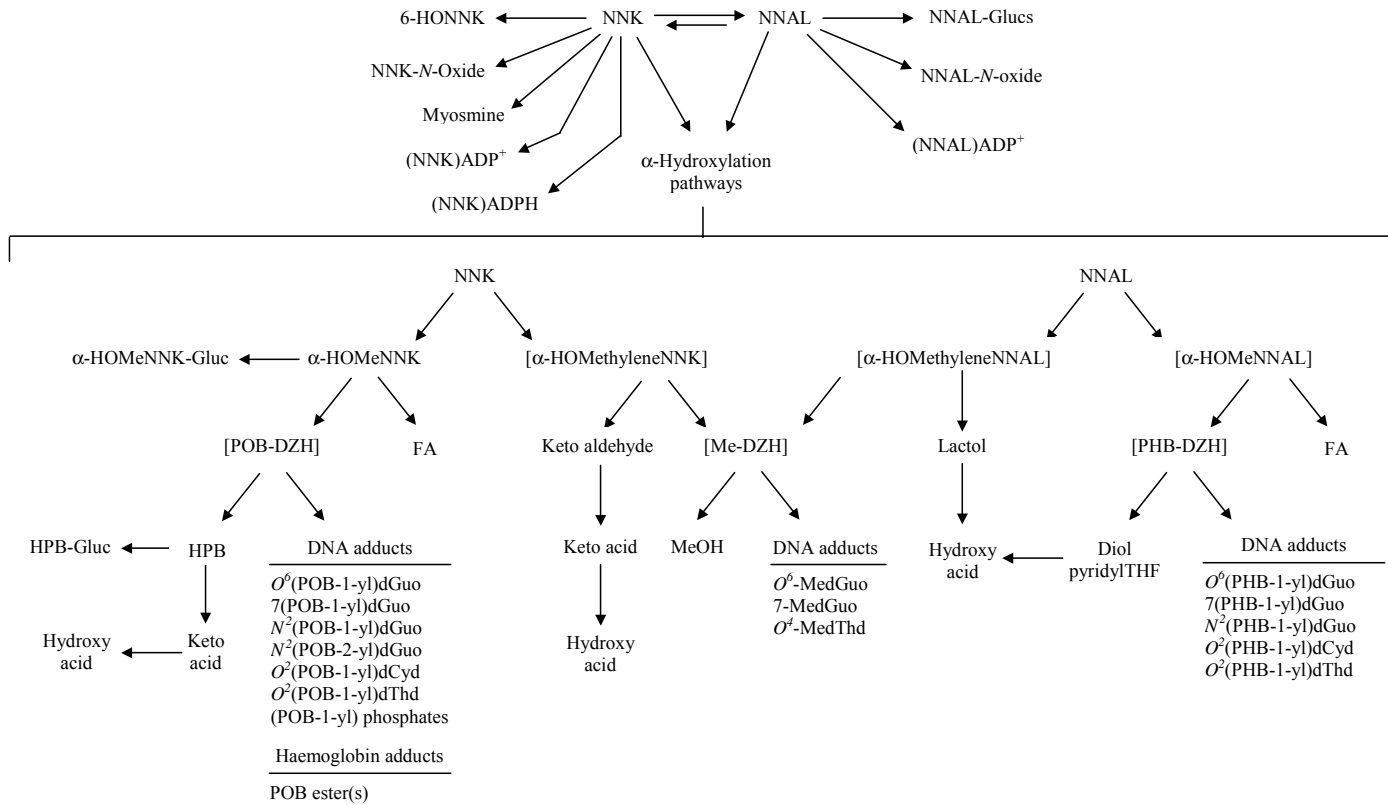
NNAL and NNAL-Gluc are excreted in the urine more slowly than would be expected, based on their structures, after cessation of smoking or smokeless tobacco use (Hecht *et al.*, 1999a, 2002). One week after smoking cessation, 34.5% of baseline NNAL plus NNAL-Gluc was detected in urine, whereas the corresponding values for the structurally related compounds cotinine and nicotine were 1.1 and 0.5%, respectively. Even 6 weeks after cessation, 7.6% of the original levels of NNAL plus NNAL-Gluc remained. The distribution half-life of NNAL and NNAL-Gluc was 3–4 days, while the elimination half-life was 40–45 days. Total body clearance of NNAL was estimated to be 61.4 ± 35.4 mL/min, and the volume of distribution in the β -phase was estimated to be 3800 ± 2100 L, which indicates substantial distribution into tissues (Hecht *et al.*, 1999a). After cessation of smokeless tobacco use, the distribution half-lives of NNAL (1.32 ± 0.85 versus 3.35 ± 1.86 days) and NNAL-Gluc (1.53 ± 1.22 versus 3.89 ± 2.43 days) were significantly shorter than those in smokers. There were no significant differences in the terminal half-lives. Ratios of (S)-NNAL:(R)-NNAL and (S)-NNAL-Gluc:(R)-NNAL-Gluc in urine were significantly (3.1–5.7 times) higher 7 days after cessation than at baseline in both smokeless tobacco users and smokers, which indicates stereoselective retention of (S)-NNAL in humans. From these results, the authors suggest that there is a receptor in the body, possibly in the lung, for (S)-NNAL (Hecht *et al.*, 2002).

(iii) *Metabolism*

Introduction

The metabolic pathways of NNK and NNAL and the modes of formation of their adducts are summarized in Figure 2. Structures of the NNK and NNAL metabolites are

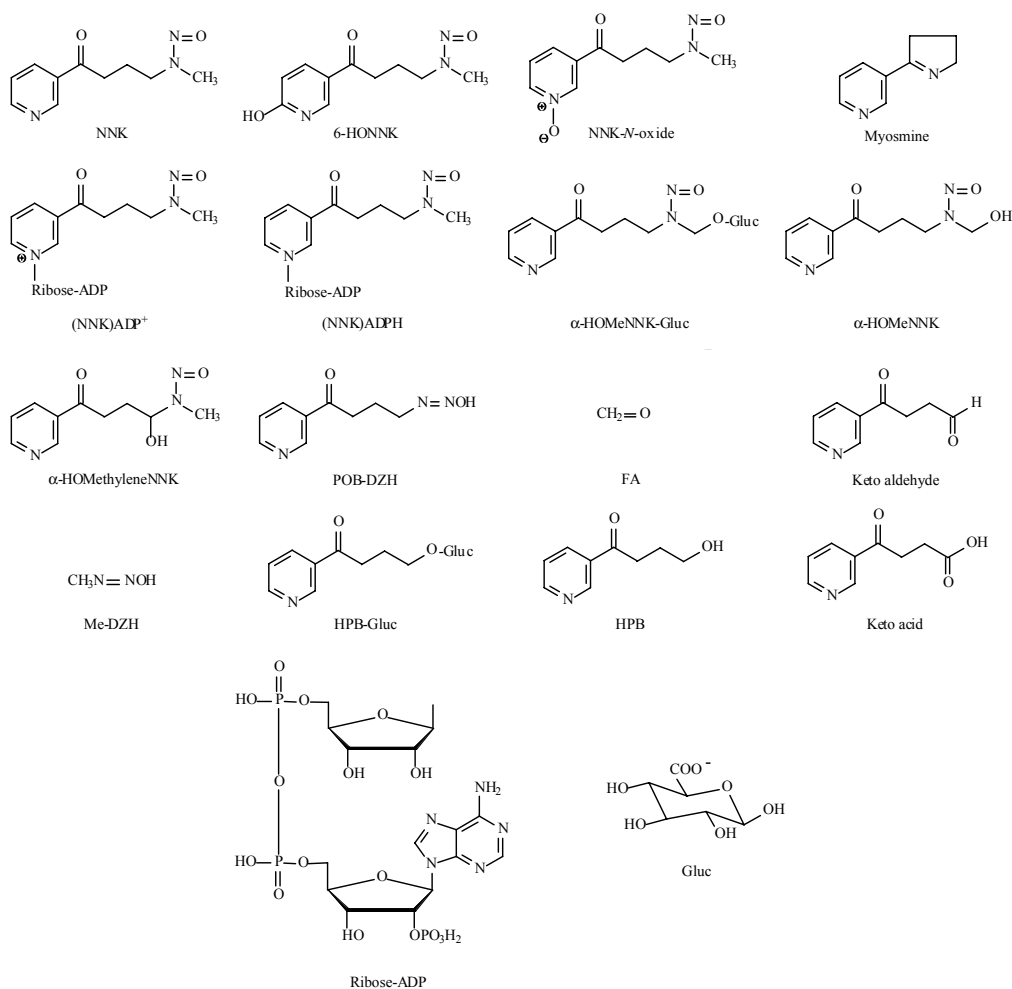
Figure 2. Metabolism of NNK and NNAL and formation of adducts, based on studies in laboratory animals and humans



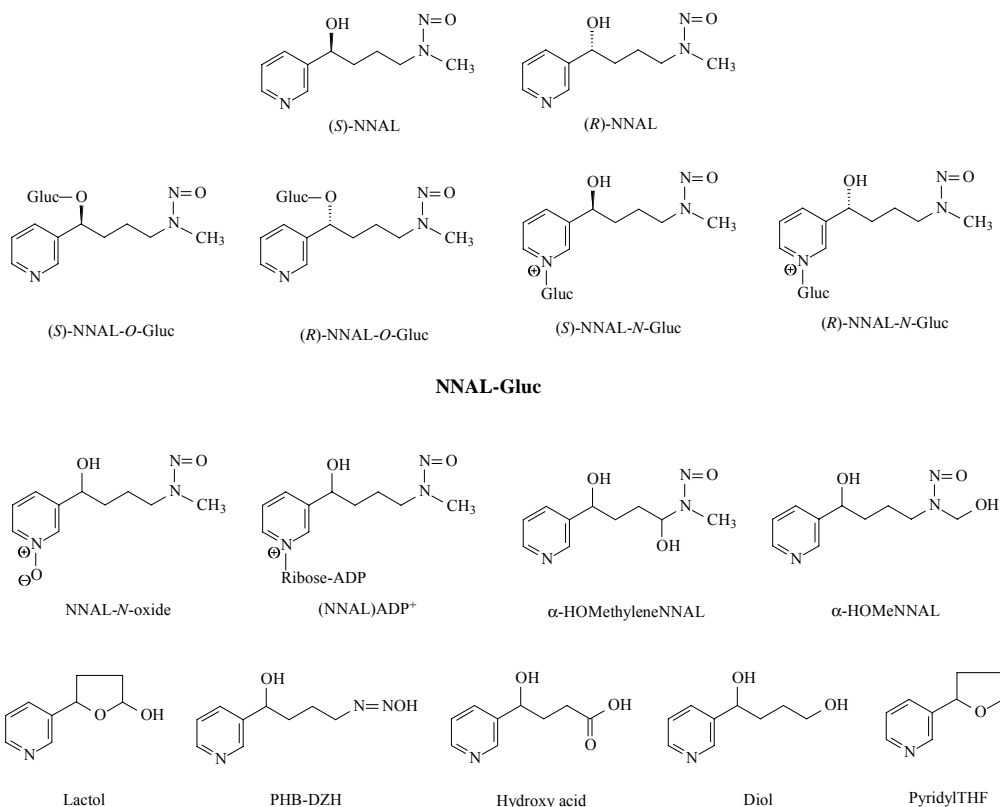
ADP⁺, adenosine dinucleotide phosphate; ADPH, adenosine dinucleotide phosphate (reduced form); dCyd, deoxycytidine; dGuo, deoxyguanosine; dThd, deoxythymidine; DZH, diazohydroxide; Gluc, glucuronide; FA, formaldehyde; HO, hydroxy; HOME, hydroxymethyl; HOMethylene, hydroxymethylene; HPB, 4-hydroxy-1-(3-pyridyl)-1-butanone or keto alcohol; MedGuo, methyldeoxyguanosine; Me-DZH, methaneDZH; MedThd, methyldeoxythymidine; MeOH, methanol; NNAL, 4-(methylnitrosamino)-1-(3-pyridyl)-1-butanol; NNK, 4-(methylnitrosamino)-1-(3-pyridyl)-1-butanone; PHB, 4-hydroxy-4-(3-pyridyl)-1-butyl; PHB-DZH, 4-hydroxy-4-(3-pyridyl)-1-butaneDZH; POB, 4-oxo-4-(3-pyridyl)-1-butyl or pyridyloxobutyl; POB-DZH, 4-oxo-4-(3-pyridyl)-1-butaneDZH; THF, tetrahydrofuran

illustrated in Figures 3 and 4, and structures of the adducts are shown in Figure 5. This information is based on studies *in vitro*, in laboratory animals and in humans. Specific pathways that have been observed in *in-vitro* studies with human tissues or enzymes or in humans are discussed below (see Hecht, 1998).

Figure 3. Structures of NNK and metabolites



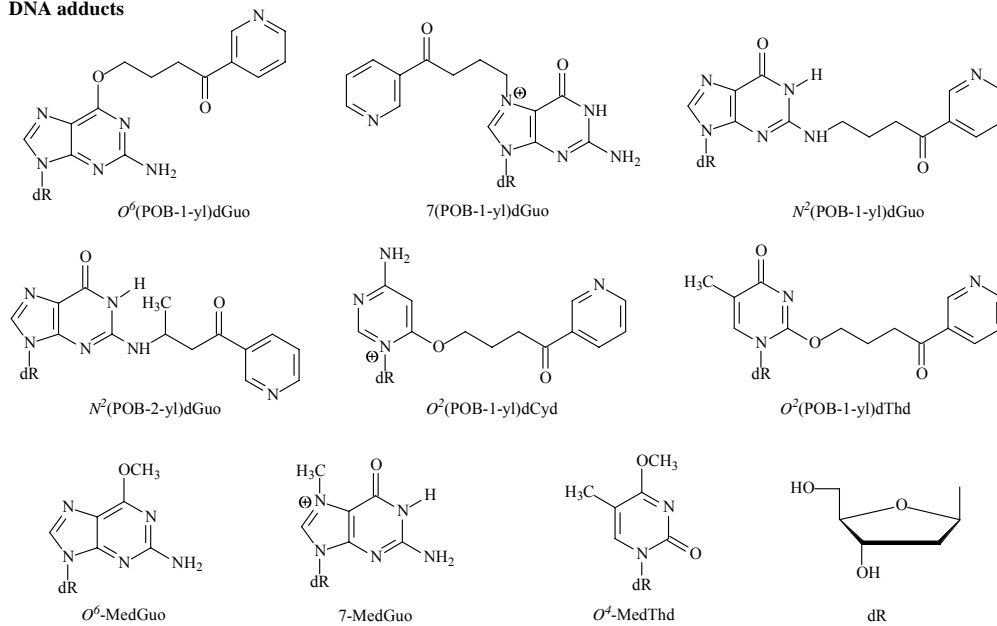
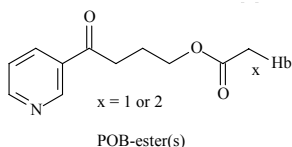
DZH, diazohydroxide; FA, formaldehyde; Gluc, glucuronide; HO, hydroxy; HOMe, hydroxymethyl; HOMethylene, hydroxymethylene; HPB, 4-hydroxy-1-(3-pyridyl)-1-butanone or keto alcohol; Me-DZH, methaneDZH; NNK, 4-(methylnitrosamino)-1-(3-pyridyl)-1-butanone; (NNK)ADP⁺, (NNK)adenosine dinucleotide phosphate; (NNK)ADPH, (NNK)adenosine dinucleotide phosphate (reduced form); POB-DZH, 4-oxo-4-(3-pyridyl)-1-butanoneDZH

Figure 4. Structures of NNAL and metabolites

DZH, diazohydroxide; Gluc, glucuronide; HOME, hydroxymethyl; HOMethylene, hydroxymethylene; NNAL, 4-(methylnitrosamino)-1-(3-pyridyl)-1-butanol; (NNAL)ADP⁺, (NNAL)adenosine dinucleotide phosphate; PHB-DZH, 4-hydroxy-4-(3-pyridyl)-1-butaneDZH; THF, tetrahydrofuran
See Figure 3 for structures of Gluc and ribose-ADP.

NNK can be converted to the pyridine oxidation products 4-(methylnitrosamino)-1-[3-(6-hydroxypyridyl)]-1-butanone (6-HONNK) and NNK-*N*-oxide. Denitrosation of NNK followed by oxidation produces myosmine. NNK can replace nicotinamide in NADP⁺ or NADPH, to yield NNK adenosine dinucleotide phosphate ((NNK)ADP⁺) and (NNK)ADPH (reduced form). Carbonyl reduction of NNK produces NNAL which can be conjugated by glucuronidation giving four diastereomers of NNAL-Gluc (Figure 4): two isomers of 4-(methylnitrosamino)-1-(3-pyridyl)-1-(*O*-β-D-glucopyranuronosyl)butane (NNAL-*O*-Gluc) and two isomers of 4-(methylnitrosamino)-1-(3-pyridyl)-*N*-β-D-glucopyranuronosyl)-1-butanolonium inner salt (NNAL-*N*-Gluc). NNAL is also converted to NNAL-*N*-oxide and NNAL(ADP⁺).

α-Hydroxylation of NNK and NNAL leads to DNA and haemoglobin adducts. Hydroxylation of the NNK methyl group gives 4-(hydroxymethylnitrosamino)-1-(3-pyridyl)-1-

Figure 5. Structures of DNA adducts and haemoglobin adducts derived from NNK**DNA adducts****Haemoglobin adducts**

dCyd, deoxycytidine; dGuo, deoxyguanosine; dThd, deoxythymidine; dR, deoxyribose; Me, methyl; POB, 4-oxo-4-(3-pyridyl)-1-butyl or pyridyloxobutyl

Adducts derived from NNAL have the same structures except that an hydroxy group replaces the carbonyl group in the adducted portion of the molecule.

butanone (α -HOMeNNK) which can be conjugated as a glucuronide, α -HOMeNNK-Gluc. α -HOMeNNK spontaneously decomposes to 4-oxo-4-(3-pyridyl)-1-butanediazohydroxide (POB-DZH) and formaldehyde. POB-DZH reacts with water to give 4-hydroxy-1-(3-pyridyl)-1-butanone (HPB) which can be conjugated as its glucuronide, HPB-Gluc. POB-DZH also reacts with DNA and haemoglobin to produce a series of adducts (Figures 2 and 5). α -Hydroxylation of the NNK methylene group produces 4-(methylnitrosamino)-1-(3-pyridyl)-1-(4-hydroxy)butanone (α -HOMethyleneNNK). This metabolite spontaneously decomposes to 4-(3-pyridyl)-4-oxobutanal (keto aldehyde) and methanediazohydroxide (Me-DZH). Keto aldehyde is further metabolized to 4-(3-pyridyl)-4-oxobutanoic acid (keto acid) which in turn can be converted to 4-hydroxy-4-(3-pyridyl)butanoic acid (hydroxy acid).

Me-DZH reacts with water to yield methanol and with DNA to produce methyl adducts as shown in Figures 2 and 5. NNAL similarly undergoes α -hydroxylation at its methylene group to yield 4-(methylnitrosamino)-1-(3-pyridyl)-1-(4-hydroxy)butanol (α -HOMethyleneNNAL) and at its methyl group to yield 4-(hydroxymethylnitrosamino)-1-(3-pyridyl)-1-butanol (α -HOMeNNAL). α -HOMethyleneNNAL spontaneously decomposes to Me-DZH and 5-(3-pyridyl)-2-hydroxytetrahydrofuran (lactol), which can be converted to hydroxy acid. α -HOMeNNAL spontaneously decomposes to 4-hydroxy-4-(3-pyridyl)-1-butanediazohydroxide (PHB-DZH) and formaldehyde. PHB-DZH reacts with water to yield 4-(3-pyridyl)butane-1,4-diol (diol), cyclizes to 2-(3-pyridyl)tetrahydrofuran (pyridylTHF) and reacts with DNA and haemoglobin to produce the adducts shown in Figures 2 and 5.

In-vitro studies in human tissues and cells

NNK

A variety of human tissues that includes cultured bronchus, peripheral lung, trachea, buccal mucosa, oesophagus and bladder metabolize NNK (Castonguay *et al.*, 1983c; Hecht, 1998), as do microsomes from human tissues such as liver, lung, cervix, placenta and pancreas (Hecht, 1998; Jalas *et al.*, 2005). A common observation in all of these studies is extensive conversion to NNAL. NNK is converted to NNAL in cultured human tissues (50–80%) (Castonguay *et al.*, 1983c), human red blood cells (Murphy & Coletta, 1993) and human liver microsomes and cytosol (18 and 25%, respectively). The enantiomeric composition in the liver was 64% (*S*)-NNAL in microsomes and 90% (*S*)-NNAL in cytosol (Upadhyaya *et al.*, 2000). Human cervical cells and human cervical microsomes formed (*R*)-NNAL while human cervical cytosol produced mainly (*S*)-NNAL (Prokopczyk *et al.*, 2001). Five enzymes that mediate conversion of NNK to NNAL in humans have been identified to date: microsomal 11 β -hydroxysteroid dehydrogenase type 1 and cytosolic carbonyl reductase, which both belong to the superfamily of the short-chain dehydrogenases/reductases, and three members of the aldo-keto reductase superfamily (Maser, 2004).

Microsomes from human liver catalyse the α -hydroxylation of NNK to keto alcohol and keto aldehyde and the pyridine-*N*-oxidation to NNK-*N*-oxide. The rates of these reactions are lower than that of carbonyl reduction to NNAL (Smith *et al.*, 1992a; Patten *et al.*, 1996; Staretz *et al.*, 1997a; Jalas *et al.*, 2005) and reported Michaelis constant (K_m) values are relatively high. Correlation studies and the use of chemical inhibitors and inhibitory antibodies have suggested a role for cytochrome P450s (CYPs) 1A2, 2A6 and 3A4 in the formation of keto alcohol or keto aldehyde (Smith *et al.*, 1992a; Patten *et al.*, 1996; Hecht, 1998; Jalas *et al.*, 2005). Microsomes from human lung catalyse the conversion of NNK to keto aldehyde, hydroxy acid and NNK-*N*-oxide. The rate of metabolism of NNK to keto aldehyde was very low (less than 0.05 pmol/mg/min) whereas the rate in liver microsomes was 1–5 pmol/mg/min (Smith *et al.*, 1992a). One study suggested that lipoxigenase may be involved in the metabolism of NNK by human lung, but another study demonstrated the contrary (Smith *et al.*, 1995; Bedard *et al.*, 2002). The contribution of CYP2A6 and/or CYP2A13, as well as CYP2B6 to the α -hydroxylation of NNK and NNAL by human lung samples were suggested by selected chemical and antibody inhibi-

tion in some subjects (Jalas *et al.*, 2003a; Smith *et al.*, 2003). One of the difficulties in studying xenobiotic metabolism in human lung microsomes is the low level of CYP activity. CYP levels in lung microsomes are reported to be between 1 and 10 pmol/mg microsomal protein (Shimada *et al.*, 1992; Guengerich, 1993); the average concentration in 60 liver microsomal samples was 344 ± 167 pmol/mg hepatic microsomal protein (Shimada *et al.*, 1994). CYP-catalysed activity levels and mRNA levels are also much lower in the lung than in the liver (Shimada *et al.*, 1996; Ding & Kaminsky, 2003). However, CYPs have been reported to be expressed in particular regions of the lung which may result in higher localized concentrations (Anttila *et al.*, 1997; Hukkanen *et al.*, 2002). A diffusible inhibitor of CYP activity has been reported to be present in human lung microsome preparations; it was also reported that 7-ethoxycoumarin-*O*-deethylase activity in rat lung microsomes was inhibited by pre-incubation with human lung microsomes (Lorenz *et al.*, 1979).

Human fetal nasal microsomes metabolized NNK by α -hydroxylation to HPB and keto aldehyde with low K_m (6.7 ± 0.8 μ M and 6.5 ± 1.1 μ M, respectively) and antibody inhibition studies indicated that CYP2A13 (K_m , 2.8–11.3 μ M; Table 11) was involved (Wong *et al.*, 2005a).

CYPs are the major catalysts of NNK α -hydroxylation in humans and rodents. Table 11 summarizes the steady-state kinetic parameters for CYP-mediated NNK metabolism (Jalas *et al.*, 2005). Based on the K_m data in Table 11, the relative efficiencies in NNK metabolism by human CYP are (from greatest catalyst to least): 2A13 > 2B6 > 2A6 > 1A2 ~ 1A1 > 2D6 ~ 2E1 ~ 3A4. Similar results are obtained when the ratio maximum velocity (V_{max})/ K_m is considered. The actual involvement of these enzymes in NNK metabolism *in vivo* depends on many factors that include relative expression levels, the amount of CYP oxido-reductase expressed in a given tissue, tissue localization and inducibility of individual CYPs, and the concentration of NNK in human tissues. Among hepatic CYPs, 2B6 has the highest affinity for NNK. However, low levels of this enzyme are present in most liver samples (Gervot *et al.*, 1999). CYP2A6 is also present at relatively low levels, and accounts for < 1% to 4% of the total CYP content (Shimada *et al.*, 1996). Levels of CYP1A2 are four- to 20-fold higher than those of CYP2A6 (Shimada *et al.*, 1996). Therefore, despite its somewhat higher K_m and lower V_{max}/K_m , CYP1A2 is most probably as important a catalyst of NNK α -hydroxylation in human liver as CYP2A6. CYP3A4 may also play a role in hepatic NNK α -hydroxylation, since it is often present at concentrations that are 10–50 times greater than those of CYP2A6 (Shimada *et al.*, 1994). It is not possible to rule out completely the presence of CYP2A13, the best known human catalyst of NNK metabolism, in the liver. However, the very low hepatic mRNA levels of CYP2A13 relative to CYP2A6 suggest that, if this enzyme is present, it is so at very low levels. Results to date do not identify that any single CYP in the liver is a key player in NNK activation. Several enzymes, including CYP1A2, CYP2A6, CYP2B6 and CYP3A4, clearly play a role. The relative contribution of any one of these CYPs varies among individuals, and their relative abundance and catalytic efficiencies suggest that rarely, if ever, is one of them the dominant catalyst (Jalas *et al.*, 2005).

Table 11. Steady-state kinetic parameters for cytochrome P450 (CYP)-mediated NNK metabolism

Species/enzyme	NNK concentration range (μM)	Metabolite	Kinetic parameters			Expression system	Reference
			V _{max} ^a	K _m (μM)	V _{max} /K _m ^b		
Human CYP1A1	1–500	Keto aldehyde	4.44 ± 0.41	1400 ± 148	3.2 × 10 ⁻³ ± 5 × 10 ⁻⁴	Gentest Supersomes ^c	Smith <i>et al.</i> (1995)
		HPB	0.824 ± 0.118	371 ± 6	2.2 × 10 ⁻³ ± 3 × 10 ⁻⁴		
Human CYP1A2	1–1000	Keto aldehyde	0.51 ± 0.04	1180 ± 60	4.3 × 10 ⁻⁴ ± 4 × 10 ⁻⁵	Purified, reconstituted protein as above, DMSO control as above, but with 50 nM PEITC added as above, but with 100 nM PEITC added as above, but with 200 nM PEITC added	Smith <i>et al.</i> (1996)
		HPB	1.7 ± 0.05	380 ± 30	4.5 × 10 ⁻³ ± 4 × 10 ⁻⁴		
		HPB	1.96 ± 0.07	400 ± 10	4.9 × 10 ⁻³ ± 2 × 10 ⁻⁴		
			2.09 ± 0.20	760 ± 10	2.8 × 10 ⁻³ ± 3 × 10 ⁻⁴		
			2.06 ± 0.21	820 ± 20	2.5 × 10 ⁻³ ± 3 × 10 ⁻⁴		
			2.05 ± 0.25	1240 ± 70	1.7 × 10 ⁻³ ± 2 × 10 ⁻⁴		
Human CYP1A2 ^d	10–350	HPB	4.2 ± 0.2	309 ± 16	0.014 ± 0.001	Hep G2 cell lysate	Smith <i>et al.</i> (1992a)
Human CYP2A6	5–2000	Keto aldehyde	0.437	392	1.11 × 10 ⁻³	Baculovirus-infected <i>Spodoptera frugiperda</i> (Sf9) cells	Patten <i>et al.</i> (1996)
		HPB	0.163	349	4.67 × 10 ⁻⁴		
Human CYP2A6 (+ b ₅) ^e	5–2000	Keto aldehyde	1.03	118	8.73 × 10 ⁻³	Baculovirus-infected Sf9 cells	Patten <i>et al.</i> (1996)
		HPB	0.419	141	2.97 × 10 ⁻³		
Human CYP2A13	2–160	Keto aldehyde	4.1 ± 0.6	11.3 ± 3.5	0.36 ± 0.12	Baculovirus-infected Sf9 cells	Su <i>et al.</i> (2000)
		HPB	1.2 ± 0.2	13.1 ± 5.1	0.092 ± 0.039		
Human CYP2A13	2–100	Keto aldehyde	14.5 ± 0.8	4.6 ± 0.4	3.2 ± 0.3	Purified, reconstituted protein	Zhang <i>et al.</i> (2002)
		HPB	5.7 ± 0.7	2.8 ± 0.5	2.0 ± 0.4		
Human CYP2A13 (Arg 257 Cys)	2–100	Keto aldehyde	8.4 ± 0.8	6.2 ± 0.7	1.4 ± 0.2	Purified, reconstituted protein	Zhang <i>et al.</i> (2002)
		HPB	3.2 ± 0.5	4.8 ± 1.0	0.67 ± 0.17		
Human CYP2A13	0.25–50	Keto aldehyde	13.8 ± 0.8	3.6 ± 0.7	3.9 ± 0.8	Baculovirus-infected Sf9 cells	Jalas <i>et al.</i> (2003a)
		HPB	4.6 ± 0.2	3.2 ± 0.5	1.4 ± 0.2		

Table 11 (contd)

Species/enzyme	NNK concentration range (μM)	Metabolite	Kinetic parameters			Expression system	Reference
			V_{\max}^a	K_m (μM)	V_{\max}/K_m^b		
Human CYP2B6	2.5–150	Keto aldehyde and HPB ^f	0.18 ± 0.01	33 ± 0.7	$5.5 \times 10^{-3} \pm 3 \times 10^{-4}$	BD Biosciences Discovery Labware Supersomes	Dicke <i>et al.</i> (2005)
Human CYP2D6	5–2000	Keto aldehyde HPB	0.105 4.01	1061 5525	9.9×10^{-5} 7.3×10^{-4}	Baculovirus-infected Sf9 cells	Patten <i>et al.</i> (1996)
Human CYP2D6	5–2000	Keto aldehyde HPB	0.13 6.04	1075 5632	2×10^{-4} 1×10^{-3}	Chinese hamster ovary cells	Patten <i>et al.</i> (1996)
Human CYP2E1 (+ b ₅) ^e	5–2000	Keto aldehyde HPB	0.026 1.17	720 3334	3.6×10^{-5} 3.5×10^{-4}	Baculovirus-infected Sf9 cells	Patten <i>et al.</i> (1996)
Human CYP3A4	5–8000	Keto aldehyde HPB	0.787 0.086	3091 1125	2.6×10^{-4} 7.6×10^{-5}	Chinese hamster ovary cells	Patten <i>et al.</i> (1996)
Rabbit CYP2A10/2A11	2.9–154	Keto aldehyde HPB	1.38 1.30	15 9.0	0.092 0.14	Purified, reconstituted protein	Hong <i>et al.</i> (1992)
Rabbit CYP2A10/2A11 (+ b ₅) ^e	2.9–154	Keto aldehyde HPB	0.849 0.575	28.6 16.3	0.0297 0.0353	Purified, reconstituted protein	Hong <i>et al.</i> (1992)
Rabbit CYP2A10/2A11 (+ 80 μM nicotine)	2.9–154	Keto aldehyde HPB	1.33 1.26	40.2 29.5	0.033 0.043	Purified, reconstituted protein	Hong <i>et al.</i> (1992)
Rabbit CYP2G1	2.9–154	Keto aldehyde HPB	0.735 ND	186	3.95×10^{-3}	Purified, reconstituted protein	Hong <i>et al.</i> (1992)
Rat CYP1A1	1–5000	Keto aldehyde HPB	2.2 ± 0.1 0.68 ± 0.03	180 ± 34 140 ± 26	0.013 ± 0.002 $4.9 \times 10^{-3} \pm 9 \times 10^{-4}$	Gentest Supersomes	Jalas <i>et al.</i> (2005)
Rat CYP1A2	1–5000	Keto aldehyde HPB	5.0 ± 0.1 6.1 ± 0.09	180 ± 22 200 ± 11	0.028 ± 0.003 0.034 ± 0.002	Gentest Supersomes	Jalas <i>et al.</i> (2005)
Rat CYP2A3	0.25–50	Keto aldehyde HPB	10.8 ± 0.4 8.2 ± 0.3	4.6 ± 0.5 4.9 ± 0.5	2.3 ± 0.3 1.7 ± 0.2	Baculovirus-infected Sf9 cells	Jalas <i>et al.</i> (2003a)

Table 11 (contd)

Species/enzyme	NNK concentration range (μM)	Metabolite	Kinetic parameters			Expression system	Reference
			V_{\max}^a	K_m (μM)	V_{\max}/K_m^b		
Rat CYP2B1	10–1300	Keto aldehyde	0.0897 ± 0.003	191 ± 20	$4.70 \times 10^{-4} \pm 5.2 \times 10^{-5}$	Purified, reconstituted protein	Guo <i>et al.</i> (1991a)
		HPB	0.333 ± 0.016	318 ± 5	$1.05 \times 10^{-3} \pm 5 \times 10^{-5}$		
		NNK- <i>N</i> -oxide	0.295 ± 0.006	131 ± 10	$2.25 \times 10^{-3} \pm 1.7 \times 10^{-4}$		
Rat CYP2C6	1–5000	Keto aldehyde	2.5 ± 0.1	1300 ± 130	$1.9 \times 10^{-3} \pm 2 \times 10^{-4}$	Gentest Supersomes	Jalas <i>et al.</i> (2005)
		HPB	16 ± 0.5	1400 ± 89	0.011 ± 0.0008		
		NNK- <i>N</i> -oxide	1.5 ± 0.06	1100 ± 110	$1.4 \times 10^{-3} \pm 4 \times 10^{-4}$		
Mouse CYP2A4	1–5000	Keto aldehyde	190 ± 23	3900 ± 995	0.049 ± 0.014	Baculovirus-infected Sf9 cells	Felicia <i>et al.</i> (2000)
Mouse CYP2A4	0.5–3000	Keto aldehyde	7.3 ± 0.4	97 ± 19	0.075 ± 0.015	Baculovirus-infected Sf9 cells	Jalas <i>et al.</i> (2003b)
		HPB	1.8 ± 0.1	67 ± 17	0.027 ± 0.007		
Mouse CYP2A5	0.25–100	HPB	4.0 ± 0.4	1.5 ± 0.6	2.7 ± 1.8	Baculovirus-infected Sf9 cells	Felicia <i>et al.</i> (2000)
Mouse CYP2A5	0.25–50	Keto aldehyde	2.0 ± 0.1	4.3 ± 0.8	0.47 ± 0.09	Baculovirus-infected Sf9 cells	Jalas <i>et al.</i> (2003b)
		HPB	6.5 ± 0.2	4.5 ± 0.4	1.4 ± 0.1		

Adapted from Jalas *et al.* (2005)

DMSO, dimethyl sulfoxide; HPB, 4-hydroxy-1-(3-pyridyl)-1-butanone; K_m , Michaelis constant; NNK, 4-(Methylnitrosamino)-1-(3-pyridyl)-1-butanone; PEITC, phenethyl isothiocyanate; ND, not detected; OPB, 4-oxo-4-(3-pyridyl)butanol or keto aldehyde; V_{\max} , maximum velocity

^a Units are pmol product/min/(pmol CYP).

^b Units are pmol product/min/(pmol CYP)/ μM .

^c V_{\max} units were converted using the published CYP concentration of 34 pmol CYP/(mg protein) (Smith *et al.*, 1995). Supersomes that contain co-expressed CYP and oxidoreductase were purchased from Gentest (Woburn, MA).

^d The V_{\max} value was computed based on a CYP1A2 concentration of 13 pmol/(mg protein); this is an upper limit, the lowest possible V_{\max} value is 3.1 ± 0.1 pmol/min/(pmol CYP) based on 18 pmol/(mg protein). See Aoyama *et al.* (1990).

^e Cytochrome b₅ was added at a 3:1 b₅:CYP molar ratio. b₅:CYP molar ratio is corrected according to the original reference (Patten *et al.*, 1996).

^f HBP:keto aldehyde (OPB) ratio \approx 10:1

In the lung, CYP2A13 may be the key catalyst of NNK α -hydroxylation (Su *et al.*, 2000; J alas *et al.*, 2003a). However, the level of CYP2A13 protein in the lung is unknown. The relative levels of human lung CYPs are not well characterized. CYP1A1 (when induced in smokers) and CYP1B1 are probably present at relatively high levels in this tissue (Shimada *et al.*, 1992; Spivack *et al.*, 2001). CYP1A1 is a catalyst of NNK metabolism but is much less efficient than CYP2A13 (Table 11). Metabolism of NNK by CYP1B1 has not been studied. Based on reported expression levels, other enzymes that may contribute to NNK activation in the lung are CYP2B6 and CYP3A5 (Table 11; Hukkanen *et al.*, 2002; Smith *et al.*, 2003). The kinetic parameters for CYP3A5-catalysed NNK metabolism have not been determined.

NNAL

Human liver microsomes convert NNAL to NNAL-*O*-Gluc and NNAL-*N*-Gluc (Wiener *et al.*, 2004a). The hepatic enzymes UGT2B7 and UGT1A9 appear to be important catalysts for conversion of NNAL to NNAL-*O*-Gluc while UGT1A4 plays a significant role in the formation of NNAL-*N*-Gluc (Ren *et al.*, 2000; Wiener *et al.*, 2004a). Large variations in the ability to glucuronidate NNAL have been observed among liver microsomal specimens from different humans. Polymorphisms in the *UGT1A4* and *UGT2B7* genes were associated with altered levels of NNAL glucuronidation in these specimens (Wiener *et al.*, 2004b). Thus, interindividual differences in the conversion of NNK to NNAL and of NNAL to NNAL-Gluc could be important in determining individual susceptibility to the carcinogenic effects of NNK.

Human liver microsomes convert NNAL to lactol, diol, hydroxy acid, NNAL-*N*-oxide and NNK. Conversion to NNK occurs at the fastest rate (Staretz *et al.*, 1997b). There was no significant difference in the rates of metabolism of (*S*)- and (*R*)-NNAL by human liver microsomes (Upadhyaya *et al.*, 2000). Human CYP2A13 catalyzed the conversion of racemic NNAL to lactol, diol and NNAL-*N*-oxide with K_m values of 36 ± 3 , 40 ± 3 and 30 ± 7 μ M, respectively (J alas *et al.*, 2003a).

In-vivo studies

Overview

The metabolism of NNK in humans was definitively established by studies that demonstrated the presence of its metabolites in the urine of smokeless tobacco users, smokers and nonsmokers exposed to secondhand smoke. NNK metabolites identified and quantified to date are NNAL, NNAL-*O*-Gluc, NNAL-*N*-Gluc and NNAL-*N*-oxide. NNAL and NNAL-Gluc have also been detected in plasma. These metabolites have been reported only in individuals exposed to tobacco or tobacco smoke, and their levels are too high for them to derive from the small amounts of NNAL in tobacco products. The only possible source is NNK. In addition, haemoglobin and DNA adducts that could arise from either NNK or NNN have been quantified in human blood and tissues.

NNAL and NNAL-Gluc

Studies on NNAL and NNAL-Gluc in human urine have been reviewed (Hecht, 2002; IARC, 2004) (see also Section 1.4.1(c)). Mean levels reported in the urine of smokeless tobacco users, smokers and nonsmokers exposed to secondhand tobacco smoke are summarized in Table 12.

Table 12. Total NNAL in the urine of smokeless tobacco users, smokers and nonsmokers exposed to secondhand tobacco smoke

No. of subjects	pmol/mL	pmol/mg creatinine	nmol/24 h	Reference
Smokeless tobacco users				
7 <i>toombak</i> users	1270	NR	NR	Murphy <i>et al.</i> (1994)
39 smokeless tobacco users	NR	4.4	NR	Kresty <i>et al.</i> (1996)
13 smokeless tobacco users	4.22	3.55	6.60	Hecht <i>et al.</i> (2002)
10 snuff dippers	4.20	NR	NR	Carmella <i>et al.</i> (2002)
55 snuff dippers	NR	3.25	NR	Carmella <i>et al.</i> (2003)
41 snuff dippers	NR	3.0	NR	Hatsukami <i>et al.</i> (2004)
54 snuff dippers	NR	3.3	NR	Lemmonds <i>et al.</i> (2005)
Smokers				
11 smokers	NR	NR	11.4	Carmella <i>et al.</i> (1993)
61 smokers	NR	3.76	NR	Carmella <i>et al.</i> (1995)
11 smokers	NR	NR	3.28	Hecht <i>et al.</i> (1995)
20 smokers	NR	NR	3.22	Meger <i>et al.</i> (2000)
13 smokers	NR	3.90	NR	Taioli <i>et al.</i> (1997)
27 smokers	1.95	2.70	3.14	Hecht <i>et al.</i> (1999a)
18 smokers	NR	3.69	NR	Hurt <i>et al.</i> (2000)
10 smokers	1.22	NR	NR	Carmella <i>et al.</i> (2002)
99 smokers	NR	2.07	NR	Hecht <i>et al.</i> (2004a)
41 smokers	NR	2.60	NR	Carmella <i>et al.</i> (2003)
34 smokers	NR	3.5	NR	Hughes <i>et al.</i> (2004)
38 smokers	NR	2.3	NR	Hatsukami <i>et al.</i> (2004)
84 smokers	NR	1.6	NR	Hecht <i>et al.</i> (2004b)
7 smokers	2.36	NR	5.32	Byrd & Ogden (2003)
12 smokers	2.8	NR	NR	Breland <i>et al.</i> (2003)
11 smokers	NR	1.34	NR	Sellers <i>et al.</i> (2003)
Nonsmokers exposed to secondhand tobacco smoke				
5 exposed men	NR	NR	0.127	Hecht <i>et al.</i> (1993a)
9 exposed hospital workers	0.059	NR	NR	Parsons <i>et al.</i> (1998)
29 exposed nonsmokers	NR	NR	0.027	Meger <i>et al.</i> (2000)
23 exposed women	0.050	NR	NR	Anderson <i>et al.</i> (2001)
74 exposed children	0.056	NR	NR	Hecht <i>et al.</i> (2001)
16 casino patrons	0.033	0.037	NR	Anderson <i>et al.</i> (2003)
19 restaurant workers	0.066	0.070	0.107	Tulunay <i>et al.</i> (2005)
27 newborns of smoking mothers	0.14	NR	NR	Lackmann <i>et al.</i> (1999)

NNAL, 4-(methylnitrosamino)-1-(3-pyridyl)-1-butanol (NNAL); NR, not reported

Smokeless tobacco users

Snuff dippers/tobacco chewers in the USA excreted 6.6 nmol/24 h total NNAL (NNAL plus NNAL-Gluc) in urine (Hecht *et al.*, 2002) (Table 12). Swedish snuff users excreted 48% less total NNAL than snuff dippers who used products marketed in the USA (Hatsukami *et al.*, 2004). Assuming that total NNAL represents 20% of the NNK dose, uptake of NNK amounts to 33 nmol per day in snuff dippers/chewers and 17 nmol per day in Swedish snuff users. The total dose of NNK would be 4.8 $\mu\text{mol/kg}$ bw over 30 years of snuff dipping/chewing and 2.5 $\mu\text{mol/kg}$ bw over 30 years of *snus* use. Rats treated with 0.5 ppm of NNK in the drinking-water for 2 years (total dose, 73 $\mu\text{mol/kg}$ bw) had an increased incidence of exocrine pancreatic tumours (Rivenson *et al.*, 1988) (see Section 3.1.4(b)). The total dose in the rat study was about 15–29 times higher than the estimated total human dose achieved over 30 years of snuff dipping/chewing or *snus* use. Lower doses of NNK have not been tested for induction of pancreatic tumours, but tumorigenicity of NNK in the rat pancreas is enhanced by a high-fat diet (Hoffmann *et al.*, 1993a).

Toombak users excreted an average of 1270 pmol/mL urine total NNAL, which was approximately 300 times higher than that excreted by snuff dippers/chewers or Swedish snuff users (4.2 pmol/mL) (Murphy *et al.*, 1994; Carmella *et al.*, 2002). Applying the above calculation, the 30-year total dose of NNK in *toombak* users would be about 1440 $\mu\text{mol/kg}$ bw (298 mg/kg bw). NNN levels in the saliva of *toombak* users were approximately 30 times greater than those of NNK (Idris *et al.*, 1992). Thus, the corresponding NNN dose could be estimated as 43 200 $\mu\text{mol/kg}$ bw (9.04 g/kg bw). These estimated total doses of NNK (1440 $\mu\text{mol/kg}$ bw) and NNN (43 200 $\mu\text{mol/kg}$ bw) can be compared with the total doses of NNK (240 $\mu\text{mol/kg}$ bw) and NNN (1400 $\mu\text{mol/kg}$ bw) which induced a significantly increased incidence of oral cavity tumours when swabbed repeatedly in the oral cavity of Fischer 344 rats (Hecht *et al.*, 1986b). Thus, 30-year *toombak* users are exposed to total doses of NNK and NNN that are approximately six and 31 times higher than those required to induce oral tumours in rats.

The ratio of (S)-NNAL-O-Gluc:(R)-NNAL-O-Gluc was 1.9 and that of NNAL-O-Gluc:NNAL-N-Gluc was 7.1 in the urine of *toombak* users (Murphy *et al.*, 1994; Carmella *et al.*, 2002) and 3.6 in the urine of snuff dippers (Carmella *et al.*, 2002). Free NNAL comprised 31% of total NNAL in the urine of *toombak* users (Murphy *et al.*, 1994) and 35% of total NNAL in the urine of snuff dippers (Carmella *et al.*, 2002).

When snuff dippers who used products marketed in the USA switched to a brand of Swedish snuff over a 4-week period, a statistically significant average reduction of about 48% in total urinary NNAL was observed. However, when snuff dippers switched to a nicotine patch for 4 weeks, there was a significantly greater reduction of about 90% in total NNAL, which showed that a switch to *snus* is inferior to abstinence from smokeless tobacco with respect to NNK uptake (Hatsukami *et al.*, 2004).

In one study of snuff dippers and tobacco chewers, a significant association between urinary levels of total NNAL and the presence of oral leukoplakia was observed (Kresty *et al.*, 1996).

Smokers

Smokers excrete about 3.2 nmol/24 h total NNAL (Table 12). Assuming that total NNAL represents 20% of NNK dose, daily uptake of NNK would be 16.5 nmol, or 180 μ mol (2.4 μ mol/kg bw; 0.5 mg/kg bw) over 30 years of smoking. The lowest total dose of NNK shown to induce a significantly increased incidence of lung tumours in rats, as part of a dose–response relationship, was 1.8 mg/kg bw (8.7 μ mol/kg bw), 3.6 times higher than the dose of a smoker (Belinsky *et al.*, 1990) (see Section 3.1.2(a)).

The enantiomeric distribution of NNAL in urine was 54% (*R*)-NNAL and 46% (*S*)-NNAL whereas the diastereomeric distribution of NNAL-Gluc was 68% (*R*)-NNAL-Gluc and 32% (*S*)-NNAL-Gluc (Carmella *et al.*, 1999). (*R*)-NNAL is the more tumorigenic NNAL enantiomer in A/J mice (Upadhyaya *et al.*, 1999). The ratio of NNAL-*O*-Gluc:NNAL-*N*-Gluc was 1.3 in smokers (Carmella *et al.*, 2002). Free NNAL comprised a mean of 38% of total NNAL in smokers, and gave an NNAL-Gluc:NNAL ratio of 1.6 (Carmella *et al.*, 2002). A wide range of NNAL-Gluc:NNAL ratios has been observed and there is evidence for a high ratio (6–11) phenotype in a minority of smokers (Carmella *et al.*, 1995).

Consistently, total NNAL correlates with total cotinine in smokers (Hecht, 2002), number of cigarettes per day and 1-hydroxypyrene in urine. The increase in total NNAL with number of cigarettes per day was not linear (Joseph *et al.*, 2005). As cotinine is a marker for the uptake of nicotine, total NNAL is a marker for the uptake of NNK.

Five recent studies have employed NNAL and NNAL-Gluc, as well as other biomarkers, to investigate approaches to tobacco harm reduction. Two concerned the effects of reducing numbers of cigarettes smoked per day and whether this would have a significant effect on the uptake of NNK. One study of 23 subjects found a moderate reduction of NNAL-Gluc and total NNAL (Hurt *et al.*, 2000). A second study of 102 smokers examined NNAL and NNAL-Gluc in the urine of smokers who reduced their smoking by up to 75% over a 6-week period. Statistically significant reductions in NNAL, NNAL-Gluc and total NNAL were observed at most intervals, but the observed decreases were generally modest, were always proportionally lower than the reductions in the number of cigarettes smoked per day and were sometimes transient (Hecht *et al.*, 2004a). Apparently, smokers compensate in their smoking behaviour when they smoke fewer cigarettes per day, and thereby decrease the expected reduction in carcinogen uptake. Three studies examined the effects of switching to brands with lower NNK delivery, as measured by standardized machine methods. In one study of the Omni cigarette, which, according to machine measurement, delivers less NNK than traditional brands, no significant decrease in the level of total NNAL was observed (Hughes *et al.*, 2004). A second study of Omni did demonstrate a significant reduction in total NNAL compared with the smokers' usual brand, but less than that achieved by cessation with medicinal nicotine (Hatsukami *et al.*, 2004). A significant reduction in total NNAL was also observed in smokers who switched to the Advance cigarette (Breland *et al.*, 2003).

Levels of NNAL and NNAL-Gluc were measured in the urine of 84 Singapore Chinese smokers, who were interviewed about their intake of cruciferous vegetables (Hecht *et al.*,

2004b). There was a significant correlation between increased consumption of glucobrassicins (precursors of indole-3-carbinols) from these vegetables and decreased levels of NNAL in the urine, after adjustment for number of cigarettes smoked per day; similar trends were observed for NNAL-Gluc and total NNAL. These results are consistent with those of previous studies that demonstrated that indole-3-carbinol, an in-vivo hydrolysis product of glucobrassicins, decreased the levels of urinary NNAL, probably by inducing hepatic metabolism of NNK (Morse *et al.*, 1990a; Taioli *et al.*, 1997).

Urine samples from 175 smokers of regular, light or ultra-light cigarettes were analysed for total NNAL (Hecht *et al.*, 2005). There were no statistically significant differences in urinary levels of total NNAL among smokers of these types of cigarettes, and no correlation between levels of tar and total NNAL. These results are consistent with epidemiological studies that showed no difference in the risk for lung cancer among smokers of different types of cigarettes (Burns *et al.*, 2001; Harris *et al.*, 2004).

Nonsmokers exposed to secondhand tobacco smoke

Levels of total NNAL in the urine of nonsmokers exposed to secondhand tobacco smoke are typically about 1–5% of those in smokers (Table 12). Correlations between levels of urinary cotinine and total NNAL have consistently been observed in studies of nonsmokers exposed to secondhand tobacco smoke (Hecht, 2002; IARC, 2004). Most studies on NNAL in the urine of nonsmokers have been reviewed in a previous monograph which concluded: “The data demonstrating uptake of NNK, a lung carcinogen in rodents, by nonsmokers are supportive of a causal link between exposure to secondhand tobacco smoke and development of lung cancer” (IARC, 2004). Two studies have appeared since that time. In one, total NNAL was quantified before and after a 4-h visit to a gambling casino where smoking was allowed. Paired samples showed statistically significant mean increases in total cotinine (cotinine plus its glucuronide) and total NNAL in urine after the visit (Anderson *et al.*, 2003). A second study examined the uptake of total nicotine, total cotinine and total NNAL in nonsmokers who worked in restaurants and bars that permit smoking (Tulunay *et al.*, 2005). Urine samples were collected for 24 h on working and non-working days. The results showed significant increases in urinary levels of total nicotine, total cotinine and total NNAL on working days compared with non-working days.

NNAL-N-oxide

Levels of NNAL-*N*-oxide ranged from 0.06 to 1.4 pmol/mg creatinine (mean, 0.53 pmol/mg creatinine) in the urine of smokers and from 0.02 to 1.2 pmol/mg creatinine (mean, 0.41 pmol/mg creatinine) in the urine of smokeless tobacco users. NNK-*N*-oxide was not detected in the urine. The amounts of NNAL-*N*-oxide in urine were about 20 and 50% of the amounts of NNAL-Gluc and NNAL, respectively. Thus, pyridine-*N*-oxidation is less important than glucuronidation as a detoxification pathway for NNK and NNAL in humans (Carmella *et al.*, 1997).

Haemoglobin adducts

Haemoglobin adducts of NNK and NNN are formed upon reaction of a common intermediate, POB-DZH, with aspartate or glutamate in haemoglobin. In the case of NNK, POB-DZH is generated by CYP-mediated hydroxylation of the methyl group to give α -HOMeNNK (Figures 2 and 5). The POB-aspartate and -glutamate esters in haemoglobin can readily be hydrolysed by base treatment to release HPB, which can be quantified by gas chromatography–mass spectrometry (Carmella *et al.*, 1990a; Hecht, 1998). The presence of HPB-releasing haemoglobin adducts in humans provides strong evidence for the metabolic activation of NNK and/or NNN, although another possible source — nitrosation of myosmine — has been proposed (Wilp *et al.*, 2002).

The highest levels of HPB-releasing haemoglobin adducts have been found in smokeless tobacco users. Mean levels (fmol/g haemoglobin) were 517 in snuff-dippers, 236 in nasal snuff users and 148 in *toombak* users (Carmella *et al.*, 1990a; Falter *et al.*, 1994; Murphy *et al.*, 1994). Lower levels were reported in smokers. Mean levels (fmol/g haemoglobin) in smokers and nonsmokers in four studies were 79.6 and 29.3 (Carmella *et al.*, 1990a), 54.7 and 26.7 (Branner *et al.*, 1998), 61 and 34 (Falter *et al.*, 1994) and 26 and 19 (Atawodi *et al.*, 1998). Levels of HPB-releasing haemoglobin adducts were not higher in nonsmokers exposed to secondhand tobacco smoke than in non-exposed nonsmokers (Branner *et al.*, 1998).

DNA adducts

NNK can form adducts by two α -hydroxylation pathways (Figure 2). α -Methyl hydroxylation produces α -HOMeNNK, which spontaneously decomposes to POB-DZH. POB-DZH can also be formed by 2'-hydroxylation of NNN. POB-DZH reacts with DNA to give a variety of adducts (Figures 2 and 5), some of which release HPB upon acid or neutral thermal hydrolysis. POB-DZH-derived adducts in DNA can be quantified by treating the DNA with acid and measuring released HPB by gas chromatography–mass spectrometry. α -Methylene hydroxylation of NNK or NNAL ultimately produces Me-DZH, which can react with DNA to produce *O*⁶-methyldeoxyguanosine (*O*⁶-MedGuo), 7-MedGuo, *O*⁴-methyldeoxythymidine (*O*⁴-MedThd) and other adducts (Figure 2).

HPB-releasing DNA adducts were detected in human lung (Foiles *et al.*, 1991). Mean levels (fmol/mg DNA) were 11 ± 16 in nine smokers and 0.9 ± 2.3 in eight nonsmokers. Mean adduct levels in tracheobronchus were 16 ± 18 in four smokers and 0.9 ± 1.7 in four nonsmokers. In another study, HPB-releasing adducts were not detected in lung samples from four individuals, two of whom were confirmed smokers (detection limit reported as 8–50 fmol/mg DNA) (Blömeke *et al.*, 1996).

Methyl DNA adducts have been detected in tissues or cells of smokers and nonsmokers in several studies. Levels of 7-MedGuo were higher in pulmonary alveolar cells or bronchial tissues of smokers than nonsmokers (Mustonen *et al.*, 1993; Petruzzelli *et al.*, 1996) in two studies, while a third showed no difference (Kato *et al.*, 1995). Sample sizes and their origins were insufficient to judge the effects of smoking in four other studies (Wilson *et al.*, 1989; Shields *et al.*, 1990; Kato *et al.*, 1993; Blömeke *et al.*, 1996). Levels

of 7-alkylguanines in DNA from larynx tissue increased with the amount of smoking (Szyfter *et al.*, 1996). Levels of 7-MedGuo plus 7-(2-hydroxyethyldeoxyguanosine) were higher in lymphocytes of smokers compared with nonsmokers (Kumar & Hemminki, 1996). There was no effect of smoking or exposure to secondhand tobacco smoke on levels of *O*⁶-MedGuo in human peripheral and cord blood DNA (Georgiadis *et al.*, 2000), and no difference in *O*⁶-MedGuo levels in placenta from smokers and nonsmokers (Foiles *et al.*, 1988). Some of the methyl DNA adducts detected in these studies may have originated from NNK, but there are other sources of methyl DNA adducts in cigarette smoke, notably *N*-nitrosodimethylamine.

(iv) *Excretion*

Urine is the only route of excretion of NNK metabolites for which data from studies with humans are currently available (see Section on metabolism above and Table 12). Studies in laboratory animals indicate that urine is the major route of excretion of NNK metabolites (see Section 4.1.2(d)).

(b) *N'*-Nitrosonornicotine (NNN)

(i) *Absorption*

NNN has been detected in the saliva of snuff dippers, chewers of betel quid with tobacco, users of *khaini*, *gudhaku*, *toombak* and *mishri* and reverse smokers. The data are presented in Section 1.4.2(a).

Absorption of NNN has been demonstrated by detection of NNN and NNN-*N*-Gluc in the urine in smokeless tobacco users and smokers (Stepanov & Hecht, 2005; see Section 4.1.1(b)(iv)).

(ii) *Distribution*

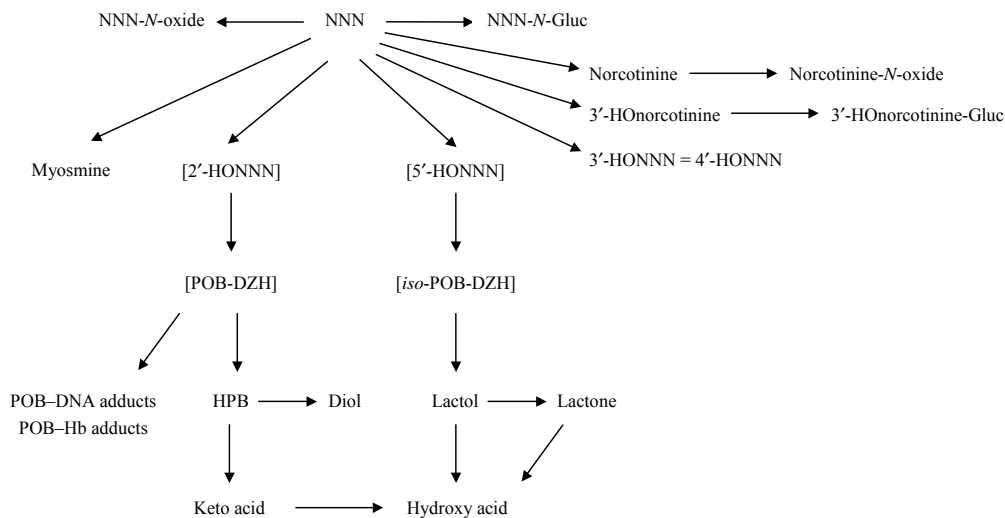
NNN was detected in two of 17 samples of pancreatic juice from smokers at levels of 68.1 and 242 ng/mL juice. It was not detected in the pancreatic juice from nine nonsmokers (Prokopczyk *et al.*, 2002). Pyridyloxobutyl-haemoglobin adducts have been detected in smokeless tobacco users and smokers, and pyridyloxobutyl-DNA adducts have been detected in smokers. These adducts could arise from NNN or NNK and are discussed in the section on NNK.

(iii) *Metabolism*

Introduction

The metabolic pathways of NNN and modes of DNA adduct formation are shown in Figure 6, and structures of the metabolites are illustrated in Figure 7. This information is based on studies *in vitro*, in laboratory animals and in humans. Specific pathways that have been observed in in-vitro studies with human tissues or enzymes or *in vivo* in humans are discussed below.

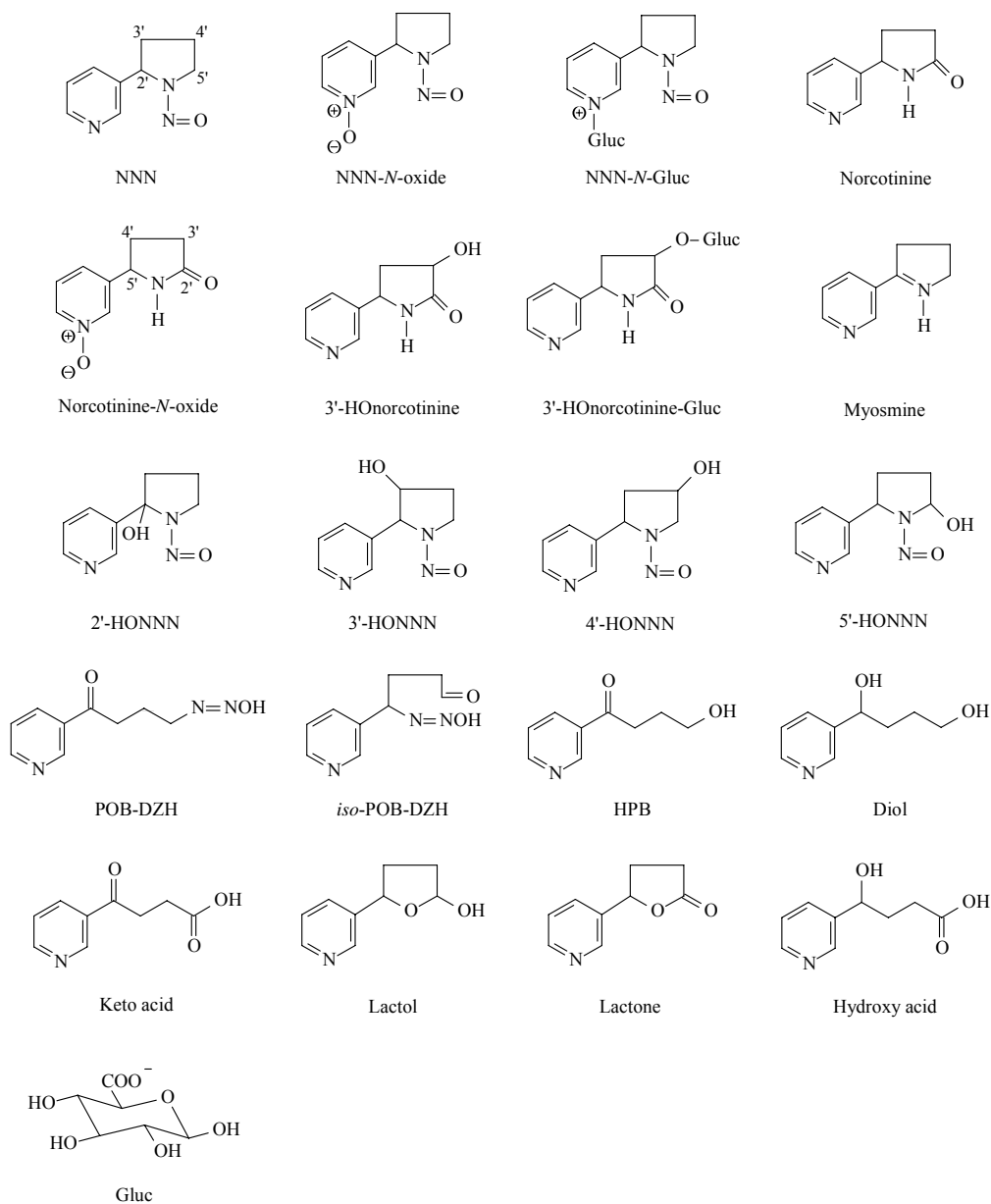
Figure 6. Metabolism of NNN and formation of adducts, based on studies in laboratory animals and humans



DZH, diazohydroxide; Gluc, glucuronide; Hb, haemoglobin; HO, hydroxy; HPB, 4-hydroxy-1-(3-pyridyl)-1-butanone or keto alcohol; NNN, *N*'-nitrosornicotine; POB, 4-oxo-4-(3-pyridyl)-1-butyl or pyridyloxobutyl

NNN can undergo pyridine *N*-oxidation to yield NNN-*N*-oxide and pyridine *N*-glucuronidation to yield NNN-*N*-Gluc. Denitrosation and oxidation of NNN yields myosmine or norcotinine, and the latter can undergo pyridine *N*-oxidation to yield norcotinine-*N*-oxide. NNN also is metabolized to 3'-hydroxynorcotinine (3'-HONorcotinine) but it is not clear whether this proceeds via norcotinine or by an independent pathway. 3'-HONorcotinine undergoes glucuronidation on its hydroxyl group to yield 3'-HONorcotinine-Gluc.

Hydroxylation of the pyrrolidine ring of NNN produces 2'-hydroxy-NNN (2'-HONNN), 3'-HONNN, 4'-HONNN and 5'-HONNN. While 3'-HONNN and 4'-HONNN are stable metabolites, 2'-HONNN and 5'-HONNN, which are α -hydroxynitrosamines, are unstable. 2'-HONNN spontaneously undergoes ring opening to yield POB-DZH. POB-DZH reacts with water to form HPB. POB-DZH also reacts with DNA and haemoglobin to form adducts that are believed to have structures identical to those formed by the POB-DZH pathway in NNK metabolism. HPB can be further oxidized to keto acid or reduced to diol. 5'-HONNN spontaneously undergoes ring opening to produce 1-(3-pyridyl)-4-oxo-1-butanediazohydroxide (*iso*-POB-DZH), which reacts with water to form 5-(3-pyridyl)-2-hydroxytetrahydrofuran (lactol). Lactol can be oxidized to 5-(3-pyridyl)tetrahydrofuran-2-one (lactone) or 4-hydroxy-4-(3-pyridyl)butanoic acid (hydroxy acid). Thus, HPB and keto acid are indicative of the metabolic activation of NNN by 2'-hydroxylation whereas the lactol and the hydroxy acid are indicative of the metabolic activation of NNN by 5'-hydroxylation.

Figure 7. Structures of NNN and metabolites

DZH, diazohydroxide; Gluc, glucuronide; HO, hydroxy; HPB, 4-hydroxy-1-(3-pyridyl)-1-butanone or keto alcohol; NNN, *N*'-nitrosanornicotine; POB, 4-oxo-4-(3-pyridyl)-1-butyl or pyridyloxobutyl

In-vitro studies in human tissues and cells

Metabolism of NNN by human tissues *in vitro* has been reviewed (Hecht, 1998). NNN-*N*-oxide and hydroxy acid (from 5'-hydroxylation) have been detected after incubation of cultured human tissues — buccal mucosa, trachea, oesophagus, bronchus, peripheral lung and urinary bladder — with NNN (Castonguay *et al.*, 1983c). Smaller amounts of keto acid (from 2'-hydroxylation) were also observed (Castonguay *et al.*, 1983c). Adult and fetal human oesophageal cultures metabolized NNN to hydroxy acid (5'-hydroxylation), keto acid (2'-hydroxylation) and NNN-*N*-oxide (Chakradeo *et al.*, 1995). Human oesophageal microsomes also metabolized NNN by 5'-hydroxylation and 2'-hydroxylation; and the latter was partially inhibited by troleandomycin, an inhibitor of CYP3A (Smith *et al.*, 1998).

Human liver microsomes metabolically activate NNN by 5'-hydroxylation to yield lactol and by 2'-hydroxylation to yield keto alcohol. Consistently, 5'-hydroxylation predominates (Hecht, 1998). Overall rates of metabolic activation of NNN were greater than those of NNK, NNAL or benzo[*a*]pyrene in human liver microsomes (Staretz *et al.*, 1997a). At concentrations of 0.8–1 μM NNN, metabolism by human liver microsomes was mainly by 5'-hydroxylation and the reaction was strongly correlated with coumarin 7-hydroxylation, which suggests the involvement of CYP2A6 (Patten *et al.*, 1997). 2'-Hydroxylation correlated with 6 β -hydroxylation of testosterone, a CYP3A4-specific activity (Patten *et al.*, 1997).

CYPs have been identified as the major catalysts of NNN metabolic activation by α -hydroxylation. Human CYP2A6 metabolized NNN exclusively by 5'-hydroxylation, with a K_m of 2.1 μM (Patten *et al.*, 1997). The K_m s for 5'-hydroxylation of (*R*)-NNN and (*S*)-NNN were 22 μM and 2.3 μM , respectively (Wong *et al.*, 2005b). Rates of metabolism of NNN by CYP2E1 and 2D6 were much lower (Patten *et al.*, 1997). Metabolism of NNN by expressed human CYP3A4 was specific for 2'-hydroxylation (HPB formation) with a K_m of 304 μM (Patten *et al.*, 1997). Human CYP2A13 metabolized both (*R*)- and (*S*)-NNN by 5'-hydroxylation to lactol, with K_m s of 24 and 23 μM , respectively, and metabolized (*R*)-NNN to HPB with a K_m of 21 μM (Wong *et al.*, 2005b). Studies with *Salmonella typhimurium* strains that co-express human CYPs demonstrated that CYP2A6 was the most effective catalyst of NNN metabolic activation among 11 CYPs tested (Fujita & Kamataki, 2001).

In summary, studies with human tissues clearly demonstrate the metabolic activation of NNN; 5'-hydroxylation predominates in liver microsomes and both 2'-hydroxylation and 5'-hydroxylation are observed to comparable extents in oesophageal microsomes. NNN metabolism has also been observed in a variety of cultured tissues. Human CYP2A6 and CYP2A13 are effective catalysts of NNN α -hydroxylation.

In-vivo studies

NNN-*N*-Gluc has been detected in the urine of smokeless tobacco users and smokers (Stepanov & Hecht, 2005). Keto acid and the enantiomers of hydroxy acid have been quantified in the urine of smokers and abstinent smokers who used nicotine replacement therapy to test the hypothesis that (*S*)-hydroxy acid could be a biomarker of metabolic

activation of NNK and NNN while (*R*)-hydroxy acid would be formed predominantly from nicotine as indicated by studies with rats (Hecht *et al.*, 1999b; Trushin & Hecht, 1999). (*R*)-Hydroxy acid was the major enantiomer in human urine. The amount of (*S*)-hydroxy acid was far greater than that which could be formed from NNK and NNN. Both (*S*)-hydroxy acid and keto acid were formed in substantial amounts from nicotine, which precludes their use as biomarkers of NNN uptake in smokers.

HPB-releasing haemoglobin adducts and DNA adducts have been detected in tobacco users. These adducts can be formed either from NNK or from 2'-hydroxylation of NNN, and are discussed in section 4.1.1(a)(iii).

(iv) *Excretion*

NNN and NNN-*N*-Gluc have been detected in the urine of smokeless tobacco users and smokers (Stepanov & Hecht, 2005). The data are presented in Section 1.4.2(b).

(c) *N'*-Nitrosoanabasine (NAB)

(i) *Absorption*

NAB has been detected in the saliva of users of *toombak*, *khaini* tobacco and *gudhaku*. The data are presented in Section 1.4.3(a).

Absorption of NAB by smokeless tobacco users and smokers has been demonstrated by detection of NAB and NAB-*N*-Gluc in urine (Stepanov & Hecht, 2005).

(ii) *Distribution*

No data were available to the Working Group

(iii) *Metabolism*

In experiments with 11 strains of *S. typhimurium* YG7108, each of which co-expresses a form of human CYPs, CYP 3A4, 2A6, 1A1 and 3A5 were capable of converting NAB to mutagenic products. CYP3A4 was the best catalyst (Fujita & Kamataki, 2001).

(iv) *Excretion*

NAB and NAB-*N*-Gluc have been detected in the urine of smokers and smokeless tobacco users (Stepanov & Hecht, 2005). The data are presented in Section 1.4.3(b).

(d) *N'*-Nitrosoanatabine (NAT)

(i) *Absorption*

NAB has been detected in the saliva of users of *toombak*, *khaini* and *gudhaku*. The data are presented in Section 1.4.4(a).

Absorption of NAT has been demonstrated by the detection of NAT and NAT-*N*-Gluc in the urine of smokeless tobacco users and smokers (Stepanov & Hecht, 2005).

(ii) *Distribution*

No data were available to the Working Group.

(iii) *Metabolism*

In experiments with 11 strains of *S. typhimurium* YG7108, each of which co-expresses a form of human CYPs, CYP2A6 was capable of converting NAT to mutagenic products (Fujita & Kamataki, 2001).

(iv) *Excretion*

NAT and NAT-*N*-Gluc have been detected in the urine of smokers and smokeless tobacco users (Stepanov & Hecht, 2005). The data are presented in Section 1.4.4(b).

4.1.2 *Experimental systems*

(a) *NNK and NNAL*

Studies on the absorption, distribution, metabolism and excretion of NNK in experimental systems have been comprehensively reviewed (Hecht, 1998). The reader is referred to that review for detailed coverage of the literature. Selected studies from the previous review that illustrate important points as well as more recent studies pertinent to the evaluation are presented below.

(i) *Absorption*

Beagle dogs were exposed to a single spray bolus of dissolved NNK in the distal trachea (0.48 nmol/dog) (Gerde *et al.*, 1998). NNK was rapidly absorbed and extensively metabolized in the tracheal mucosa. Most NNK appeared rapidly in the blood that drains the airway mucosa, but a phase of slow clearance was also observed. During absorption, NNK was distributed within the entire depth of the mucosa to the tracheal cartilage. A portion was bound to the mucin component of the mucous lining. First-pass metabolism and activation of NNK in the airway mucosa were sufficiently rapid to cause levels of binding at the site of absorption that were 20-fold those at distal tissues, which indicates a mechanism by which NNK could act as a carcinogen at the site of entry. In a comparison of NNK and benzo[*a*]pyrene, it was concluded that NNK is diffused into the mucosa sufficiently rapidly for blood perfusion to limit clearance, whereas benzo[*a*]pyrene is diffused into the mucosa more slowly. NNK passes into the blood about 100 times more rapidly than benzo[*a*]pyrene. NNK and its metabolites swiftly disperse throughout the mucosa, whereas benzo[*a*]pyrene and its activated metabolites are confined to the target epithelium. NNK was metabolized in the airway mucosa at least 15 times faster than benzo[*a*]pyrene, but NNK metabolites bound less effectively than those of benzo[*a*]pyrene at the site of entry. The rapid absorption of NNK at the site of entry could lead to accumulation at peripheral sites in the lung, which is consistent with its ability to induce adenocarcinoma (Gerde *et al.*, 1998). Rapid absorption of NNK has also been observed after admi-

nistration to rodents and monkeys by various routes (Castonguay *et al.*, 1983b; Tjälve & Castonguay, 1983; Castonguay *et al.*, 1985a; Tjälve, 1991).

(ii) *Distribution*

Autoradiographic studies demonstrate that, 1 min after intravenous administration of [carbonyl-¹⁴C]NNK to rats, radioactivity was homogeneously distributed in most tissues of the body at a level similar to that in the blood (Castonguay *et al.*, 1983b). At later time intervals, accumulation of bound radioactivity was observed in tissues such as the lung and nasal mucosa, which are targets of NNK carcinogenicity. Relatively large amounts of unbound radioactivity are also observed in the stomach contents and melanin-containing tissues, due to the basicity of NNK and NNAL (Castonguay *et al.*, 1983b; Tjälve & Castonguay, 1983; Castonguay *et al.*, 1985a; Hecht, 1998). These studies show that NNK is distributed rapidly and homogeneously throughout the body and has the ability to cross cellular membranes freely and partition evenly in the intra- and extracellular tissue water (Castonguay *et al.*, 1983b). Initially, strong labelling was observed in parts of the nasal mucosa, in the liver, bronchial mucosa, adrenal cortex, preputial gland, salivary gland and stomach contents. At later time points, radioactivity persisted in certain tissues and was seen in the kidney, urinary bladder and gastrointestinal contents (Castonguay *et al.*, 1983b). Similar results have been obtained in autoradiographic and other studies carried out in Syrian golden hamsters, dogs and marmoset monkeys by various routes of administration (Tjälve & Castonguay, 1983; Castonguay *et al.*, 1985a; Gerde *et al.*, 1998; Tjälve, 1991).

Micro-autoradiographic studies in Fischer 344 rats injected with [CH₃-³H]NNK showed that the highest degree of labelling in the lung was in the Clara cells (Belinsky *et al.*, 1987a); in the nasal passages, the highest degree of labelling was in Bowman's glands, Steno's gland and serous glands of the respiratory mucosa, with a lower degree of labelling in the respiratory and olfactory epithelia (Belinsky *et al.*, 1987b). Similar results were obtained with [carbonyl-¹⁴C]NNK (Tjälve *et al.*, 1985; Tjälve, 1991).

Pharmacokinetic studies of NNK and NNAL in rats demonstrated large volumes of distribution of NNK (321 ± 137 mL) and NNAL (2772 ± 1423 mL) (Wu *et al.*, 2002). The enantiomers of NNAL appear to be distributed differently in the body, as indicated by the apparent volumes of distribution: 1792 ± 570 mL for (*S*)-NNAL and 645 ± 230 mL for (*R*)-NNAL, a difference that was significant (Zimmerman *et al.*, 2004). These data suggest extensive tissue binding that is greater for (*S*)-NNAL. Tissue distribution studies demonstrated that (*S*)-NNAL was retained in the lung 24 h after administration; the (*S*):(*R*) ratio increased from 1.1 1 h after administration to 4.23 24 h after administration (Zimmerman *et al.*, 2004). An increase of this magnitude was observed only in the lung, which suggests that (*S*)-NNAL is stereoselectively retained in the rat lung, possibly at a receptor site. This tissue distribution of NNAL may partially explain the initial accumulation of radioactivity in certain rat tissues, as seen by autoradiography, as well as the relatively long retention of (*S*)-NNAL seen in smokers and smokeless tobacco users.

(iii) *Metabolism*

Extensive studies of the metabolism of NNK have been carried out *in vitro* and *in vivo* in a variety of species including rats, hamsters, mice, rabbits, pigs and monkeys (reviewed in Hecht, 1998). Figure 2 summarizes the metabolism of NNK determined from these investigations. Virtually all systems examined conform to this general scheme, with major pathways of metabolism generally being reduction to NNAL and α -hydroxylation of NNK and NNAL. In the conversion of NNK to NNAL, (*S*)-NNAL is the predominant enantiomer formed in rat and mouse liver and lung microsomes and cytosol, as well as red blood cells (Upadhyaya *et al.*, 2000).

In-vitro studies of NNK metabolism

In-vitro studies of NNK metabolism have been comprehensively reviewed (Hecht, 1998). Studies of the kinetic parameters for NNK metabolism mediated by microsomal preparations from tissues of laboratory animals (Table 13) and relevant CYP enzymes (Table 11) are discussed below. Other selected studies of NNK metabolism *in vitro* are also included.

Monkey

Kinetic parameters for NNK metabolism have been reported for patas monkey lung and liver microsomes (Table 13; Smith *et al.*, 1997). In the lung, HPB is formed with the greatest efficiency, followed by NNK-*N*-oxide, the keto aldehyde and NNAL (Table 13; Smith *et al.*, 1997). K_m values for keto aldehyde, HPB and NNK-*N*-oxide formation were about 5–10 μ M. The K_m for NNAL formation was much higher, however, which is consistent with the hypothesis that this metabolite is not formed by the same enzymes that catalyse α -hydroxylation (Maser *et al.*, 1996; Maser, 1998; Maser *et al.*, 2000; Finckh *et al.*, 2001). Similar results were obtained in patas monkey liver microsomes (Table 13). The kinetic parameters for NNK metabolism by expressed monkey CYPs have not been reported, but antibody and chemical inhibition studies imply that members of the CYP1A and 2A subfamilies are important catalysts of NNK metabolism (Smith *et al.*, 1997). The metabolism of NNK was also studied in short-term cultures of patas and cynomolgus monkey lung, and in Fischer 344 rat lung for comparison. Substantial amounts of metabolites from the α -hydroxylation pathway of metabolic activation were observed, together with the formation of NNK-*N*-oxide and NNAL. The metabolism of NNK by cultured monkey lung was generally similar to that observed in rat lung, which indicates that there are no major species differences between rodents and non-human primates in the pulmonary metabolism of NNK (Hecht *et al.*, 2000).

Rabbit

NNK metabolism by rabbit nasal, but not liver or lung, microsomes has been studied; kinetic parameters have not been reported (Hong *et al.*, 1992; Hecht, 1998). Kinetic parameters for CYPs purified from rabbit nasal microsomes — CYP2A10/2A11 (a mixture of two CYPs previously referred to as NMa) and CYP2G1 (previously NMb) — have been

Table 13. Apparent steady-state kinetic parameters for microsome-mediated NNK metabolism

Species/tissue	Metabolite	Kinetic parameters			Experimental conditions	Reference
		V_{max}^a	K_m (μ M)	V_{max}/K_m^b		
Female Patas monkey lung	Keto aldehyde	5.3 \pm 0.4	10.3 \pm 0.8	0.51 \pm 0.06	1–20 μ M NNK; 30-min incubation, 0.5 mg/mL microsomal protein.	Smith <i>et al.</i> (1997)
	HPB	19.1 \pm 0.8	4.9 \pm 0.2	3.9 \pm 0.2		
	NNK- <i>N</i> -oxide	11.0 \pm 0.3	5.4 \pm 0.2	2.0 \pm 0.01		
	NNAL ^c	479 \pm 35	902 \pm 21	0.53 \pm 0.04		
Female Patas monkey liver	Keto aldehyde	37.7 \pm 1.9	8.2 \pm 0.3	4.6 \pm 0.3	1–50 μ M NNK; 20-min incubation, 0.25 mg/mL microsomal protein.	
	HPB	37.4 \pm 1.0	8.1 \pm 0.2	4.6 \pm 0.2		
	NNAL ^c	3470 \pm 103	474 \pm 28	7.3 \pm 0.5		
Male Sprague-Dawley rat lung	Keto aldehyde	11.7 \pm 1	28.9 \pm 1.2	0.40 \pm 0.04	1–50 μ M NNK, 30-min incubation, 0.25 mg/mL microsomal protein.	Smith <i>et al.</i> (1992a)
	HPB	14.6 \pm 1.0	7.0 \pm 0.5	2.1 \pm 0.2		
	NNK- <i>N</i> -oxide	35.1 \pm 2.3	10.4 \pm 0.9	3.4 \pm 0.4		
	NNAL	195.3 \pm 9	178 \pm 10	1.1 \pm 0.1		
Male Fischer 344 rat liver	Formaldehyde	1478	5	296	12.5–4000 μ M NNK, 0.55 mg/mL microsomal protein.	Castonguay <i>et al.</i> (1991)
	Formaldehyde	197	534	0.37		
Male Sprague-Dawley rat liver	Keto aldehyde	153 \pm 16	234 \pm 38	0.65 \pm 0.13	5–200 μ M NNK, 5-min incubation, 0.75 mg/mL microsomal protein.	Guo <i>et al.</i> (1992)
	HPB	156 \pm 8	211 \pm 20	0.74 \pm 0.08		
	Keto aldehyde	381 \pm 51	149 \pm 32	2.6 \pm 0.6	As above, but animals were treated with 3-methylcholanthrene	
	HPB	270 \pm 43	246 \pm 54	1 \pm 0.3		
	Keto aldehyde	329 \pm 35	119 \pm 22	2.8 \pm 0.6	As above, but animals were treated with phenobarbital.	
	HPB	358 \pm 27	177 \pm 20	2.0 \pm 0.3		
	NNK- <i>N</i> -oxide	140 \pm 10	57 \pm 9	2.5 \pm 0.4	As above, but animals were treated with pregnenolone 16 α -carbonitrile.	
	Keto aldehyde	550 \pm 44	133 \pm 21	4.1 \pm 0.7		
	HPB	247 \pm 18	187 \pm 24	1.3 \pm 0.2		
NNK- <i>N</i> -oxide	167 \pm 15	103 \pm 21	1.6 \pm 0.4			
Male Sprague-Dawley rat nasal mucosa	Keto aldehyde	2833 \pm 81	9.6 \pm 0.3	295 \pm 12	1–100 μ M NNK, 10-min incubation, 0.013 mg/mL microsomal protein.	Smith <i>et al.</i> (1992a)
	HPB	3275 \pm 60	10.1 \pm 0.2	324 \pm 9		

Table 13 (contd)

Species/tissue	Metabolite	Kinetic parameters			Experimental conditions	Reference
		V _{max} ^a	K _m (μM)	V _{max} /K _m ^b		
Female A/J mouse lung	Formaldehyde	57.2 ± 2.2	5.6 ± 0.9	10.2 ± 1.7	1–20 μM NNK, 30-min incubation, 0.25 mg/mL microsomal protein.	Smith <i>et al.</i> (1990)
	HPB	56.0 ± 3.8	5.6 ± 0.9	10.0 ± 1.7		
	Keto acid	4.2 ± 0.5	9.2 ± 1.0	0.456 ± 0.074		
	NNK- <i>N</i> -oxide	54.2 ± 1.3	4.7 ± 0.9	11.5 ± 2.2		
	NNAL ^c	1322 ± 10	2541 ± 15	0.52 ± 0.005		
	Keto aldehyde	58.9 ± 2.6	23.7 ± 2.6	2.5 ± 0.3		
Female A/J mouse lung	HPB	32.5 ± 2.5	3.6 ± 0.9	9.0 ± 2.4	0.5–100 μM NNK, 30-min incubation, 0.25 mg/mL microsomal protein.	Peterson <i>et al.</i> (1991a)
	Keto aldehyde	34.0	4.9	6.9	1–10 μM NNK, 30-min incubation, 0.25 mg/mL microsomal protein.	Smith <i>et al.</i> (1993)
Female A/J mouse lung	HPB	38.1	2.6	15	As above, but animals were treated with PEITC (1 μmol/g diet).	Smith <i>et al.</i> (1993)
	NNK- <i>N</i> -oxide	60.0	1.8	33		
	Keto aldehyde	31.8	5.0	6.4		
	HPB	35.1	2.9	12		
	NNK- <i>N</i> -oxide	51.0	1.8	28	As above, but animals were treated with PEITC (3 μmol/g diet).	
	Keto aldehyde	25.7	4.7	5.5		
	HPB	23.0	2.4	9.6		
	NNK- <i>N</i> -oxide	36.7	1.6	23		
	Keto aldehyde	84.7 ± 2.8	4.5 ± 0.4	19 ± 2	0.25–20 μM NNK, 30-min incubation, 0.25 mg/mL microsomal protein.	
	HPB	62.8 ± 1.3	1.9 ± 0.2	33 ± 4		
	NNK- <i>N</i> -oxide	83.3 ± 3.6	2.0 ± 0.3	42 ± 7	As above, but with PEITC (400 nM) added to the incubation mixtures.	
	Keto aldehyde ^d	89.2 ± 6.3	24.0 ± 2.7	3.7 ± 0.5		
	HPB ^d	60.4 ± 1.8	14.9 ± 0.8	4.1 ± 0.2		
	NNK- <i>N</i> -oxide ^d	85.8 ± 4.6	17.9 ± 1.7	4.8 ± 0.5		
Keto aldehyde	71 ± 3	4.8 ± 0.7	15 ± 2	0.25–50 μM NNK, 15-min. incubation, 0.25 mg/mL microsomal protein.	Jalas <i>et al.</i> (2003b)	
HPB	93 ± 3	3.0 ± 0.4	31 ± 4			
NNK- <i>N</i> -oxide	109 ± 4	2.1 ± 0.3	52 ± 8			

Table 13 (contd)

Species/tissue	Metabolite	Kinetic parameters			Experimental conditions	Reference	
		V_{\max}^a	K_m (μM)	V_{\max}/K_m^b			
Female A/J mouse liver	Keto aldehyde	245 ± 17	24 ± 4	10 ± 2	0.5–100 μM NNK, 15-min incubation, 0.25 mg/mL microsomal protein. As above, but with 2.5 μM 4-HPO added As above, but with 5.0 μM 4-HPO added As above, but with 10 μM 4-HPO added As above, but with 20 μM 4-HPO added 1–100 μM NNK, 10-min incubation, 0.25 mg/mL microsomal protein. 1–10 μM NNK, 10-min incubation, 0.50 mg/mL microsomal protein. As above, but animals were treated with PEITC (3 $\mu\text{mol/g}$ diet).	Nunes <i>et al.</i> (1998)	
	HPB	100 ± 7	18 ± 4	5.6 ± 1.3			
	Keto aldehyde ^d	213 ± 41	23 ± 12	9.3 ± 5.2			
	HPB ^d	77 ± 13	17 ± 8	4.5 ± 2.3			
	Keto aldehyde ^d	210 ± 16	24 ± 4	8.8 ± 1.6			
	HPB ^d	69 ± 11	17 ± 8	4.1 ± 2.0			
	Keto aldehyde ^d	170 ± 14	22 ± 5	7.7 ± 1.9			
	HPB ^d	71 ± 4	18 ± 3	3.9 ± 0.7			
	Keto aldehyde ^d	78 ± 1	22 ± 8	3.5 ± 1.3			
	HPB ^d	44 ± 5	18 ± 5	2.4 ± 0.7			
	Keto aldehyde	173 ± 6	19.1 ± 2	9.1 ± 0.7			Peterson <i>et al.</i>
	HPB	239 ± 11	73.8 ± 6.8	3.2 ± 0.3			(1991a)
	Keto aldehyde	132 ± 11	5.5 ± 0.3	24 ± 2			Smith <i>et al.</i> (1993)
	HPB	60.4 ± 3.1	5.1 ± 0.2	11.8 ± 0.8			
NNK-N-oxide	8.0 ± 0.6	8.8 ± 0.5	0.91 ± 0.09				
Keto aldehyde	77.0 ± 9.3	5.4 ± 0.4	14.3 ± 2.0				
HPB	39.3 ± 2.5	5.3 ± 0.3	7.4 ± 0.6				
NNK-N-oxide	5.6 ± 0.7	9.1 ± 0.3	0.62 ± 0.08				

Adapted from Jalas *et al.* (2005)

HPB, 4-hydroxy-1-(3-pyridyl)-1-butanone; 4-HPO, 4-hydroxy-1-phenyl-1-octanone; K_m , Michaelis constant; NNAL, 4-(methylnitrosamino)-1-(3-pyridyl)-1-butanol; NNK, 4-(Methylnitrosamino)-1-(3-pyridyl)-1-butanone; PEITC, phenethyl isothiocyanate; V_{\max} , maximum velocity

^a Units are pmol/mg/min.

^b Units are pmol/mg/min/ μM .

^c NNK concentrations up to 1000 μM were used to determine kinetic parameters for NNAL formation.

^d Values are V_{\max}' , K_m' , and V_{\max}'/K_m' , respectively, due to the presence of an inhibitor in the incubation mixtures.

determined (Hong *et al.*, 1992). In the absence of exogenous cytochrome b_5 , reconstituted CYPs 2A10/2A11 exhibited K_m values for NNK α -hydroxylation that were similar to those for human CYP2A13 (Table 12; Hong *et al.*, 1992; Su *et al.*, 2000; Zhang *et al.*, 2002). CYPs 2A10/2A11 exhibited lower K_m and higher V_{max}/K_m values for the keto aldehyde formation than those determined using CYP2G1 (Table 11; Hong *et al.*, 1992). Nicotine was a competitive inhibitor of CYP2A10/2A11-mediated NNK metabolism (Table 11; Hong *et al.*, 1992).

Rat

Studies in isolated perfused liver and lung demonstrated that, at a concentration of 35 nM, NNK was rapidly eliminated (Schrader *et al.*, 1998). The clearance was almost exclusively mediated by metabolism. The kinetics of NNK metabolism in the liver was substantially faster than that in the lung but, on a per gram basis, lung clearance was faster. Products of α -hydroxylation were the major metabolites in the liver and NNK-*N*-oxide was the major metabolite in the lung, followed by α -hydroxylation products. Studies in rat lung and liver cells gave similar results and indicated a correlation between metabolite profiles in lung cells and urinary metabolites obtained after treatment of rats with NNK and modifiers (Schneider *et al.*, 1999). A study of NNK metabolism in rat alveolar type II cells demonstrated substantial metabolism by α -hydroxylation at low concentrations of NNK (50 nM), a concentration probably relevant to human exposure (Schrader *et al.*, 2000).

The kinetics of NNK metabolism have been studied extensively using microsomes prepared from Sprague-Dawley and Fischer rat lung, liver and nasal mucosa (Table 13). In rat lung, NNK-*N*-oxide is the major NNK metabolite, followed by HPB, NNAL and the keto aldehyde (Hecht, 1998). K_m values for HPB and NNK-*N*-oxide formation were similar to those in patas monkey lung (Table 13). The kinetic parameters of NNK metabolism in rat liver and the effects of various inducers of CYP on these parameters have been evaluated in several studies. The K_m values for the keto aldehyde and HPB formation by rat liver microsomes were higher than those in human or patas monkey liver microsomes (Table 13; Guo *et al.*, 1992; Patten *et al.*, 1996; Smith *et al.*, 1997). Treatment of rats with phenobarbital, which induces expression of CYP2B enzymes (Soucek & Gut, 1992; Whitlock & Denison, 1995), led to detectable levels of NNK-*N*-oxide and slightly increased the efficiency of POB and HPB formation (Table 13; Guo *et al.*, 1992). Treatment of rats with pregnenolone 16 α -carbonitrile, an inducer of CYP3A enzymes (Heuman *et al.*, 1982; Soucek & Gut, 1992; Whitlock & Denison, 1995), also led to enhanced efficiency of keto aldehyde and HPB formation, as well as to the formation of NNK-*N*-oxide (Table 13; Guo *et al.*, 1992).

Microsomes prepared from rat nasal mucosa are better catalysts of NNK bioactivation than any other microsomal system investigated to date (Table 13). The K_m values for HPB formation were comparable in rat lung and nasal mucosa, whereas the K_m for the keto aldehyde formation by rat nasal mucosal microsomes was threefold lower than that in lung microsomes (Table 13). The much higher catalytic efficiency of NNK metabolism in rat nasal mucosal microsomes than lung or liver was clearly due to the larger V_{max} values in

the nasal mucosa (Table 13). These data are consistent with a role for CYP2A3 (discussed below) as an important catalyst of NNK α -hydroxylation in lung and nasal mucosa.

The kinetic parameters for NNK metabolism by rat CYPs have been studied only for two enzymes — CYP2A3 and 2B1 (Table 12; Guo *et al.*, 1991a; J alas *et al.*, 2003a). CYP2A3 is expressed in both the nasal mucosa and lung, but not the liver (Su *et al.*, 1996). Both protein and mRNA levels are much greater in the nasal mucosa than in the lung (Su *et al.*, 1996; Gopalakrishnan *et al.*, 1999). CYP2A3 catalyses α -hydroxylation of NNK much more efficiently than CYP2B1. A comparison of the primary sequence of rat and human CYP2A enzymes showed that rat CYP2A3 was 85 and 87% identical to human CYPs 2A6 and 2A13, respectively. CYP2A3 catalyses NNK metabolism with an efficiency similar to that of human CYP2A13 (Honkakoski & Negishi, 1997; J alas *et al.*, 2003a). The high catalytic efficiency of CYP2A3 for NNK α -hydroxylation most probably plays a role in the carcinogenicity of NNK to the rat lung and nasal mucosa (J alas *et al.*, 2005).

CYP2B1 also catalyses the α -hydroxylation of NNK, but with much higher K_m and lower V_{max} values than CYP2A3 (Table 11; Guo *et al.*, 1991a). CYP2B1, unlike CYP2A3, also catalyses NNK-*N*-oxide formation (Table 11; Guo *et al.*, 1991a). Rat CYP2B1 and CYP2C6, together with human CYP2C8, are the only CYP enzymes reported to catalyse the *N*-oxidation of NNK (Guo *et al.*, 1991a; Smith *et al.*, 1992a; Lacroix *et al.*, 1993; J alas *et al.*, 2005). Because NNK-*N*-oxide formation represents quantitatively the major CYP-catalysed pathway of NNK metabolism in the rat lung, studies have examined the enzyme(s) responsible for this reaction (Smith *et al.*, 1992b). Anti-2B1 antibodies do not inhibit the formation of this metabolite by rat lung microsomes (Smith *et al.*, 1992b). Furthermore, phenobarbital treatment of rats induced the formation of NNK-*N*-oxide catalysed by rat liver microsomes (Table 13), but did not significantly enhance the rate of formation of this metabolite catalysed by rat lung microsomes (Guo *et al.*, 1992).

Kinetic parameters for NNK metabolism for rat CYPs 1A1, 1A2, and 2C6 are also presented in Table 11 (J alas *et al.*, 2005). Rat CYP1A1, similarly to human CYP1A1 (with which it shares 78% primary sequence identity; Soucek & Gut, 1992) preferentially catalyses keto aldehyde formation, but with much lower K_m values (Table 11; Smith *et al.*, 1995; J alas *et al.*, 2005). The V_{max}/K_m values for keto aldehyde formation were an order of magnitude higher for the rat enzyme compared with the human enzyme, but these values were similar for HPB formation (Table 11; Smith *et al.*, 1995; J alas *et al.*, 2005). In contrast to rat CYP1A1, rat CYP1A2 does not exhibit the regioselectivity observed with the orthologous human enzyme (primary sequence identity, 70%; Soucek & Gut, 1992) (Table 11; Smith *et al.*, 1992a, 1996; J alas *et al.*, 2005).

Rat CYP2C6, similarly to rat CYP2B1 and human CYP2C8, catalyses the *N*-oxidation in addition to α -hydroxylation of NNK (Table 11; Guo *et al.*, 1991a; Smith *et al.*, 1992b; Lacroix *et al.*, 1993; J alas *et al.*, 2005). The K_m values for CYP2C6 were much higher than those for CYP2B1, but higher V_{max} values led to V_{max}/K_m values that were similar between the two enzymes (except in the case of HPB formation) (Table 11; Guo *et al.*, 1991a; J alas *et al.*, 2005). Rat CYP2C6 catalyses HPB formation about 10-fold more efficiently than

CYP2B1 (Table 11; Guo *et al.*, 1991a; Jalas *et al.*, 2005). Rat CYPs 2D1, 2D2, 3A1 and 3A2 do not metabolize NNK (Jalas *et al.*, 2005).

Mouse

Lung microsomes from female A/J mice have been used by several laboratories to determine the kinetic parameters of NNK metabolism (Table 13). The reported K_m values were consistently in the 1–10 μM range for keto aldehyde, HPB and NNK-*N*-oxide (Smith *et al.*, 1990; Peterson *et al.*, 1991a; Smith *et al.*, 1993; Jalas *et al.*, 2003b). Similarly to results with rat lung microsomes, NNK-*N*-oxide was the major metabolite (Table 13). In female A/J mouse liver microsomes, NNK was converted to keto aldehyde, HPB and NNK-*N*-oxide (Table 13). The K_m values were similar in mouse lung and liver microsomes, but the V_{\max} values were generally higher for liver microsome-mediated formation of keto aldehyde and HPB (Table 13).

Kinetic parameters for NNK metabolism have been determined for mouse CYPs 2A4 and 2A5 (Felicia *et al.*, 2000; Jalas *et al.*, 2003b). CYP2A4 and CYP2A5 are more than 90% identical to human CYPs 2A6 and 2A13 and are expressed in many mouse tissues, including the liver and lung (Honkakoski & Negishi, 1997). These two mouse CYP2A enzymes differ in primary sequence by only 11 amino acids (of 494), but exhibit strikingly different substrate specificities (Lindberg & Negishi, 1989; Honkakoski & Negishi, 1997). Mutation of only one amino acid residue (Phe 209) in CYP2A5 to the corresponding residue in CYP2A4 (Leu 209) is sufficient to convert the substrate specificity of CYP2A5 to that of a 2A4-like enzyme (Lindberg & Negishi, 1989). Investigation of the kinetic parameters of NNK metabolism by these two highly similar CYPs revealed significant differences in their ability to catalyse NNK α -hydroxylation (Table 11; Felicia *et al.*, 2000). CYP2A5 exhibits a much lower K_m value and preferentially hydroxylates the α -methyl carbon of NNK, whereas CYP2A4 exhibits a much higher K_m value and preferentially catalyses the α -methylene hydroxylation of NNK (Table 11; Felicia *et al.*, 2000; Jalas *et al.*, 2003b). The K_m value for CYP2A5-mediated α -methyl hydroxylation of NNK is the lowest among those of the CYPs listed in Table 11.

Hamster

Kinetic parameters for NNK metabolism were determined in tissue slices from the lung, liver and kidney of female Syrian golden hamsters (Richter *et al.*, 2000). High and low K_m and V_{\max} values were observed in the lung and liver for the formation of most NNK metabolites including hydroxy acid, keto acid, HPB, diol, NNK-*N*-oxide, NNAL-*N*-oxide and NNAL. K_m values ranged from 0.04 to 1952 μM . In the lung, α -hydroxylation accounted for 13–31% of metabolism. The liver showed the highest capacity for NNK metabolism, and α -hydroxylation accounted for 12–25% of the metabolites. The kidney showed a low capacity for NNK metabolism with α -hydroxylation accounting for < 3% of the metabolites. Conversion of NNK to NNAL was greatest in the kidney, followed by the liver and lung.

Summary

In the species that have been studied, a number of CYP2A enzymes are excellent catalysts of NNK α -hydroxylation, but more research is needed to clarify the contribution of individual CYPs to microsome-mediated NNK metabolism in animals. The K_m values for NNK α -hydroxylation in patas monkey lung and liver microsomes are consistent with the involvement of a CYP2A13 orthologue, but further study is required. The K_m values observed using rat lung microsomes are consistent with the involvement of CYP2A3 which is closely related to human CYP2A13 or mouse CYP2A5. The rat liver does not express a CYP2A6 or 2A13 orthologue (Honkakoski & Negishi, 1997; Gopalakrishnan *et al.*, 1999) and the K_m values for NNK metabolism by liver microsomes are consistent with the involvement of CYP2B1. Kinetic data on NNK metabolism by other rat CYPs is needed to assess better the involvement of individual enzymes in this species. The K_m values for NNK metabolism in mouse lung and liver microsomes are similar to those determined for CYP2A5. It seems probable that CYP2A5 plays a role in NNK bioactivation in mice; however, additional studies are needed to define better the contribution of CYP2A5 in both the lung and liver. Table 14 summarizes K_m values and regioselectivity in NNK metabolism for both laboratory animal and human CYPs.

In-vitro studies of NNAL metabolism

Rat liver microsomes convert NNAL to lactol and hydroxy acid (products of α -methylene hydroxylation), to diol and pyridylTHF (products of α -methyl hydroxylation), as well as to NNAL-*N*-oxide, NNAL(ADP)⁺ and NNK (Peterson *et al.*, 1994; Staretz *et al.*, 1997b; Upadhyaya *et al.*, 2000). In rat pancreatic microsomes, only NNAL(ADP)⁺ was observed (Peterson *et al.*, 1994). Rat liver microsomes and co-factors convert NNAL predominantly to (*R*)-NNAL-*O*-Gluc; the uridine diphospho (UDP)-glucuronosyl transferase, UGT2B1, is an important catalyst of this reaction (Ren *et al.*, 1999).

Kinetic parameters for NNAL metabolism catalysed by microsomes have only been reported for A/J mouse lung microsomes (Table 15). K_m values for NNAL and NNK metabolism were similar (Tables 13 and 15), but V_{max} values for NNAL were almost an order of magnitude lower. Thus, *in vivo*, metabolic activation of NNAL may be a less important source of DNA-reactive electrophiles than metabolic activation of NNK.

NNAL-*N*-oxide was the major metabolite formed from (\pm)-, (*R*)- and (*S*)-NNAL in mouse lung microsomes (Table 15; Jalas & Hecht, 2003). NNAL-*N*-oxide was formed from (*S*)-NNAL at much greater maximal rates than from the other two substrates, but the K_m value was also higher for (*S*)-NNAL; this resulted in relatively similar V_{max}/K_m values for NNAL-*N*-oxide formation among all three substrates (Table 15; Jalas & Hecht, 2003).

Kinetic parameters for NNAL metabolism have also been determined with hamster liver, lung and kidney tissue slices (Richter *et al.*, 2000). NNAL was converted to hydroxy acid, NNAL-*N*-oxide and NNK in all three tissue preparations, as well as to NNK-*N*-oxide in the liver and to diol in the lung (Richter *et al.*, 2000). K_m values for these metabolites ranged from 1.6 μ M for NNK formation in the lung to 1624 μ M for NNAL-*N*-oxide formation in the same tissue (Richter *et al.*, 2000).

Table 14. Summary of K_m values and regioselectivity for cytochrome P450-mediated NNK metabolism

Metabolic pathway	Low K_m (< 50 μ M)	Intermediate K_m (50–500 μ M)	High K_m (> 500 μ M)	Regioselectivity
α -Methylene hydroxylation	Human 2A13 Rabbit 2A10/2A11 Rat 2A3 Mouse 2A5	Human 2A6 Rabbit 2G1 Rat 1A1 Rat 1A2 Rat 2B1 Mouse 2A4	Human 1A1 Human 1A2 Human 2D6 Human 2E1 Human 3A4 Rat 2C6	α -Methylene > α -methyl Human 1A1 Human 2A13 Human 3A4 Rabbit 2G1 Rat 1A1
α -Methyl hydroxylation	Human 2B6 Human 2A13 Rabbit 2A10/2A11 Rat 2A3 Mouse 2A5	Human 1A1 Human 1A2 Human 2A6 Rat 1A1 Rat 1A2 Rat 2B1 Mouse 2A4	Human 2D6 Human 2E1 Human 3A4 Rat 2C6	α -Methylene \equiv α -methyl Human 2A6 Rabbit 2A10/2A11 Rat 1A2 Rat 2A3
N-Oxidation		Rat 2B1	Rat 2C6	α -Methylene < α -methyl Human 1A2 Human 2B6 Human 2D6 Human 2E1 Rat 2B1 Rat 2C6 Mouse 2A5

Adapted from Jalas *et al.* (2005) K_m , Michaelis constant

Table 15. Apparent steady-state kinetic parameters for A/J mouse lung microsomal-mediated metabolism of NNAL

Substrate	Metabolite	Kinetic parameters			Experimental conditions	Reference
		V_{\max}^a	K_m (μM)	V_{\max}/K_m^b		
(±)-NNAL	Lactol	6.6 ± 0.3	5.7 ± 0.9	1.2 ± 0.2	0.25–50 μM NNAL; 45-min incubation; 0.3 mg/mL microsomal protein.	Jalas & Hecht (2003)
	Diol	6.0 ± 0.3	3.7 ± 0.7	1.6 ± 0.3		
	NNAL- <i>N</i> -oxide	20 ± 0.4	2.2 ± 0.2	9.1 ± 0.8		
(R)-NNAL	Lactol	6.5 ± 0.4	5.7 ± 1	1.1 ± 0.2		
	Diol	5.8 ± 0.3	5.0 ± 0.9	1.2 ± 0.2		
	NNAL- <i>N</i> -oxide	13 ± 0.4	2.0 ± 0.2	6.5 ± 0.7		
(S)-NNAL	Lactol	14 ± 0.8	9.9 ± 1.5	1.4 ± 0.2		
	Diol	15 ± 0.6	7.8 ± 1	1.9 ± 0.3		
	NNAL- <i>N</i> -oxide	103 ± 2	9.4 ± 0.5	11 ± 0.6		

K_m , Michaelis constant; NNAL, 4-(methylnitrosamino)-1-(3-pyridyl)-1-butanol; V_{\max} , maximum velocity

^a Units are pmol/mg/min.

^b Units are pmol/mg/min/ μM .

The kinetic parameters for CYP-mediated NNAL metabolism have been reported only for three enzymes — mouse CYP2A5, rat CYP2A3 and human CYP2A13 (Table 16; J alas & Hecht, 2003; J alas *et al.*, 2003a). Similarly to results with mouse lung microsomes, the K_m values for CYP2A5-mediated NNAL metabolism were similar to those for CYP2A5-mediated NNK metabolism and were largely independent of substrate stereochemistry (Tables 11 and 16). In contrast, the V_{max} values were generally more than an order of magnitude lower for the NNAL substrates (Tables 12 and 16). Thus, NNK is clearly a much better substrate for CYP2A5 than NNAL (or the individual enantiomers) (Tables 11 and 16). Rat CYP2A3 metabolizes NNAL with an efficiency similar to mouse CYP2A5 and human CYP2A13, but the K_m values are slightly higher for the human enzyme (Table 16; J alas *et al.*, 2003a).

In-vivo studies of NNK metabolism

The literature on in-vivo studies of NNK metabolism has been reviewed comprehensively (Hecht, 1998). Only selected studies are discussed below.

Monkey

Intravenous injection of NNK into patas monkeys resulted in rapid and extensive metabolism by α -hydroxylation and the formation of keto acid and hydroxy acid (Hecht *et al.*, 1993b). These metabolites accounted for a relatively large proportion of serum and urinary metabolites at all time-points. The other major metabolic pathway was reduction to NNAL, which was detected both unconjugated and as NNAL-*O*-Gluc, of which (*S*)-NNAL-*O*-Gluc predominated. NNAL-*O*-Gluc accounted for 15–20% of the urinary metabolites in monkeys given 0.1 $\mu\text{g}/\text{kg}$ bw NNK, a dose similar to that of a smoker. Pharmacokinetic parameters for NNK metabolism were similar to those observed in baboons, which indicates rapid metabolism of NNK in primates (Adams *et al.*, 1985a). A comparison of pharmacokinetic parameters in rats, mice and hamsters showed that clearance of NNK varied predictably with body weight, similar to observations with NDMA, which implies that common phenomena govern the pharmacokinetics of these nitrosamines (Hecht *et al.*, 1993b).

Rat

Studies of the metabolism of NNK in rats consistently demonstrate rapid and extensive conversion of NNK to products of α -hydroxylation, pyridine-*N*-oxidation and carbonyl reduction. Less than 1% of the dose is excreted unchanged in the urine. Rapid metabolism of NNK is observed in all tissues examined; the highest amounts of α -hydroxylation are observed in the nasal mucosa, liver and lung, which are target tissues of NNK carcinogenesis (reviewed in Hecht, 1998).

The pharmacokinetics and metabolism of NNK (8.4 $\mu\text{mol}/\text{kg}$ bw intravenously) were studied in bile duct-cannulated Fischer 344 rats (Wu *et al.*, 2002). After 24 h, approximately 85% of NNK was recovered (17.5% from bile and 67.6% from urine), which is consistent with previous studies (Schulze *et al.*, 1992; Hecht, 1998). Pharmacokinetic

Table 16. Steady-state kinetic parameters for human cytochrome P450 (CYP) 2A13-, rat CYP2A3- and mouse CYP2A5-mediated metabolism of NNAL

Species/ enzyme	Substrate	Metabolite	Kinetic parameters			Expression system	Reference
			V_{\max}^a	K_m (μM)	V_{\max}/K_m^b		
Human CYP2A13	(±)-NNAL	Lactol	1.50 ± 0.05	36 ± 3	0.042 ± 0.004	Baculovirus- infected Sf9 cells	Jalas <i>et al.</i> (2003a)
		Diol	0.79 ± 0.02	40 ± 3	0.020 ± 0.002		
		NNAL- <i>N</i> -oxide	0.12 ± 0.01	30 ± 7	0.0040 ± 0.0010		
Rat CYP2A3	(±)-NNAL	Lactol	0.41 ± 0.01	3.8 ± 0.5	0.11 ± 0.01		
		Diol	0.98 ± 0.02	16 ± 1	0.061 ± 0.004		
		NNAL- <i>N</i> -oxide	0.046 ± 0.003	2.6 ± 0.7	0.018 ± 0.005		
Mouse CYP2A5	(±)-NNAL	Lactol	0.55 ± 0.02	1.7 ± 0.3	0.32 ± 0.06	Baculovirus- infected Sf9 cells	Jalas & Hecht (2003)
		Diol	0.47 ± 0.01	5.1 ± 0.5	0.092 ± 0.009		
		NNAL- <i>N</i> -oxide	0.17 ± 0.01	4.7 ± 1.1	0.036 ± 0.009		
		NNK	0.78 ± 0.04	14 ± 1.8	0.056 ± 0.008		
	(R)-NNAL	Lactol	0.42 ± 0.02	2.1 ± 0.5	0.20 ± 0.05		
		Diol	1.2 ± 0.03	11 ± 0.8	0.11 ± 0.008		
		NNAL- <i>N</i> -oxide	ND				
		NNK	0.31 ± 0.03	16 ± 3.9	0.019 ± 0.005		
	(S)-NNAL	Lactol	0.45 ± 0.03	0.78 ± 0.26	0.58 ± 0.22		
		Diol	0.17 ± 0.01	1.3 ± 0.4	0.13 ± 0.04		
		NNAL- <i>N</i> -oxide	0.16 ± 0.01	1.1 ± 0.4	0.15 ± 0.05		
		NNK	0.78 ± 0.03	4.2 ± 0.6	0.19 ± 0.03		

K_m , Michaelis constant; ND, not detected; NNAL, 4-(methylnitrosamino)-1-(3-pyridyl)-1-butanol; NNK, 4-(Methylnitrosamino)-1-(3-pyridyl)-1-butanone; Sf9, *Spodoptera frugiperda*; V_{\max} , maximum velocity

^a Units are pmol/min/pmol CYP.

^b Units are pmol/min/pmol CYP/ μM .

analysis indicated that NNK had a short urinary half-life (2.6 h), a large volume of distribution (321 ± 137 mL) and a total body clearance of 12.8 ± 2.0 mL/min. (*R*)-NNAL-Gluc was the major metabolite in bile and represented approximately 14% of the total NNK dose. Nearly all NNAL-Gluc were excreted as the (*R*)-diastereomer. The major metabolite in urine was keto acid (26% of the dose). Urinary excretion of NNAL and hydroxy acid comprised about 30% of the dose. Metabolism of NNK to (*S*)-NNAL appeared to favour α -hydroxylation of (*S*)-NNAL and stereoselective localization in the lung while metabolism of NNK to (*R*)-NNAL appeared to lead to detoxification through glucuronidation and biliary excretion (Wu *et al.*, 2002).

In a study designed to probe the effects of nicotine on NNK metabolism, Holzman rats received acute (36 h) or chronic (2 week) subcutaneous infusions of nicotine at rates that produced serum nicotine concentrations that were two to three times the venous nicotine concentrations usually measured in smokers (Keyler *et al.*, 2003). A single intraperitoneal dose of NNK (39 nmol/kg bw) was administered 24 h before the end of each infusion. Neither acute nor chronic nicotine infusion had any effect on the extent of NNK metabolism by α -hydroxylation; some small effects on pyridine-*N*-oxidation were observed. The results indicate that nicotine infusion has no effect on the carcinogenic pathways of NNK metabolism in the rat.

Mouse

A/J mice treated intraperitoneally with NNK (0.005–500 μ mol/kg bw) excreted hydroxy acid (18–37% of urinary metabolites), keto acid (11–27%), (*R*)-NNAL-*O*-Gluc (ND–22%), NNAL-*N*-oxide (6–14%), NNK-*N*-oxide (ND–10%), NNAL (ND–29%) and 6-hydroxy-NNK (1%) in the 48-h urine, similar to results obtained in rats (Morse *et al.*, 1990b; Desai *et al.*, 1993; Hecht, 1998). At lower doses of NNK, levels of α -hydroxylation products increased while the levels of NNAL and NNAL-*O*-Gluc decreased. NNAL glucuronidation is quantitatively an unimportant metabolic pathway at low doses of NNK (Morse *et al.*, 1990b).

Following a 2-h nose-only exposure to mainstream cigarette smoke, mice were administered NNK intraperitoneally (7.5 μ mol). Control mice were sham-exposed and treated with the same dose of NNK (Brown *et al.*, 2001a). The pattern of urinary metabolites was affected by smoke exposure. Mice exposed to smoke excreted 25% more NNAL, 15% less hydroxy acid and 42% less keto acid than control mice. Other metabolites (NNAL-Gluc and NNAL-*N*-oxide) were not affected. These results indicate that mainstream cigarette smoke causes a shift in metabolism which leads to lesser α -hydroxylation and greater excretion of NNAL.

Hamster

As in rats and mice, NNK is extensively metabolized by α -hydroxylation and other pathways in Syrian golden hamsters (Hecht, 1998). Female Syrian golden hamsters treated subcutaneously with NNK (80 nmol/kg) excreted 96% of the dose as urinary metabolites within 24 h of treatment (Richter & Tricker, 2002). α -Hydroxylation to keto acid (30.7% of

radioactivity in urine) and hydroxy acid (22.3%), and detoxification to NNAL-*N*-oxide (24.2%) accounted for almost 80% of the NNK metabolites in the 24-h urine. Smaller amounts of diol, HPB, NNAL-*O*-Gluc, NNK-*N*-oxide and NNAL were observed. Concurrent treatment with nicotine, cotinine or 2-phenethyl isothiocyanate (PEITC) decreased total α -hydroxylation from 58.1% (control) to 49.6% (nicotine), 41.2% (cotinine) and 54.6% (PEITC), with concomitant increases in NNAL (Richter & Tricker, 2002).

In-vivo studies of NNAL metabolism

Earlier studies demonstrate that the NNK/NNAL equilibrium favours NNAL in rodents and primates, and report some pharmacokinetic parameters for NNAL metabolism. Conversion of (*R*)-NNAL-*O*-Gluc to metabolites of NNAL and NNK was also observed (reviewed in Hecht, 1998).

Rat

Male Fischer 344 rats were treated intravenously with racemic [5-³H] NNAL (8.5 μ mol/kg) (Wu *et al.*, 2002). After 24 h, 43% of the dose was recovered from urine and 20% from bile. Urinary elimination half-lives were 9.5 h for NNAL, 7.8 h for hydroxy acid and 8 h for keto acid. Total body clearance of NNAL was 8.65 ± 2.6 mL/min and volume of distribution was 2772 ± 1423 mL. (*R*)-NNAL-Gluc was the major metabolite in bile and accounted for 16% of the NNAL dose. The urinary excretion profile following NNAL administration was similar to that of NNK except that less keto acid was excreted. Enantiomeric ratios for NNAL were evaluated in plasma, urine and bile. (*R*)-NNAL was the predominant form excreted. In the lung, 1 h after administration of racemic NNAL, 49% of the total metabolites was NNAL, with lesser amounts of NNAL-*N*-oxide (19%), hydroxy acid (10%) and keto acid (7%). NNAL levels in the liver were comparable with those in the lung; significant amounts of (*R*)-NNAL-Gluc and hydroxy acid were also observed. NNK was also identified in the lung and liver samples. Four hours after administration, NNAL remained the most abundant metabolite in the lung, but lower amounts were found in the liver and kidney. Enantiomeric ratios demonstrated that (*S*)-NNAL predominated in the lung and liver 4 h after administration. At 24 h after administration, the (*S*):(*R*) ratio was 57 in the lung, 1.2 in the liver and 3.4 in the kidney. NNAL made up 75% of total metabolites in the lung 24 h after administration. Collectively, the results demonstrated stereoselective excretion of (*R*)-NNAL-*O*-Gluc and retention of (*S*)-NNAL in the rat lung (Wu *et al.*, 2002).

Male Fischer 344 rats were treated intravenously with [5-³H] (*R*)-NNAL (0.11–0.65 mg/kg) or (*S*)-NNAL (0.198–1.07 mg/kg) (Zimmerman *et al.*, 2004). After 24 h, 65% of the dose of (*S*)-NNAL was recovered (15% from the bile and 48% from urine), while almost 90% of the (*R*)-NNAL dose was recovered (44% from the bile and 45% from urine). Thus, excretion of (*S*)-NNAL was substantially less than that of (*R*)-NNAL, principally due to the difference in biliary excretion of (*R*)-NNAL-Gluc. The volume of distribution of (*S*)-NNAL (1792 ± 570 mL) was significantly greater than that of (*R*)-NNAL (645 ± 230 mL). Urinary elimination half-lives of metabolites were significantly shorter

after administration of (*R*)-NNAL (4.2 h) than after that of (*S*)-NNAL (6.3 h). Urinary metabolite profiles of the two enantiomers were markedly different. For (*R*)-NNAL, major metabolites consisted largely of unchanged NNAL, hydroxy acid and (*R*)-NNAL-Gluc. For (*S*)-NNAL, more keto acid and less hydroxy acid, more NNK-*N*-oxide and less NNAL were formed than in the case of (*R*)-NNAL; NNK was also observed. Tissue retention of metabolites demonstrated that a larger proportion of the dose was retained in the liver, lung and kidney 24 h after administration of (*S*)-NNAL compared with (*R*)-NNAL. There was significant and rapid conversion of (*S*)-NNAL to NNK in the tissues. At 24 h after administration of (*S*)-NNAL, 78% of lung metabolites was NNAL, with an (*S*):(*R*) ratio of 4.2, a shift from a ratio of 1.1 at 1 h after dosing, which indicated selective retention of (*S*)-NNAL in the lung. At 24 h after administration of (*R*)-NNAL, no quantifiable metabolites were found in the lung. These results demonstrate that (*R*)-NNAL, the less carcinogenic NNAL enantiomer (in mice), is excreted more rapidly than (*S*)-NNAL, while (*S*)-NNAL is selectively retained in the lung and is extensively converted to NNK.

Mouse

Racemic and enantiomeric NNAL as well as (*R*)-NNAL-Gluc (20 μ mol) were administered intraperitoneally to female A/J mice and urine was collected (Upadhyaya *et al.*, 1999). The metabolites of racemic NNAL were hydroxy acid (10% of the dose), NNAL-*N*-oxide (3.1%), NNAL (20%) and (*S*)-NNAL-Gluc (16%). The profile of metabolites from the enantiomers was quite similar to that of racemic NNAL, except that (*S*)-NNAL was metabolized less effectively to (*R*)-NNAL-Gluc than (*R*)-NNAL. The formation of (*S*)-NNAL-Gluc from (*R*)-NNAL indicates that (*R*)-NNAL was converted to NNK *in vivo*. Minor amounts of urinary metabolites other than (*S*)-NNAL-Gluc were detected when (*S*)-NNAL-Gluc was administered to mice.

Haemoglobin adducts of NNK and NNAL

Adducts with globin are formed in rats by both the α -methylene and α -methyl hydroxylation pathways of NNK (Carmella & Hecht, 1987; Hecht, 1998). Depending on dose, species and protocol employed, approximately 15–40% of the pyridyloxobutyl adducts are released as HPB upon mild base hydrolysis (Carmella & Hecht, 1987; Murphy *et al.*, 1990a; Peterson *et al.*, 1990; Murphy & Coletta, 1993). The HPB-releasing adducts are esters, most probably with aspartate, glutamate or the terminal carboxy groups of globin (Carmella *et al.*, 1992). Pyridyloxobutyl cysteine adducts do not appear to be formed in measurable amounts in rats (Carmella *et al.*, 1990b). Co-incubation of rat hepatocytes and human red blood cells results in the formation of HPB-releasing adducts, as seen *in vivo* (Murphy & Coletta, 1993). Therefore, α -HOMeNNK or its glucuronide are sufficiently stable to migrate out of the hepatocyte and into the red blood cell. Human red blood cells alone can activate NNK but not to HPB-releasing adducts (Murphy & Coletta, 1993). In rats, both methyl and pyridyloxobutyl haemoglobin adducts increase linearly with the dose over a more than 3000-fold range (Murphy *et al.*, 1990a). DNA adducts in the liver and lung also increase over this range but the relationship with dose is non-linear.

The utility of HPB-releasing haemoglobin adducts as a biomarker of the overall carcinogenic effect of NNK was demonstrated in studies in which treatment of rats with PEITC or 6-phenylhexyl isothiocyanate resulted in a significant decrease in HPB-releasing adducts over an 18-month period compared with rats treated with NNK only; concurrently, a significant decrease in lung tumour induction was observed in the rats treated with isothiocyanates and NNK (Hecht *et al.*, 1996a,b). In rats treated with a mixture of benzo[*a*]-pyrene (2 ppm in diet; 2 mg/kg) and NNK (2 ppm in drinking-water; 2 µg/mL), HPB-releasing haemoglobin adducts were significantly inhibited by concurrent treatment with dietary PEITC, or a mixture of PEITC and benzyl isothiocyanate, but not with benzyl isothiocyanate alone. Concurrently with the inhibition of HPB-releasing haemoglobin adducts, a decrease in HPB-releasing DNA adducts was observed in the rat lung, but not in the liver, as was an increase in the levels of NNAL and NNAL-Gluc excreted in urine (Boysen *et al.*, 2003). HPB-releasing haemoglobin adducts are also formed upon treatment of rats with NNAL (Hecht & Trushin, 1988).

DNA adducts of NNK and NNAL

In experimental systems, DNA adducts have been measured by high-performance liquid chromatography–radioflow detection after administration of [³H]-labelled compounds, or by gas chromatography–mass spectrometry of released HPB. The latter technique has also been used in human studies (see Section 4.1.1(a)(iii)).

Studies of DNA adduct formation by NNK and NNAL have been extensively reviewed (Hecht, 1998). Highlights and recent studies are presented below.

In-vitro studies

All data indicate that there are two major types of NNK–DNA adducts: methyl adducts formed by α -methylene hydroxylation and pyridyloxobutyl adducts formed by α -methyl hydroxylation. Adduct formation is summarized in Figures 2 and 5. α -Methylene hydroxylation of NNK leads to the formation of Me-DZH and/or the methyl diazonium ion, which react with DNA to form 7-MedGuo, *O*⁶-MedGuo and *O*⁴-MedThd. Other adducts are probably also produced, based on studies of other methylating nitrosamines and nitroso-ureas (Singer & Grunberger, 1983). DNA methylation by NNK is observed in a number of in-vitro studies with different systems that are capable of activating its metabolism, including rat lung cells and lung, liver or nasal mucosal microsomes (with added DNA), rat oral tissue and hamster lung (Devereux *et al.*, 1988; Rossignol *et al.*, 1989; Murphy *et al.*, 1990a; Guo *et al.*, 1991b; Hecht, 1998).

The chemistry of the intermediates that result from α -methyl hydroxylation of NNK has been studied in detail. Since α -HOMeNNK (Figure 2) is not very stable, this metabolite has been generated *in situ* by solvolysis of 4-(acetoxymethylnitrosamino)-1-(3-pyridyl)-1-butanone (NNKOAc) and 4-(carbethoxynitrosamino)-1-(3-pyridyl)-1-butanone. Extensive studies conclusively demonstrate that the major DNA adducts formed by this pathway *in vitro* and *in vivo*, which account for at least 50% of the DNA binding, release HPB (Figure 3) upon acid or neutral thermal hydrolysis (Hecht & Trushin, 1988;

Hecht *et al.*, 1988b; Spratt *et al.*, 1989; Murphy *et al.*, 1990a; Peterson *et al.*, 1990; Peterson & Hecht, 1991; Foiles *et al.*, 1992; Trushin *et al.*, 1994; Staretz *et al.*, 1997c; Hecht, 1998). These adducts are produced via POB-DZH but not by HPB itself (Hecht *et al.*, 1988). The HPB-releasing adducts have different stabilities in DNA, and are released in a triphasic manner (Peterson *et al.*, 1991b). Adducts that release HPB upon neutral thermal hydrolysis have recently been identified as 7(POB-1-yl)dGuo and O^2 (POB-1-yl)dCyd (Wang *et al.*, 2003; Hecht *et al.*, 2004c). Other adducts formed by this pathway that have been identified are shown in Figures 2 and 5 (Haglund *et al.*, 2002; Wang *et al.*, 2003; Hecht *et al.*, 2004c). A similar group of adducts is formed upon methyl hydroxylation of NNAL (Figures 2 and 5; Upadhyaya *et al.*, 2003; Hecht *et al.*, 2004c).

Pyridyloxobutyl adducts inhibit O^6 -alkylguanine–DNA alkyltransferase (AGT), the enzyme responsible for the repair of O^6 -MedGuo. Since O^6 -MedGuo is also formed by metabolic activation of NNK, this phenomenon is probably important in the persistence of O^6 -MedGuo in NNK-exposed tissues (Peterson *et al.*, 1993).

In-vivo studies

Since O^6 -methylguanine (O^6 -MeGua) and 7-MeGua were first detected in the liver and lung of NNK-treated Fischer 344 rats (Castonguay *et al.*, 1984b), substantial research has been carried out on the occurrence and biological significance of methyl and pyridyloxobutyl adducts that result from the metabolic activation of NNK (Hecht, 1998).

Rat

Levels of 7-MeGua are 7.5–25 times higher than those of HPB released in the whole lung, depending on dose, with lower ratios at lower doses (Murphy *et al.*, 1990b). Levels of HPB-releasing adducts are about twice those of O^6 -MeGua, which are about 10 times greater than those of O^4 -MedThd (Belinsky *et al.*, 1986; Staretz *et al.*, 1997c). Consistently, the highest levels of O^6 -MeGua and HPB-releasing adducts are found in Clara cells of the rat lung, with lower amounts in type II cells, macrophages and small cells (Belinsky *et al.*, 1987a; Belinsky *et al.*, 1988; Devereux *et al.*, 1988; Staretz *et al.*, 1997c). The dose–response relationship for adduct formation in whole lung and lung cell types is non-linear. Adduct levels at the lowest doses are higher than would be expected by linear extrapolation from higher doses, e.g. efficiency of alkylation increases considerably at low doses (Belinsky *et al.*, 1987a; Devereux *et al.*, 1988; Belinsky *et al.*, 1990; Murphy *et al.*, 1990b; Staretz *et al.*, 1997c). One interpretation of these data is the presence of CYPs in the rat lung, such as CYP2A3, which efficiently catalyse α -hydroxylation at low concentrations of NNK. A second interpretation relates specifically to O^6 -MeGua. Pyridyloxobutyl adduct concentrations increase at low doses of NNK, which may lead to greater inhibition of AGT and consequent higher levels of O^6 -MeGua (Peterson *et al.*, 1993).

During chronic treatment with high doses of NNK, O^6 -MeGua increases consistently in the rat lung (Belinsky *et al.*, 1986). At lower doses over a 4-day period, O^6 -MeGua persists to a greater extent in Clara cells than in other cell types (Belinsky *et al.*, 1988). This is partly because of lower levels of AGT in Clara cells than in other cell types after treatment with

NNK. Treatment with NNK inhibits AGT, which is probably due to DNA pyridyloxobutylation. However, when NNK was administered over the full 20-week course to induce lung tumours in rats, *O*⁶-MeGua levels decreased by 82% in the Clara cells during the treatment period and were lower than those in the macrophages at 20 weeks (Staretz *et al.*, 1997c). The decrease is due to inhibition of CYP-catalysed α -methylene hydroxylation by NNK, as demonstrated in a study of α -methylene hydroxylation by isolated rat pulmonary microsomes after 20 weeks of treatment with NNK (Staretz *et al.*, 1997b).

Structure-activity studies suggest that both DNA methylation and pyridyloxobutylation are important in NNK-induced lung tumorigenesis in rats. Neither NDMA, which only methylates DNA, nor NNN, which pyridyloxobutylates but does not methylate DNA, is an effective lung carcinogen in rats (Hecht *et al.*, 1980a; Hoffmann *et al.*, 1984; Hecht *et al.*, 1986b). NNK yields greater amounts of *O*⁶-MeGua than NDMA in Clara cells, but not in alveolar type II cells, and is metabolized somewhat more effectively to a pyridyloxobutylating agent than NNN in rat lung cells (Devereux *et al.*, 1988; Belinsky *et al.*, 1989a). Such differences in binding and metabolism may partially account for the distinctly greater pulmonary carcinogenicity of NNK than that of NDMA or NNN. However, only NNK provides the combination of DNA methylation and pyridyloxobutylation that appears to be critical for rat lung tumorigenesis. NNK-induced rat lung tumours arise in type II cells (Belinsky *et al.*, 1990). Levels of HPB-releasing adducts in type II cells of NNK-treated rats correlate with lung tumour incidence over a range of doses, which suggests that pyridyloxobutylation is an important pathway (Staretz *et al.*, 1997c). Levels of *O*⁶-MeGua in Clara cells also correlate with lung tumour incidence over a wide dose range, which suggests some role of this adduct in spite of the fact that the Clara cell is probably not the cell of origin of the tumours (Belinsky *et al.*, 1990). The effects of PEITC on levels of HPB-releasing adducts in type II cells and other cell types of the lung correlate well with inhibition of NNK-induced lung tumorigenesis by PEITC, which provides further evidence for the importance of these adducts (Staretz *et al.*, 1997c). PEITC also inhibits *O*⁶-MeGua levels in Clara cells to the same extent that it inhibits lung tumorigenesis, but this is not seen in other cell types (Staretz *et al.*, 1997c). PEITC selectively inhibits HPB-releasing DNA adducts in the lung, but not in the liver of NNK-treated rats (Boysen *et al.*, 2003). Collectively, the available data indicate that HPB-releasing adducts and *O*⁶-MeGua are both important in lung tumour induction by NNK in rats.

Levels of DNA methylation in rat nasal mucosa are frequently higher than those in other tissues of NNK-treated animals (Belinsky *et al.*, 1986; Hecht *et al.*, 1986b; Belinsky *et al.*, 1987b). This is a consequence of the high NNK α -hydroxylation activity mediated by CYPs of the nasal mucosa. Although both α -methylene and α -methyl hydroxylation of NNK occur at similar rates in nasal mucosa microsomes (Smith *et al.*, 1992b), DNA methylation is greater than pyridyloxobutylation (Trushin *et al.*, 1994). These data indicate that, in rat nasal mucosa, α -HOMethyleneNNK is more effective as a DNA methylating agent than α -HOMeNNK is as a pyridyloxobutylating agent, possibly due to differences in the reactivity of the resulting alkylating agents, or to other factors such as glucuronidation of α -HOMeNNK (Hecht, 1998).

In spite of the relatively low levels of HPB-releasing adducts formed in rat nasal mucosa after treatment with NNK, these adducts appear to be important in tumour induction. NNK and NNN have similar carcinogenic activities toward the nasal mucosa, but NDMA has little activity (Hecht *et al.*, 1986b; Trushin *et al.*, 1994). NNK and NNN both pyridyloxobutylate nasal mucosa DNA to form HPB-releasing adducts (Trushin *et al.*, 1994). NNN does not methylate DNA whereas NDMA methylates but does not pyridyloxobutylate nasal DNA. These results support the role of DNA pyridyloxobutylation in rat nasal tumorigenesis. Studies with deuterated analogues of NNK further support this conclusion. Thus, [methylene-D₂]NNK is a stronger nasal carcinogen than either [methyl-D₃]NNK or NNK (Hecht *et al.*, 1987; Trushin *et al.*, 1994). Moreover, DNA pyridyloxobutylation by [methylene-D₂]NNK exceeds that by NNK while levels of *O*⁶-MedGuo from [methylene-D₂]NNK are significantly lower than those from NNK or [methyl-D₃]NNK (Trushin *et al.*, 1994). Collectively, these data provide strong support for the proposal that DNA pyridyloxobutylation is critical in rat nasal carcinogenesis by NNK (Hecht, 1998).

Levels of 7-MeGua are 13–49 times greater than those of HPB-releasing adducts in rat liver, and levels of the latter are generally greater than those of *O*⁶-MeGua (Murphy *et al.*, 1990b). The 7-MeGua:HPB-releasing adduct ratio at lower doses is lower in the liver than in the lung (Murphy *et al.*, 1990b). At low doses, levels of HPB-releasing adducts are lower in the liver than in the lung (Murphy *et al.*, 1990b; Boysen *et al.*, 2003). At high doses, the formation of 7-MeGua is saturated in the lung, but not in the liver, whereas the formation of HPB-releasing adducts is saturated in both tissues (Murphy *et al.*, 1990b). The higher levels of HPB-releasing adducts than of *O*⁶-MeGua are probably due to differences in repair (Belinsky *et al.*, 1986, 1990; Peterson *et al.*, 1991b). During chronic NNK treatment, *O*⁶-MeGua reaches a maximum in both hepatocytes and non-parenchymal cells, then declines rapidly due to induction of AGT (Belinsky *et al.*, 1986). The removal of HPB-releasing adducts from hepatic DNA appears to be slower than that of *O*⁶-MeGua (Belinsky *et al.*, 1986; Peterson *et al.*, 1991b).

Treatment of rats with a single dose of NNK or NNAL resulted in the formation of 7-MeGua and *O*⁶-MeGua (Hecht & Trushin, 1988). In hepatic DNA, levels of these adducts were similar 1–48 h after treatment with NNK or NNAL, while adduct levels in nasal mucosa and lung were somewhat higher after treatment with NNK than with NNAL. HPB-releasing adducts were formed with both NNK and NNAL in the liver; levels of the NNK-derived adducts were somewhat higher (Hecht & Trushin, 1998).

Mouse

Lung tumours are induced rapidly by a single dose of 10 µmol NNK in A/J mice (Hecht *et al.*, 1989). This model has been used extensively to examine mechanistic phenomena as well as the modifying effects of chemopreventive agents (Hecht, 1998). Levels of 7-MeGua are greater than those of *O*⁶-MeGua, which in turn exceed those of HPB-releasing adducts (Peterson & Hecht, 1991). Levels of 7-MeGua and *O*⁶-MeGua reached a maximum 4 h after injection of 10 µmol NNK, whereas the levels of released HPB were maximal after 24 h (Peterson & Hecht, 1991). Levels of 7-MeGua and released HPB

decrease with time, but *O*⁶-MeGua is persistent, such that its levels exceed those of 7-MeGua 15 days after treatment (Peterson & Hecht, 1991). Levels of *O*⁶-MedGua were highest in type II cells and Clara cells, followed by small cells and whole lung (Devereux *et al.*, 1993).

Persistent *O*⁶-MeGua is the critical determinant of lung tumour induction in A/J mice (Peterson & Hecht, 1991), but does not account for differences in sensitivity to NNK-induced lung tumorigenesis between A/J and C57BL/6 mice (Devereux *et al.*, 1993). In A/J mice, acetoxymethylmethylnitrosamine (AMMN), which can only methylate DNA, is highly tumorigenic whereas NNKOAc and NNN, which only pyridyloxobutylate DNA, are weakly active (Peterson & Hecht, 1991). [Methylene-D₂]NNK is significantly less tumorigenic than NNK or [methyl-D₃]NNK and also forms significantly less *O*⁶-MeGua (Hecht *et al.*, 1990). Similarly, (4*R*)[4D]NNK is significantly less tumorigenic than either NNK or (4*S*)[4D]NNK, and also leads to lower levels of persistent *O*⁶-MeGua (Jalas *et al.*, 2003b). There is an inflection in the dose–response curve for lung tumour induction by NNK in A/J mice, with an increase above a dose of 2–3 μmol NNK, at which persistent *O*⁶-MeGua begins to be measurable (Peterson & Hecht, 1991). Evidently, AGT activity is saturated above this dose. Levels of *O*⁶-MedGua measured 96 h after treatment of A/J mice correlate strongly with tumour multiplicity, independent of the source of the methylating agent, e.g. NNK, AMMN or AMMN plus NNKOAc (Peterson & Hecht, 1991). In addition, GC→AT transitions in codon 12 of the *K-ras* gene are observed in a high percentage of lung tumours induced by NNK in A/J mice (see Section 4.4.2(a)(ii)), consistent with the importance of *O*⁶-MeGua (Belinsky *et al.*, 1989b). Human methylguanin–DNA methyltransferase transgenic mice, which express high levels of AGT in the lung, were crossbred with A/J mice. Human AGT was expressed throughout the lung and, after treatment with NNK, these mice had lower levels of *O*⁶-MeGua, lower tumour multiplicity and size of tumours in the lung and a lower frequency of *K-ras* mutations in the lung tumours than non-transgenic mice (Liu *et al.*, 1999).

The pyridyloxobutylation pathway is important in increasing the activity of the methylation pathway in A/J mouse lung tumorigenesis since NNKOAc markedly increases the tumorigenicity of AMMN over a wide dose range (Peterson & Hecht, 1991). NNKOAc enhances the persistence of *O*⁶-MeGua in the lung of AMMN-treated mice due to the ability of HPB-releasing adducts to inhibit AGT (Peterson *et al.*, 1993; Liu *et al.*, 1996; Peterson *et al.*, 2001). The ability of NNKOAc to enhance the persistence of *O*⁶-MeGua in the lung was similar to that of *O*⁶-benzylguanin, a known inhibitor of AGT (Peterson *et al.*, 2001). The pyridyloxobutyl adduct, *O*⁶(POB-1-yl)Gua, was detected in the liver, but not in the lung, of A/J mice treated with NNK (Thomson *et al.*, 2003). This adduct was also detected in the lung and liver of mice treated with NNKOAc, in the presence but not absence of *O*⁶-benzylguanin, which indicates that *O*⁶(POB-1-yl)Gua is repaired in part by AGT (Thomson *et al.*, 2003). Further studies demonstrated that *O*⁶(POB-1-yl)Gua is repaired by mammalian AGT and that the rate of repair is highly dependent on protein structure (Mijal *et al.*, 2004). Inefficient repair of *O*⁶(POB-1-yl)Gua by bacterial AGT explains the high mutagenic activity of this adduct in bacterial systems (Pauly *et al.*, 2002).

Adduct measurements have been made in A/J mouse liver after treatment with NNK, although tumour induction in this tissue is infrequent (Belinsky *et al.*, 1989b). As in the lung, the relative levels of adduct formation are 7-MeGua > *O*⁶-MeGua > HPB-releasing adducts (Morse *et al.*, 1990a; Peterson *et al.*, 1990; Morse *et al.*, 1991). Levels of HPB-releasing adducts are higher in liver than in the lung, as are levels of 7-MeGua and *O*⁶-MeGua (Morse *et al.*, 1990a; Peterson *et al.*, 1990; Morse *et al.*, 1991; Peterson & Hecht, 1991). The relatively high level of adducts in the liver is consistent with metabolic studies that show efficient α -hydroxylation with little or no pyridine-*N*-oxidation in this tissue, in contrast to the lung where pyridine-*N*-oxidation is a major competing detoxification pathway. Despite the high DNA adduct levels in A/J mouse liver, tumours are observed in the lung and this is clearly related to susceptibility factors inherent in this mouse strain (Hecht, 1998).

Hamster

Initial levels of 7-MeGua and *O*⁶-MeGua are similar in rat and hamster liver after a single dose of NNK (Liu *et al.*, 1992). However, *O*⁶-MeGua is repaired more rapidly in rats (half-time, 12 h), while only 14% of the initial *O*⁶-MeGua is repaired 72 h after treatment in hamsters. 7-MeGua also persists longer in hamster than in rat liver. NNK rapidly depletes AGT in both rat and hamster liver, but AGT recovers in rats and not in hamsters. These results do not correlate with tumour induction by NNK. Whereas NNK is a weak hepatocarcinogen in rats, it does not induce liver tumours in hamsters. The results suggest that *O*⁶-MeGua is not important in the hepatocarcinogenesis of NNK.

Other types of DNA damage

Single-strand breaks are observed in hepatocytes incubated with NNK and in the livers of NNK-treated animals (Hecht, 1998), and are probably produced by spontaneous or enzymatic depurination of adducts such as 7-MeGua or 7(POB-1-yl)Gua. Among the metabolites of NNK, keto aldehyde has received the most attention as a source of single-strand breaks. However, the single-strand breaks induced by keto aldehyde appear to have different properties (for example, pH dependence) from those caused by NNK, which indicates that NNK single-strand breaks do not result from keto aldehyde (Demkowicz-Dobrzanski & Castonguay, 1991). NNK single-strand breaks are repaired slowly and damage persists for 2–3 weeks after a single treatment with NNK in rats and hamsters (Jorquera *et al.*, 1994). One study demonstrated an increase in NNK-induced single-strand breaks in human lung cells after generation of superoxide by hypoxanthine/xanthine oxidase (Weitberg & Corvese, 1993).

Treatment with NNK causes increases in levels of the promutagenic adduct 8-oxo-deoxyguanosine in mouse and rat lung, and in fetal liver following transplacental exposure of mice to NNK (Chung & Xu, 1992; Sipowicz *et al.*, 1997).

(iv) *Excretion*

Urine was the major route of excretion of NNK and NNAL metabolites with a pyridine ring in all studies with rodents and primates (Hecht, 1998).

In rats, 47% of a dose of [¹⁴C-methyl]NNK was excreted in the expired air (Castonguay *et al.*, 1983b). From 7 to 17% of an NNK dose was excreted in the bile of rats, mainly as (*R*)-NNAL-*O*-Gluc (Schulze *et al.*, 1992; Wu *et al.*, 2002). After intravenous administration of individual NNAL enantiomers, metabolites of (*S*)-NNAL (15% of the total dose) and (*R*)-NNAL (44% of the total dose) were excreted in the bile of rats (Zimmerman *et al.*, 2004).

Male rhesus monkeys received a single intravenous dose of radioactive NNK (4.6–9.8 µg/kg) and urine was collected for 10 days (Meger *et al.*, 1999). Within the first 24 h, 86% of the dose was excreted. NNK-derived radioactivity was still detectable in urine 10 days after treatment. Patterns of metabolites in the urine during the first 6 h closely resembled those seen in patas monkeys (Hecht *et al.*, 1993b); end-products of NNK metabolic activation represented more than 50% of total radioactivity. At later time-points, the pattern shifted toward NNAL and NNAL-*O*-Gluc. There was no preferential biliary excretion of NNAL-Gluc compared with rats.

(b) *NNN*

(i) *Absorption*

Studies of the absorption, distribution, metabolism and excretion of NNN in experimental systems have been comprehensively reviewed (Hecht, 1998), and the reader is referred to that review for detailed coverage of the literature. Selected studies from this review which illustrate important points as well as more recent studies that are pertinent to the evaluation are presented below.

The penetration of NNN across porcine skin and various regions of the oral mucosa was determined. Specimens of porcine skin, keratinized gingival and non-keratinized mucosa from the floor of the mouth and cheek were studied. Skin showed a lower permeability than the oral regions, and the floor of the mouth was generally the most permeable site. The non-keratinized oral regions were most permeable to NNN (Squier, 1986). Concentrations of 25% ethanol and above significantly increased the permeability of oral mucosa to NNN, but this increase ceased with 50% ethanol. The permeability of oral mucosa to NNN was also increased by nicotine (0.2–2%). Combined use of nicotine and ethanol significantly increased the penetration of NNN across oral mucosa compared with ethanol alone (Du *et al.*, 2000). Permeability of rat skin and buccal mucosa to NNN was significantly increased in rats maintained on a diet that contained 6.7% ethanol compared with rats kept on an isocaloric diet without ethanol (Squier *et al.*, 2003).

(ii) *Distribution*

Whole-body and micro-autoradiographic studies of the distribution of NNN in rats, mice, marmoset monkeys and mini-pigs have been reviewed (Tjälve, 1991). In general, NNN is rapidly distributed throughout the body, which reflects an ability of this

compound to pass freely across biological membranes and distribute evenly in the intra- and extracellular tissue water. However, accumulation of radioactivity has been observed in certain tissues. In rats, 5 min after intravenous injection of [2'-¹⁴C]NNN, the radioactivity was distributed homogeneously throughout most of the body and levels in tissues did not exceed the level in blood. However, high uptake was observed in a few tissues including the mucosa of the ethmoturbinates and the mucosa that covers the naso- and maxillo-turbinates. High radioactivity was also present in the submaxillary salivary glands, lacrimal glands, Zymbal glands, tarsal glands of the eyelids, preputial glands and stomach contents. The radioactivity in the nasal and tracheo-bronchial mucosa and the mucosa of the oesophagus and tongue was non-extractable, and a low level of non-extractable radioactivity was found in the liver, whereas that in other tissues was extractable (Brittebo & Tjälve, 1981). Whole-body autoradiography of mice treated intravenously with [2'-¹⁴C]NNN showed a similar spectrum of tissue localization of bound metabolites as that in rats; the only difference was in the salivary glands which accumulated radioactivity in mice but not in rats (Brittebo & Tjälve, 1980; Waddell & Marlowe, 1980; Tjälve, 1991). Whole-body autoradiograms taken 15–220 min after intracardiac administration of [5-³H]NNN to miniature pigs showed high levels of radioactivity in the mandibular and parotid salivary glands, Harder's gland, lacrimal glands, glands of the snout and respiratory part of the nasal cavity and melanin of the eyes and skin. Bound radioactivity was most abundant in the nasal mucosa and liver (Domellöf *et al.*, 1987). Autoradiograms obtained 4 h after intravenous injection of [2'-¹⁴C]NNN into a marmoset monkey showed the highest levels of radioactivity in the liver, nasal mucosa, melanin of the eyes, hair follicles of the skin and ceruminous ear glands. Bound radioactivity was observed in the liver and nasal mucosa (Castonguay *et al.*, 1985a).

(iii) *Metabolism*

In-vitro studies

The in-vitro metabolism of NNN has been studied in the rat liver, oesophagus, nasal mucosa, oral tissue and lung, in hamster liver and oesophagus and in mouse lung; these studies have been reviewed (Hecht, 1998), and only selected studies and more recent investigations are discussed below.

Rat liver metabolizes NNN by hydroxylation at each position of the pyrrolidine ring, which results in the formation of HPB, lactol and other secondary metabolites, 3'-HONNN and 4'-HONNN. Myosmine and NNN-*N*-oxide have also been observed (Chen *et al.*, 1978; Hecht *et al.*, 1980b; Hecht, 1998).

In cultured rat oesophagus, which is a target tissue for NNN carcinogenesis, metabolites that result from the 2'-hydroxylation pathway of metabolic activation exceed those that result from the 5'-hydroxylation pathway of metabolic activation (Hecht *et al.*, 1982). DNA isolated from rat oesophagus cultured with [5-³H]NNN contained HPB-releasing adducts (Murphy *et al.*, 1990a). Oesophageal microsomes metabolized NNN to HPB via 2'-hydroxylation and to lactol via 5'-hydroxylation. These reactions were probably mediated by a CYP enzyme, which had an apparent K_m of 49 μ M (Murphy & Spina, 1994).

Products of 2'-hydroxylation exceeded those of 5'-hydroxylation by threefold, as in cultured rat oesophagus; however, in liver microsomes, the ratio of 2':5'-hydroxylation varied between 0.23 and 0.71 depending on the concentration of NNN (Murphy & Spina, 1994). Cultured rat oesophagus metabolized (*S*)-NNN predominantly to products of 2'-hydroxylation while these products were significantly less prevalent in incubations with (*R*)-NNN. The 2':5'-hydroxylation ratio ranged from 6.22 to 8.06 at various time intervals in the incubations with (*S*)-NNN, while the corresponding ratios were 1.22–1.33 in experiments with (*R*)-NNN (McIntee & Hecht, 2000). The CYP enzyme that is responsible for the metabolic activation of NNN in rat oesophagus has not been identified. One candidate was thought to be CYP2A3, which has been identified in small amounts in the rat oesophagus (Gopalakrishnan *et al.*, 2002). CYP2A3 is an efficient catalyst of NNN α -hydroxylation (K_m , 13 μ M). However, metabolism of (*R*)- and (*S*)-NNN gives results that contrast to those observed in cultured rat oesophagus, which indicates that CYP2A3 is not involved in the catalysis of NNN α -hydroxylation in this tissue (Murphy *et al.*, 2000).

Cultured rat nasal mucosa, which is another target tissue of NNN carcinogenesis, metabolized NNN extensively by α -hydroxylation; pyridine *N*-oxidation was not observed (Brittebo *et al.*, 1983). HPB-releasing DNA adducts of NNN were detected in rat nasal mucosa cultured with NNN (Spratt *et al.*, 1989). Rat nasal mucosal microsomes catalysed both 2'- and 5'-hydroxylation of NNN, with low K_m values of 2–3 μ M. NNN inhibited coumarin 7-hydroxylation, which suggests the involvement of a CYP2A enzyme (Patten *et al.*, 1998).

Cultured rat oral tissue metabolized NNN in a fashion similar to that observed with cultured rat oesophagus, but HPB-releasing DNA adducts were not observed (Murphy *et al.*, 1990a). NNN metabolism was inhibited by nicotine and, to a lesser extent, by NNK (Murphy & Heiblum, 1990).

There is some consistency between the ratios of 2':5'-hydroxylation in different rodent tissues and their susceptibility to carcinogenesis by NNN (Hecht, 1998). The 2':5'-hydroxylation ratio is typically 2–4 in rat oesophagus and nasal mucosa, which are the main target tissues of NNN in the rat. In the liver, which is a non-target tissue, 2':5'-hydroxylation ratio is 0.3–1.4. Hamster oesophagus, which is a non-target tissue, predominantly 5'-hydroxylates NNN (Hecht *et al.*, 1982). These results are consistent with a role for 2'-hydroxylation in tumour induction by NNN and for 5'-hydroxylation in detoxification. In contrast, 5'-hydroxylation and 2'-hydroxylation occur to equal extents in hamster trachea (McCoy *et al.*, 1982) and 5'-hydroxylation exceeds 2'-hydroxylation in A/J mouse lung (Castonguay *et al.*, 1983a), both of which are target tissues of NNN carcinogenesis (Hecht, 1998).

Rat CYP2A3 and mouse CYP2A5 catalyse 5'-hydroxylation of both enantiomers of NNN with low K_m values (0.74–3.35 μ M). Mouse CYP2A4 is a poorer catalyst with K_m values of 54.1–68.5 μ M. Rat CYP2A3 and mouse CYP2A5 catalyse 2'-hydroxylation of (*R*)-NNN with K_m values of 0.73–1.64 μ M, while the K_m for mouse CYP2A4 is 66 μ M. 2'-Hydroxylation of (*S*)-NNN was not observed in studies with these enzymes (Wong *et al.*, 2005b).

2'- and 5'-Hydroxylation of NNN can lead to DNA damage. 2'-Hydroxylation generates the same intermediate — POB-DZH (Figure 6) — as methyl hydroxylation of NNK (Hecht, 1998; Wang *et al.*, 2003; Hecht *et al.*, 2004c). Formation of HPB-releasing DNA adducts is therefore expected following 2'-hydroxylation of NNN and this been observed in cultured rat oesophagus and nasal mucosa. Adducts could also be formed from 5'-HONNN via *iso*-POB-DZH, but this has not been reported (Hecht, 1998).

In-vivo studies

The effect of NNN on hepatic and pulmonary carcinogen metabolizing enzymes in male Sprague-Dawley rats was evaluated in a series of studies that used the following basic experimental protocol. Inbred male weanling Sprague-Dawley rats (19–21 days of age and weighing 35–50 g) were randomly divided into three groups of eight animals each and were placed on three different dietary regimens that consisted of a standard diet, a control semisynthetic diet and a semisynthetic deficient diet. In each set of experiments, the semisynthetic diets were either adequate (control) or deficient in vitamin A (Nair *et al.*, 1991), vitamin B complex (Ammigan *et al.*, 1990a) or protein (Ammigan *et al.*, 1989). At 12 weeks, 75% of the dose that causes 50% lethality (LD₅₀) was divided into three equal doses and was given intraperitoneally at 24-h intervals. Twenty-four hours after the last injection, overnight fasted animals were killed and the lung and liver were excised. Hepatic and pulmonary biotransformation enzymes, CYPs, cytochrome b-5, benzo[*a*]-pyrene hydroxylase, benzphetamine *N*-demethylase, glutathione *S*-transferase (GST) and glutathione (GSH) content were determined. Vitamin A and C were also determined.

NNN was more toxic to animals with nutritional deficiencies. In the vitamin A-, B complex- or protein-deficient rats, the LD₅₀ of NNN was reduced by 20–24% (Ammigan *et al.*, 1990b). These deficiencies resulted in a decrease in the basal levels of CYPs, benzo[*a*]-pyrene hydroxylase, benzphetamine demethylase, GST and GSH.

In vitamin A-sufficient and -deficient groups, treatment with NNN significantly increased the levels of phase I-activating enzymes in all treatment groups. A higher increase in hepatic and pulmonary phase I activities was observed in the deficient animals compared with the sufficient groups. An increase in the GSH/GST system was observed in the sufficient group following treatment; however, in the deficient animals, exposure to the NNN caused suppression of the hepatic and pulmonary GSH/GST systems (Nair *et al.*, 1991).

When groups of Sprague-Dawley rats fed low-protein (5% casein) or vitamin B complex-deficient diets were exposed to NNN by the same protocol, a significant increase in phase I enzymes with concurrent inhibition of the GSH/GST levels was observed compared with the corresponding control groups fed high-protein (20% casein) or vitamin B complex-sufficient diets (Ammigan *et al.*, 1989, 1990a). The hepatic pool of vitamin A was depleted while that of vitamin C was increased in Sprague-Dawley rats fed low-protein diet and exposed to NNN. Altered metabolism resulting from vitamin deficiency and/or protein-calorie malnutrition may be an important factor in the modulation of the metabolism of NNN.

The metabolism of NNN has been studied in rats, hamsters, mice, monkeys and mini-pigs (reviewed in Hecht, 1998). NNN is rapidly metabolized and eliminated primarily in urine. Hydroxy acid via 5'-hydroxylation and keto acid via 2'-hydroxylation are the major urinary metabolites of NNN in rodents, marmoset monkeys and mini-pigs (Hecht, 1998). Other metabolites that are consistently observed in the urine are NNN-*N*-oxide and norcotinine (Hecht, 1998). In patas monkeys, the major urinary metabolites are hydroxy acid, 3'-Honorcotinine, 3'-Honorcotinine-Gluc, norcotinine-*N*-oxide and norcotinine (Upadhyaya *et al.*, 2002). Small amounts of unchanged NNN are also observed in the urine of treated animals (Hecht, 1998).

In rats treated with racemic NNN, (*S*)-hydroxy acid and (*R*)-hydroxy acid represented 36% and 64% of total hydroxy acid in the urine, respectively (Trushin & Hecht, 1999). Products of 2'-hydroxylation predominated in the urine of rats treated with (*S*)-NNN while products of 5'-hydroxylation were more prevalent in the rats treated with (*R*)-NNN (McIntee & Hecht, 2000).

Haemoglobin adducts

HPB-releasing haemoglobin adducts are formed in rats treated with NNN. The adduct levels are only about 16% of those induced by NNK (Carmella & Hecht, 1987).

DNA adducts

HPB-releasing adducts are present in acid or enzyme hydrolysates of hepatic DNA from NNN-treated rats, in acid hydrolysates of pulmonary DNA from NNN-treated mice and in acid hydrolysates of DNA from the respiratory and olfactory parts of the nasal mucosa of rats treated with NNN; the levels in the respiratory mucosa are higher (reviewed in Hecht, 1998). As may be expected, *O*⁶-MeGua is not detected in the nasal mucosa or liver of rats treated with NNN (Castonguay *et al.*, 1985b).

(iv) *Excretion*

Urine is the major route of excretion of NNN and metabolites in rodents and accounts for 60–80% of the dose (Hecht, 1998).

Urine samples were collected from seven groups of eight Sprague-Dawley rats that were maintained on semisynthetic diets sufficient or deficient in vitamin A, sufficient or deficient in vitamin B complex and sufficient or deficient in protein, or on standard control diet. All groups were exposed to NNN. Urine was tested for mutagenic activity using the *Salmonella*/microsome assay. A higher mutagenic activity of urine was observed in the exposed groups on each of the deficient diets. The order of mutagenicity of all treatments was deficient diet > standard diet > nutritionally sufficient diet (Ammigan *et al.*, 1990b). Thus, NNN-exposed animals probably have greater exposure to mutagenic metabolites, which are generated by increased phase I enzymes and decreased detoxification system.

(c) *NAB*

(i) *Absorption*

No data were available to the Working Group

(ii) *Distribution*

No data were available to the Working Group

(iii) *Metabolism*

In rats treated by gavage with [2'-¹⁴C]NAB, 68.5% of the dose was excreted in the urine (Hecht & Young, 1982). 5-Hydroxy-5-(3-pyridyl)pentanoic acid, formed by 6'-hydroxylation, and NAB-*N*-oxide were detected as urinary metabolites. In cultured rat oesophagus treated with [2'-¹⁴C]NAB, 5-hydroxy-5-(3-pyridyl)pentanoic acid, formed by 6'-hydroxylation, was a major metabolite and 5-oxo-5-(3-pyridyl)pentanoic acid, formed by 2'-hydroxylation, was a minor metabolite at all time-points examined. These results contrasted with those obtained by rat oesophageal metabolism of NNN, in which 2'-hydroxylation predominated (Hecht & Young, 1982).

(iv) *Excretion*

Urine was the major route of excretion of NAB metabolites in the rat (Hecht & Young, 1982).

(d) *NAT*

(i) *Absorption*

No data were available to the Working Group.

(ii) *Distribution*

No data were available to the Working Group.

(iii) *Metabolism*

In Fischer 344 rats, the pharmacokinetics of NAT fit a two compartment model. Pharmacokinetic parameters were: half-life, 540 min; blood clearance, 128 mL/h; and apparent volume of distribution, 695 mL (Adams *et al.*, 1985b).

(iv) *Excretion*

No data were available to the Working Group.

4.2 Toxic effects

4.2.1 Humans

No data were available to the Working Group

4.2.2 *Experimental systems*

(a) *NNK and NNAL*

(i) *Animals*

NNK induced cytotoxicity in the nasal passage of male Fischer 344 rats: it damaged Steno's and Bowmans's glands and caused degeneration of the olfactory epithelium at intraperitoneal doses of 4.8–48 $\mu\text{mol/kg}$ bw daily for up to 12 days (Belinsky *et al.*, 1987b). NNK also induced mild centrilobular necrosis in the liver, which progressed to collapse of the centrilobular architecture at higher doses (Belinsky *et al.*, 1986). An intraperitoneal dose of 0.39 mmol/kg bw induced an increase in levels of alanine transaminase, aspartate transaminase and lactate dehydrogenase in male Syrian golden hamsters over 2–3 weeks (Jorquera *et al.*, 1994).

(ii) *In-vitro cellular systems*

NNK induced cytotoxicity in rat tracheal epithelial (RTE) cells at concentrations of 100–200 $\mu\text{g/mL}$ (Zhu *et al.*, 1991) and in human–hamster hybrid A_L cells at a dose of 500 $\mu\text{g/mL}$ (Zhou *et al.*, 1999). NNK caused dose- and time-dependent toxicity in hamster pancreatic duct cells *in vitro* (Baskaran *et al.*, 1994).

No data on NNAL were available to the Working Group.

(b) *NNN*

The subcutaneous LD₅₀ of NNN in male rats observed for 8 days was > 1000 mg/kg bw. In rats that died, haemorrhages were observed in the lungs and abdominal organs and epithelial-cell necrosis in the posterior nasal cavities and liver (Hoffmann *et al.*, 1975). The LD₅₀ determined in 12-week-old Sprague-Dawley rats was 200 mg/kg bw with a standard diet and 190 mg/kg bw for animals fed vitamin B- and protein-deficient diets (Ammigan *et al.*, 1990b).

(c) *NAB*

The subcutaneous LD₅₀ of NAB in Fischer rats was > 1000 mg/kg bw (Hoffmann *et al.*, 1975).

(d) *NAT*

No data were available to the Working Group.

4.3 **Reproductive and developmental effects**

No data were available to the Working Group.

4.4 Genetic and related effects

4.4.1 Humans

DNA adducts as biomarkers of exposure to NNK and NNN are discussed in Section 4.1. No data were available for NNAL, NAB or NAT.

4.4.2 Experimental systems

(a) NNK and NNAL

(i) NNK

DNA adducts as biomarkers of exposure to NNK have been discussed in Section 4.1.2.(a)(iii).

Mutagenicity, clastogenicity, cell transformation and other effects

Mutagenicity and allied effects (for details and references, see Table 17)

In-vitro studies

NNK caused a dose-dependent increase in mutations in *S. typhimurium* strains TA100 and TA1535 in the presence of a liver microsomal preparation from Aroclor-1254-induced rats.

Primary hepatocytes, a liver metabolic activation system (S9 fraction), and tracheal epithelial cells from normal and Aroclor-1254-induced rats were compared for bio-activation of NNK in the *Salmonella* mutagenicity assay. Without activation, NNK was not mutagenic in *S. typhimurium* TA1535. The bioactivation of NNK to a mutagenic metabolite was achieved by incubation with the liver S9 metabolic activation system from Aroclor-1254-induced rats or with primary hepatocytes from both untreated and Aroclor-1254-pretreated rats. In contrast, NNK incubated with rat tracheal epithelial cells from both uninduced or Aroclor-1254-induced rats produced no measurable mutagenic activity in strain TA1535 (Zhu *et al.*, 1991).

NNK was mutagenic in a *Salmonella* tester strain that carries the human *CYP2A6* and human NADPH-CYP reductase (YG7108 2A6/OR) in the absence of an exogenous metabolic activation system. In another report, NNK was shown to be mutagenic in strain TA7004 with rat and hamster metabolic activation systems, but not in TA100. It was also mutagenic in *S. typhimurium* TA98.

NNK has been used as a model mutagen in several studies that employed the *S. typhimurium* mutagenicity assay to determine the anti-mutagenic properties of various compounds (reviewed in Hecht, 1998).

NNK was mutagenic in the Mutatox test using the dark mutant M-169 of *Vibrio fischeri* (Yim & Hee, 2001).

In primary rat hepatocytes and rabbit lung cells, NNK induced DNA strand breaks without exogenous activation and unscheduled DNA synthesis.

Table 17. Genetic and related effects of 4-(methylnitrosamino)-1-(3-pyridyl)-1-butanone (NNK)

Test system	Result ^a		Dose ^b (LED or HID)	Reference
	Without exogenous metabolic system	With exogenous metabolic system		
<i>Salmonella typhimurium</i> TA100, TA1535, reverse mutation	NT	+	2 µmol/plate [414 µg/plate]	Hecht <i>et al.</i> (1983c)
<i>Salmonella typhimurium</i> TA100, TA1535, reverse mutation	NT	+	2 µmol/plate ^c [418 µg/plate]	Hecht <i>et al.</i> (1983c)
<i>Salmonella typhimurium</i> TA100, TA1535, reverse mutation	NT	-	4 µmol/plate ^d [840 µg/plate]	Hecht <i>et al.</i> (1983c)
<i>Salmonella typhimurium</i> TA100, reverse mutation	-	+	1000 µg/plate	Padma <i>et al.</i> (1989b)
<i>Salmonella typhimurium</i> TA100, reverse mutation	-	-	2000 µg/plate	Yim & Hee (2001)
<i>Salmonella typhimurium</i> TA1535, reverse mutation	-	+	1000 µg/mL	Padma <i>et al.</i> (1989b)
<i>Salmonella typhimurium</i> TA1535, reverse mutation	-	-	2500 µg/plate	Zhu <i>et al.</i> (1991)
<i>Salmonella typhimurium</i> TA1535, reverse mutation	-	+	500 µg/plate	Zhu <i>et al.</i> (1991)
<i>Salmonella typhimurium</i> TA1538, reverse mutation	-	-	1000 µg/mL	Padma <i>et al.</i> (1989b)
<i>Salmonella typhimurium</i> TA98, reverse mutation	-	-	1000 µg/plate	Padma <i>et al.</i> (1989b)
<i>Salmonella typhimurium</i> TA98, reverse mutation	-	+	20 µM [4.2 µg/mL]	Kolar & Lawson (1997)
<i>Salmonella typhimurium</i> YG7108, reverse mutation	-	NT	0.7 mM [145 µg/mL]	Kushida <i>et al.</i> (2000a,b)
<i>Salmonella typhimurium</i> YG7108 -2A6/OR ^e , reverse mutation	+	NT	0.1 mM [20.7 µg/mL]	Kushida <i>et al.</i> (2000a,b)
<i>Salmonella typhimurium</i> YG7108 -2E1/OR ^f , reverse mutation	-	NT	0.7 mM [145 µg/mL]	Kushida <i>et al.</i> (2000a,b)
<i>Salmonella typhimurium</i> TA7004, reverse mutation	-	+	2000 µg/plate	Yim & Hee (2001)
DNA strand breaks, primary rat hepatocytes <i>in vitro</i>	+	NT	5 mM [1035 µg/mL]	Liu <i>et al.</i> (1990)
DNA strand breaks, primary rat hepatocytes <i>in vitro</i>	+	NT	6.25 µmol/mL [1297 µg/mL]	Pool-Zobel <i>et al.</i> (1992)
DNA strand breaks, isolated rabbit lung cells (Type II and Clara) <i>in vitro</i>	+	NT	30 µM [6.22 µg/mL]	Becher <i>et al.</i> (1993)
DNA strand breaks, isolated rabbit alveolar macrophages <i>in vitro</i>	-	NT	300 µM [62.2 µg/mL]	Becher <i>et al.</i> (1993)
Unscheduled DNA synthesis, freshly isolated rat hepatocytes <i>in vitro</i>	+	NT	1 mM [207.5 µg/mL]	Williams & Laspia, 1979
Unscheduled DNA synthesis, rabbit lung cells <i>in vitro</i>	+	NT	2 mM [414.5 µg/mL]	Dahl <i>et al.</i> (1990)

Table 17 (contd)

Test system	Result ^a		Dose ^b (LED or HID)	Reference
	Without exogenous metabolic system	With exogenous metabolic system		
Gene mutation, Chinese hamster lung fibroblastic V79 cells, <i>Hprt</i> locus, <i>in vitro</i>	–	+	10 mM [2072 µg/mL]	Swedmark <i>et al.</i> (1994)
Sister chromatid exchange, Chinese hamster lung fibroblastic V79 cells <i>in vitro</i>	–	+	20 µg/mL	Zimonjic <i>et al.</i> (1989)
Sister chromatid exchange, Chinese hamster lung fibroblastic V79 cells <i>in vitro</i>	–	+	20 mM [4145 µg/mL]	Alaoui Jamali <i>et al.</i> (1988)
Sister chromatid exchange, Chinese hamster ovary (CHO) cells <i>in vitro</i>	NT	+	0.1 mM [20.7 µg/mL]	Lee <i>et al.</i> (1996)
Micronucleus formation, Chinese hamster lung fibroblastic V79 cells <i>in vitro</i>	–	+	5 mM [1036 µg/mL]	Alaoui Jamali <i>et al.</i> (1988)
Micronucleus formation, rat tracheal epithelial cells <i>in vitro</i>	+	NT	50 µg/mL	Zhu <i>et al.</i> (1991)
Chromosomal aberrations, Chinese hamster lung fibroblastic V79 cells <i>in vitro</i>	+	–	20 mM [4145 µg/mL]	Alaoui Jamali <i>et al.</i> (1988)
DNA strand breaks, human MRC-5 fetal lung cells <i>in vitro</i>	+	NT	5 mM [1035 µg/mL]	Weitberg & Corvese (1993, 1997)
Gene mutation, human lymphoblastoid cells, <i>HPRT</i> locus, <i>in vitro</i>	+	NT	1 µg/mL	Krause <i>et al.</i> (1999)
Sister chromatid exchange, human peripheral blood lymphocytes <i>in vitro</i>	+	NT	[0.48 mM] 100 µg/mL	Padma <i>et al.</i> (1989b)
Sister chromatid exchange, human peripheral blood lymphocytes <i>in vitro</i>	+	+	[0.096 mM] 20 µg/mL	Zimonjic <i>et al.</i> (1989)
Micronucleus formation, human AGT repair-deficient fibroblasts <i>in vitro</i>	+	NT	0.05 mM [10.4 µg/mL]	Pohlmann <i>et al.</i> (1992)
Micronucleus formation, human AGT repair-proficient fibroblasts <i>in vitro</i>	–	NT	1 mM [207.5 µg/mL]	Pohlmann <i>et al.</i> (1992)
Micronucleus formation, human-derived hepatoma HepG2 and Hep3B cells <i>in vitro</i>	–	NT	5 mM [1036 µg/mL]	Majer <i>et al.</i> (2004)
Chromosomal aberrations, human peripheral blood lymphocytes <i>in vitro</i>	+	NT	0.48 mM [100 µg/mL]	Padma <i>et al.</i> (1989b)

Table 17 (contd)

Test system	Result ^a		Dose ^b (LED or HID)	Reference
	Without exogenous metabolic system	With exogenous metabolic system		
DNA strand breaks, rat hepatocytes <i>in vivo</i>	+		12.5 mg/kg bw po 1× [60 µmol/kg bw]	Pool-Zobel <i>et al.</i> (1992)
DNA strand breaks, rat and hamster hepatocytes <i>in vivo</i>	+		0.39 mmol/kg bw [81 mg/kg bw] ip 1×	Jorquera <i>et al.</i> (1994)
Gene mutation, rat splenic T lymphocytes, <i>Hprt</i> locus, <i>in vivo</i>	-		150 mg/kg bw ip 1×	Jansen <i>et al.</i> (1996)
Micronucleus formation, Swiss male mice bone marrow <i>in vivo</i>	+		250 mg/kg bw/d ip 2×	Padma <i>et al.</i> (1989b)
Micronucleus formation, rat tracheal epithelial cells <i>in vivo</i>	+		150 mg/kg bw/d ip 3×	Zhu <i>et al.</i> (1991)

^a +, positive; -, negative; NT, not tested

^b LED, lowest effective dose; HID, highest ineffective dose; d, day; ip, intraperitoneal injection

^c [4,4-dideutero]NNK

^d [4-trideutero]NNK

^e Co-expressing human CYP 2A6 together with human NADPH-CYP reductase (OR)

^f Co-expressing human CYP 2E1 together with human NADPH-CYP reductase (OR)

NNK was mutagenic in V79 hamster cells when assayed with a metabolic activation system obtained from ethanol-treated pancreatic duct epithelial cells from humans and Syrian hamsters and from ethanol-treated CK cells (immortalized hamster pancreatic duct epithelial cells) (Kolar & Lawson, 1997). It induced mutations at the *Hprt* locus in V79 Chinese hamster cells co-cultivated with rat hepatocytes that provided metabolic activation.

NNK caused sister chromatid exchange in Chinese hamster ovary cells in the presence of metabolic activation in three studies.

NNK induced micronucleus formation in Chinese hamster lung fibroblastic V79 cells in the presence of a metabolic activation system. Micronuclei were also induced in V79 cells by NNK activated by fetal liver and lung homogenates from rat fetuses on the 15th day of the gestation (Alaoui Jamali *et al.*, 1998). In rat tracheal epithelial cells treated with NNK, micronuclei were formed without a metabolic activation system.

NNK induced chromosomal aberrations without exogenous bio-activation in Chinese hamster lung fibroblastic V79 cells.

NNK induced a dose-dependent toxicity in human–hamster hybrid A_L cell assay. Treatment with NNK at a low dose, when combined with radon α -particles, resulted in a combined mutagenic effect that was consistent with an additive model, but less than additive at higher concentrations of NNK (Zhou *et al.*, 1999). In mammalian cells, NNK induced mostly deletions (Zhou *et al.*, 1999).

NNK induced DNA strand breaks in fetal human lung cells. NNK induced mutations at the *HPRT* locus in human lymphoblastoid MCL-5 cells without metabolic activation. In human lymphocytes, NNK induced sister chromatid exchange without exogenous bioactivation in two studies. Micronucleus formation was observed in AGT repair-deficient, but not in repair-proficient human fibroblasts in the absence of exogenous activation. NNK did not induce micronuclei in human hepatoma cell lines HepG2 and Hep3B. NNK induced chromosomal aberrations without exogenous bioactivation in human lymphocytes.

In-vivo studies

NNK did not induce mutations in rat splenic T-lymphocytes *in vivo*. NNK induced DNA strand breaks in the hepatocytes of rats and hamsters (see Section 4.1.2(a)(iii)), and micronucleus formation in the bone marrow of male Swiss mice.

Mutations in transgenic systems

In vitro, human CYP2A6 was lipofected via a retroviral vector in AS52 Chinese hamster ovary cells, which contain the bacterial *gpt* gene that can be mutated to 6-thioguanine resistance. At the highest dose of NNK (1200 $\mu\text{g}/\text{mL}$), a 14-fold (339×10^{-6}) increase in mutant frequency was observed in AS52-E8 cells compared with the spontaneous frequency of 24×10^{-6} (Tiano *et al.*, 1994).

In vivo, NNK was administered intraperitoneally to *lacZ* transgenic mice (MutaTMMouse) at 125 and 250 mg/kg bw once a week for 4 weeks. The mutant frequencies in the *lacZ* and *cII* genes from lung and liver increased dose-dependently up to 10-fold compared with the controls. The proportion of G:C→A:T transition mutations in

the total number of mutants was less than the number of A:T→T:A and A:T→C:G transversions (Hashimoto *et al.*, 2004). NNK was also mutagenic in a mixture of pooled oral tissues (gingival, buccal, pharyngeal and sublingual), and in tongue and lung tissue of *lacZ* transgenic mice (MutaTM Mouse) (von Pressentin *et al.*, 1999).

K-*ras* and TP53 mutations

DNA isolated from 20 lung hyperplasias obtained after treatment of adult A/J mice with NNK was screened for the presence of activated K-*ras*. This gene was activated in 17/20 lesions; 85% of the mutations were a G:C→A:T transition within codon 12 (GGT→GAT), a mutation that is consistent with base mispairing produced by the formation of the O⁶-MeGua adduct (Belinsky *et al.*, 1992).

Activated K-*ras* gene was detected in 100% of lung tumours induced in C3H mice by treatment with NNK (50 mg/kg bw); the activating mutation detected in all samples was a G:C→A:T transition (GGT→GAT) in codon 12 (Devereux *et al.*, 1991). NNK caused GGT→GAT mutations in codon 12 of K-*ras* gene in lung tumours induced in A/J mice (Chen *et al.*, 1993; Ronai *et al.*, 1993).

The relationship between the development of peripheral lung lesions induced by NNK and K-*ras* gene mutation, and the correlations between histological alterations and the course of lung lesion development after treatment with NNK and K-*ras* gene mutation were investigated in A/J mice. K-*ras* gene mutations were identified in seven of 12 (58.3%) hyperplasias, in 42/56 (75.0%) adenomas and in three of four (75.0%) adenocarcinomas. The most frequent K-*ras* gene mutation was a G→A transition at the second base of codon 12, which accounted for 86.5% of all the mutations detected (Kawano *et al.*, 1996).

Analysis of lung tumour DNA from A/J mice treated with NNK indicated that 15/17 (88%) samples contained G→A transitions at the second base of codon 12 in the K-*ras* gene. Similarly, in lung tumours from (A/J × TSG-*p53*)F₁ hybrid mice treated with NNK, 29/30 (97%) contained G→A transitions at the second base of codon 12 of the K-*ras* gene. No mutations of the *p53* gene were found in any of the tumours analysed, which suggests minimal involvement of this gene in the development of lung adenomas. The *p53* allele in (A/J × TSG-*p53*)F₁ mice does not alter the incidence or multiplicity of NNK-induced lung tumours (Matzinger *et al.*, 1995).

Lung tumours induced by subcutaneous injection of NNK into Syrian golden hamsters were examined for mutations in the K-*ras* oncogene and the TP53 tumour-suppressor gene by direct sequencing. The K-*ras* mutation frequency in RNA isolated from pooled tumours and that in DNA isolated from individual tumours were found to be identical. Activated K-*ras* alleles were detected in 77–94% of tumours. All mutations observed except one (from a total of 65), at either codon 12 or 13, were G:C→A:T. No mutations were detected at codon 61. Examination of the same tumours for TP53 mutations showed only one point mutation. Treatment of Syrian golden hamsters with NNK resulted in a distinct mutation pattern in the K-*ras* gene whereas TP53 gene mutations may not play a major role at this stage in hamster lung tumorigenesis (Oreffo *et al.*, 1993).

Gene expression profile

Characteristic expression profiles induced by NNK at a dose of 20 mg/kg bw per day were investigated in rat liver for 14 days. Fourteen genes that are involved in DNA-damage response (five), detoxification response (six) and cell survival/proliferation (three) were up-regulated and one gene each that is involved in mitochondrial damage and dedifferentiation were down-regulated (more than two-fold). *O*⁶-MeGua-DNA methyltransferase was among one of the genes that were up-regulated. Increased expression profiles were weakly detectable at day 1 and then increased with time (Ellinger-Ziegelbauer, 2004).

Cytotoxicity and cell transformation

The cytotoxicity and transforming activity of NNK was studied by the assays of colony-forming efficiency, micronucleus formation and cell transformation in rat tracheal epithelial cells both *in vitro* and *in vivo*. Results from the *in-vitro* experiments indicated that low concentrations of NNK (0.01–25 µg/mL) caused increases in colony-forming efficiency of rat tracheal epithelial cells from 15% to more than 100%. At higher concentrations (100–200 µg/mL), NNK was significantly toxic to these cells. Treatment with NNK *in vitro* (50–200 µg/mL) significantly increased the transformation frequency in four of five (50 µg/mL) and six of eight (100 µg/mL) experiments. The *in-vivo* exposure of rats to NNK (150–450 mg/kg intraperitoneally) resulted in a 60–85% reduction in colony-forming efficiency in rat tracheal epithelial cells (Zhu *et al.*, 1991).

Immortalized human bronchial epithelial cells (BEAS-2B cells) grown in de-epithelialized rat tracheas were exposed to NNK and subcutaneously transplanted into athymic nude mice. The cells were neoplastically transformed to produce invasive adenocarcinoma with phenotypic changes similar to the progressive changes that occur during human lung carcinogenesis (Klein-Szanto *et al.*, 1992).

In-vitro transformation of spontaneously immortal hamster pancreatic duct cells has been described following exposure to 20 mM NNK for 1, 3, 5 and 7 days. Cells treated with NNK grew as a monolayer with numerous mitotic figures and multinucleated large cells. One- and 3-day NNK-treated cells grown in complete duct medium produced well-differentiated, mucinous tumours after their injection in nude mice. Analysis of DNA from these tumours for *K-ras* mutation at codons 12, 13 and 61 showed a G→A transition at codon 12 of the *K-ras* oncogene in tumour cells after 1 and 3 days of NNK treatment (Baskaran *et al.*, 1994).

In-vivo treatment with cumulative doses of 150 and 300 mg/kg bw NNK produced significant increases in transformation frequency of tracheal cells in three of three and two of three rats, respectively (Zhu *et al.*, 1991).

Yoo *et al.* (2000) showed that normal human gingival keratinocytes immortalized with human papillomavirus 16 (IHGK) were transformed by NNK to IHGKN cells. Transformation of IHGK cells resulted in the activation of vascular endothelial growth factor associated with angiogenesis. Inactivation of the G1 phase of cell-cycle regulation occurred during immortalization before cell transformation, and was sustained after carcinogen exposure.

Other effects

In cultured human oral epithelial cells, treatment with NNK resulted in increased longevity and a sustained differentiated phenotype for 8.5–10 weeks. The treated cells displayed focal growth and morphological changes suggestive of early stages of cell transformation as compared with controls in which cells were terminally differentiated (Murrah *et al.*, 1993).

A higher frequency of hyperplasia with hyperkeratosis was observed in the forestomach of hamster treated with a combination of nicotine and NNK as compared with either NNK or nicotine treatment alone. Squamous-cell papillomas were evident in the forestomach of animals treated with both NNK and nicotine (Chen *et al.*, 1994).

NNK was shown to inhibit the production of IL-12 and TNF, key molecules of immune response in rat alveolar macrophages and stimulate the production of IL-10 and prostaglandin E₂ (Therriault *et al.*, 2003). Using model compounds NNKOAc and *N*-nitro-(acetoxymethyl)methylamine (NDMAOAc), it has been demonstrated that the above effect of NNK is mediated by α -methyl hydroxylation of NNK, the same pathway that induces DNA pyridyloxobutylation (Proulx *et al.*, 2004).

(ii) NNAL

NNAL was mutagenic in *S. typhimurium* TA1535 in the presence of a liver metabolic activation system from Aroclor-1254-induced rats or hamsters in the range of 0.025–0.2 $\mu\text{mol/plate}$ [5.5–42 $\mu\text{g/plate}$] (maximum tested dose) (Brown *et al.*, 2001b).

(b) NNN

(i) Mutagenic and cytogenetic effects, DNA damage (for details and references, see Table 18)

NNN was mutagenic in *S. typhimurium* strain TA100 in three of four assays (two with and one without exogenous metabolic activation), in strain TA1535 (with activation) and in TA1530 and TA7004 (without activation). NNN was also mutagenic in *Salmonella* tester strains YG7108 that carry the human *CYPs* 2A6, 1A1, 3A4 and 3A5 in the absence of an exogenous activation system, but was not mutagenic in YG7108 itself or in YG7108 that carries *CYP2E1* (Kushida *et al.*, 2000a; Fujita & Kamataki, 2001). NNN was not mutagenic in *Salmonella* strains TA98 or TA1538 (single tests only).

NNN was a direct-acting mutagen in the Mutatox test using dark mutant M-169 of *Vibrio fischeri*, but was not mutagenic in this assay in the presence of a metabolic activation system from rat or hamster (Yim & Hee, 2001).

Using model compounds, it was shown that the putative diazohydroxide formed by 2'-hydroxylation of NNN has higher inherent mutagenicity toward *S. typhimurium* than the corresponding diazohydroxide formed by 5'-hydroxylation (Hecht & Lin, 1986).

NNN induced DNA strand breaks in primary rat hepatocytes but not in lung cells or alveolar macrophages of rabbits.

Table 18. Genetic and related effects of N'-nitrosornicotine (NNN)

Test system	Result ^a		Dose ^b (LED or HID)	Reference
	Without exogenous metabolic system	With exogenous metabolic system		
<i>Salmonella typhimurium</i> TA100, reverse mutation	–	+	2.5 µmol/plate [443 µg/plate]	Bartsch <i>et al.</i> (1980)
<i>Salmonella typhimurium</i> TA100, reverse mutation	–	+	250 µg/plate	Padma <i>et al.</i> (1989b)
<i>Salmonella typhimurium</i> , TA100, TA7004, reverse mutation	+	–	2000 µg/plate	Yim & Hee (2001)
<i>Salmonella typhimurium</i> TA100, TA7004, reverse mutation	+	–	500 µg/plate	Yim & Hee (2001)
<i>Salmonella typhimurium</i> TA1530, reverse mutation	+	NT	1000 µg/plate	Andrews <i>et al.</i> (1978)
<i>Salmonella typhimurium</i> TA1535, reverse mutation	–	+	1000 µg/plate	Padma <i>et al.</i> (1989b)
<i>Salmonella typhimurium</i> TA1538, TA 98, reverse mutation	–	–	1000 µg/plate	Padma <i>et al.</i> (1989b)
<i>Salmonella typhimurium</i> YG7108, reverse mutation	–	NT	0.7 mM [124 µg/mL]	Kushida <i>et al.</i> (2000a); Fujita & Kamataki (2001)
<i>Salmonella typhimurium</i> YG7108 -2A6/OR ^c , reverse mutation	+	NT	0.2 mM [35.5 µg/mL]	Kushida <i>et al.</i> (2000a); Fujita & Kamataki (2001)
<i>Salmonella typhimurium</i> YG7108 -2E1/OR ^d , reverse mutation	–	NT	0.7 mM [124 µg/mL]	Kushida <i>et al.</i> (2000a); Fujita & Kamataki (2001)
DNA strand breaks, primary rat hepatocytes <i>in vitro</i>	+	NT	5 mM [886 µg/mL]	Liu <i>et al.</i> (1990)
DNA strand breaks, isolated rabbit lung cells (Type II and Clara) and alveolar macrophages <i>in vitro</i>	–	NT	3 mM [531 µg/mL]	Becher <i>et al.</i> (1993)
DNA strand breaks, rat hepatocytes <i>in vitro</i>	–	NT	25 mM [4430 µg/mL]	Pool-Zobel <i>et al.</i> (1992)
Unscheduled DNA synthesis, freshly isolated rat hepatocytes <i>in vitro</i>	+	NT	1 mM [177 µg/mL]	Williams & Laspia (1979)
Unscheduled DNA synthesis, rabbit lung cells <i>in vitro</i>	–	NT	2 mM [354 µg/mL]	Dahl <i>et al.</i> (1990)
Gene mutation, Chinese hamster V79 cells, Hprt locus, <i>in vitro</i>	–	+	10 mM [1770 µg/mL]	Swedmark <i>et al.</i> (1994)
DNA strand breaks, human MRC-5 fetal lung cells <i>in vitro</i>	+	NT	5 mM [886 µg/mL]	Weitberg & Corvese (1993, 1997)
Sister chromatid exchange, human peripheral blood lymphocytes <i>in vitro</i>	–	NT	100 µg/mL	Padma <i>et al.</i> (1989b)

Table 18 (contd)

Test system	Result ^a		Dose ^b (LED or HID)	Reference
	Without exogenous metabolic system	With exogenous metabolic system		
Chromosome aberrations, human peripheral blood lymphocyte <i>in vitro</i>	–	NT	100 µg/mL	Padma <i>et al.</i> (1989b)
DNA strand breaks, Sprague-Dawley rat liver <i>in vivo</i>	+		100 mg/kg bw po × 1 [565 µmol/kg bw]	Pool-Zobel <i>et al.</i> (1992)
Micronucleus formation, Swiss male mice bone marrow <i>in vivo</i>	+		250 mg/kg bw ip × 2	Padma <i>et al.</i> (1989b)

^a +, positive; –, negative; NT, not tested

^b LED, lowest effective dose; HID, highest ineffective dose; ip, intraperitoneal injection

^c Co-expressing human CYP 2A6 together with human NADPH-cytochrome P450 reductase (OR)

^d Co-expressing human CYP 2E1 together with human NADPH-cytochrome P450 reductase (OR)

NNN induced DNA strand breaks in MRC-5 human fetal lung cells. When these MRC-5 cells were treated with NNN in combination with enzymatically generated oxygen radicals, DNA strand-breakage increased by approximately 50%, while oxygen-radical scavengers (superoxide dismutase, catalase, mannitol) significantly reduced the DNA damage caused by NNN (Weitberg & Corvese, 1993).

NNN induced DNA single-strand breaks in cultured primary rat hepatocytes (as measured by the alkaline elution assay). It did not cause any marked DNA damage (as measured by the alkaline elution assay) in isolated Clara and type II cells from rabbit lung and in isolated rabbit alveolar macrophages. NNN induced unscheduled DNA synthesis in freshly isolated hepatocytes from adult rats. NNN had genotoxic effects in primary rat hepatocytes *in vitro*, measured as DNA damage by alkaline elution and nick translation (Pool-Zobel *et al.*, 1992). NNN-induced mutations were not observed at the *Hprt* locus of V79 Chinese hamster cells after S9 metabolic activation in a co-cultivation system that used either freshly isolated rat hepatocytes or H4IIE rat hepatoma cells (Swedmark *et al.*, 1994).

NNN was mutagenic in a mixture of pooled oral tissues (gingiva, buccal cavity, pharynx and sublingua), and in tongue and oesophageal tissue in *lacZ*-transgenic mice (MutaTMMouse) (von Pressentin *et al.*, 1999).

NNN did not induce cytogenetic effects (sister chromatid exchange or chromosomal aberrations) in human peripheral blood lymphocytes.

NNN had genotoxic effects in Sprague-Dawley rat liver *in vivo*, measured as DNA damage by alkaline elution and nick translation (Pool-Zobel *et al.*, 1992). *In vivo*, NNN induced micronuclei in the bone marrow of Swiss mice.

In animal-mediated DNA-repair assays with *Escherichia coli* K-12 strains (injected intravenously just before nitrosamine treatment), intraperitoneal administration of NNN to mice caused dose-dependent genotoxic effects in indicator bacteria recovered from various organs of the treated animals. The genotoxic effect was enhanced by ethanol treatment prior to carcinogen treatment (Knasmüller *et al.*, 1994).

(ii) *Other effects*

In cultured human oral epithelial cells, treatment with NNN resulted in increased longevity and a sustained differentiated phenotype for 8.5–10 weeks. The treated cells displayed focal growth and morphological changes that were suggestive of early stages of cell transformation in comparison with control cells which were terminally differentiated (Murrah *et al.*, 1993).

Hamster cheek-pouch epithelium showed histological changes, including hyperplasia, hyperkeratosis and, in one animal, moderate dysplasia, when treated with nicotine combined with NNN. These changes were more frequent than after treatment with NNN or nicotine alone (Chen *et al.*, 1994).

Exposure of Syrian hamster buccal mucosa to NNN, five times per week for 24 weeks, did not result in clinical or histological changes (Papageorge *et al.*, 1996).

(c) *NAB*

Using genetically engineered *S. typhimurium* strain YG7108 that overexpresses human CYP, NAB induced mutation in the strains that contain CYP3A4, CYP2A6, CYP1A1 or CYP3A5. CYP3A4-carrying constructs induced the greatest mutagenicity (0.071 revertants/nmol NAB/pmol CYP) (Fujita & Kamataki, 2001).

(d) *NAT*

Using genetically engineered *S. typhimurium* strain YG7108 that overexpresses human CYP, NAT induced mutation in the strain that contains CYP2A6 (0.164 revertants/nmol NAB/pmol CYP) (Fujita & Kamataki, 2001).

4.5 Mechanistic considerations

4.5.1 *4-(Methylnitrosamino)-1-(3-pyridyl)-1-butanone (NNK)*

The formation of DNA adducts is pivotal in the carcinogenic process (Miller, 1994). If not repaired, DNA adducts cause permanent mutations due to miscoding events during the replication of adducted DNA (Singer & Essigmann, 1991; Seo *et al.*, 2000). When these mutations occur in critical regions of growth control genes, such as oncogenes and tumour-suppressor genes, cancer can result. The occurrence of multiple mutated genes in tumours that are caused by tobacco products is consistent with the extensive range of DNA damage that is caused by metabolically activated tobacco carcinogens (Hecht, 2003). However, NNK requires metabolic activation, generally through catalysis by CYP enzymes, before this genotoxic mechanism of cancer causation can occur. Extensive studies in laboratory animals have clearly demonstrated that the pathway of metabolic activation → persistent DNA adducts → mutations is critical to the carcinogenesis of NNK in the lung and nasal cavity. Fewer experimental studies have examined the genotoxic mechanism of the carcinogenicity of NNK in oral and pancreatic cells and tissues. Studies that used human cells and tissues have investigated potential parallels between experimental and human systems. Other mechanisms that contribute to the carcinogenesis of NNK have also emerged in recent years. This section examines the genotoxic and other mechanisms of the carcinogenesis of NNK, and focuses on comparisons between experimental and human systems.

(a) *Genotoxic mechanisms*

(i) *Metabolism*

A common metabolic event in virtually all systems (rodent and human) is the conversion of NNK to NNAL, during which (*S*)-NNAL predominates (Hecht, 1998, 2002). Studies in rats have demonstrated that (*S*)-NNAL is extensively distributed in the body and accumulates and persists in the lung, possibly at a receptor site (Wu *et al.*, 2002; Zimmerman *et al.*, 2004). (*S*)-NNAL is efficiently reconverted to NNK in rats (Zimmerman *et al.*, 2004). (*S*)-NNAL also persists in humans as shown by its slow excretion relative to that of (*R*)-NNAL

after cessation of tobacco use (Hecht *et al.*, 2002). Rat CYP2A3 and human CYP2A13 have similarly high catalytic efficiencies for the reconversion of (*S*)-NNAL to NNK (Tables 11 and 16; Jalas *et al.*, 2003a, 2005). The accumulation of (*S*)-NNAL in the lung may be a critical feature of the selectivity of NNK for induction of lung tumours in rodents. NNAL and its glucuronides are excreted in the urine of rodents, primates and humans (Hecht, 1998, 2002).

Rodent lung, oral mucosa, nasal mucosa and liver all metabolize NNK by α -hydroxylation at its methylene and methyl carbons to produce intermediates that bind to DNA (Hecht, 1998). These reactions are catalysed by CYP enzymes. Steady-state kinetic parameters for CYP-catalysed NNK metabolism have been reported for five rat enzymes, two mouse enzymes, two rabbit enzymes and eight human enzymes (Tables 11 and 14; Jalas *et al.*, 2005). Of these, rat CYP2A3, mouse CYP2A5, rabbit CYPs 2A10/11 and human CYPs 2A13 and 2B6 exhibit the lowest K_m values and may be the most important catalysts of NNK bioactivation in the respective species (Table 14). Members of the CYP2A sub-family appear to be the best catalysts of NNK α -hydroxylation across species, and CYP2A13, which has catalytic properties for NNK metabolism that are very similar to those of rat CYP2A3, may be particularly important in the bioactivation of NNK by the human lung (Jalas *et al.*, 2005). Rat pancreatic microsomes converted NNK to NNAL, (NNK)ADP⁺ and (NNK)ADPH, and converted NNAL to (NNAL)ADP⁺; products of α -hydroxylation were not observed (Peterson *et al.*, 1994).

NNK and/or NNAL are metabolically activated by a variety of human tissues and cells including those from the oral cavity, lung, oesophagus, cervix, urinary bladder and liver (Hecht, 1998; Prokopczyk *et al.*, 2001; Vondracek *et al.*, 2001). The extents of metabolism by α -hydroxylation are generally lesser than those observed in rodents. NNK and NNAL have been detected in human pancreatic juice (Prokopczyk *et al.*, 2002). Human pancreatic microsomes converted NNK to NNAL, but no products of α -hydroxylation of NNK or NNAL were observed (Anderson *et al.*, 1997).

(ii) DNA adducts

Methyl and pyridyloxobutyl DNA adducts of NNK have been characterized *in vitro* and *in vivo* (Hecht, 1998; Wang *et al.*, 2003; Hecht *et al.*, 2004c). Extensive studies have examined the mechanisms of lung tumour formation in A/J mice treated with a single dose of NNK. A consistent body of evidence including structure–activity studies, investigations of deuterated NNK analogues, analysis of the occurrence and persistence of DNA adducts and effects on the AGT-repair enzyme strongly implicates *O*⁶-MeGua as the critical DNA adduct in lung tumour induction by NNK in this mouse strain (Peterson & Hecht, 1991; Hecht, 1998; Peterson *et al.*, 2001; Jalas & Hecht, 2003; Jalas *et al.*, 2003b; Thomson *et al.*, 2003). *O*⁶-MeGua is known to have miscoding properties that cause G→A transitions (Loechler *et al.*, 1984). Mutations in the *K-ras* gene in A/J mouse lung tumours induced by NNK are predominantly G→A transitions, which is consistent with the important role of *O*⁶-MeGua (Hecht, 1998). A different picture emerges from studies of mechanisms of NNK-induced lung and nasal cavity carcinogenesis in Fischer 344 rats. Strong

evidence, based on structure–activity considerations and extensive studies of the formation and persistence of DNA adducts in individual cell types of the lung and different regions of the nasal mucosa and the effects of inhibitors of NNK carcinogenesis, indicate that a combination of *O*⁶-MeGua and HPB-releasing pyridyloxobutyl DNA adducts is important in lung carcinogenesis and that these latter adducts are critical in nasal cavity carcinogenesis by NNK (Hecht, 1998). Fewer studies have been carried out in oral tissue. However, it is known that rat oral tissue actively metabolizes NNK by all known pathways including α -hydroxylation, and 7-MeGua has been identified in these tissues (Murphy *et al.*, 1990a).

Methyl and pyridyloxobutyl DNA adducts have been identified in the lungs of smokers (Hecht, 1998). While the methyl adducts, 7-MeGua and *O*⁶-MeGua, may have multiple sources and are also found in nonsmokers, only NNK and NNN are probable precursors to pyridyloxobutyl DNA adducts. Cellular binding has also been observed in human oral keratinocyte cell lines exposed to NNK (Vondracek *et al.*, 2001).

(iii) *Mutations*

Mutations in the *K-ras* gene are frequently found in A/J mouse and hamster lung tumours induced by NNK (Hecht, 1998). The most common mutation is a GGT→GAT transition in codon 12 of the *K-ras* gene. In-vitro studies have demonstrated that 7-MeGua, *O*⁶-MeGua and *O*⁶(POB-1-yl)Gua are preferentially formed at the second G of codon 12 of the *K-ras* gene (Ziegel *et al.*, 2003). Both *O*⁶-MeGua and *O*⁶(POB-1-yl)Gua are known to cause predominantly G→A transition mutations (Loechler *et al.*, 1984; Pauly *et al.*, 2002). The pyridyloxobutylating agent, NNKOAc, causes GGT→TGT and GGT→GTT mutations in codon 12 in addition to GGT→GAT mutations (Ronai *et al.*, 1993). Although mutations in *K-ras* in lung tumours from mice and hamsters are consistent with the properties of the DNA adducts formed by NNK, other factors are also involved. For example, only two of 22 lung tumours induced by NNK in relatively insensitive C57BL/6 mice had *K-ras* mutations (Devereux *et al.*, 1993). In another study, treatment of mice with NNK followed by butylated hydroxytoluene increased lung tumour induction compared with NNK alone, but decreased the frequency of GGT→GAT mutations in codon 12 of *K-ras* (Matzinger *et al.*, 1994). The frequency of activation of *K-ras* and GGT→GAT mutation in codon 12 is not affected by the time after NNK treatment, nor are the proliferative activity of the lung lesions and the presence of mutations correlated. Thus, *K-ras* gene mutations appear to play a minor role in the selective growth advantage of NNK-induced lung lesions in A/J mice (Kawano *et al.*, 1996). In the Muta Mouse treated with NNK, A:T→T:A and A:T→C:G transversions were the major mutations observed in the lung and liver *cII* genes; G:C→A:T transitions were also observed, but to a lesser extent (Hashimoto *et al.*, 2004). There is no evidence of *K-ras* or *p53* mutations in lung tumours induced by NNK in rats (Hecht, 1998). No mutations have been detected in the *p53* gene from NNK-induced mouse lung tumours and only one of 24 hamster lung tumours examined had a mutation in the *p53* gene (Oreffo *et al.*, 1993; Hecht, 1998).

Mutations in codon 12 of the *K-RAS* gene are present in 24–50% of human primary lung adenocarcinomas, but are rarely seen in other types of lung tumour (Rodenhuis & Slebos, 1992; Mills *et al.*, 1995; Westra *et al.*, 1996). These mutations are more common in smokers and former smokers than in nonsmokers, which suggests that they may be induced by a component of tobacco smoke (Westra *et al.*, 1993). The most frequently observed mutation is GGT→TGT, which typically represents about 60% of the mutations in codon 12, followed by GGT→GAT (20%) and GGT→GTT (15%). The prevalence of G→T mutations has led to speculation that they may be due to polycyclic aromatic hydrocarbons, which can induce such mutations through the diol epoxide metabolic activation pathway (You *et al.*, 1989; Westra *et al.*, 1993). However, G→T mutations are also induced by NNKOAc (Ronai *et al.*, 1993). In A/J mice, the *O*⁶-MeGua pathway of NNK metabolic activation is clearly the major pathway involved in tumour induction, which is consistent with the high percentage of GGT→GAT mutations in the *K-ras* gene isolated from mouse lung tumours induced by NNK. However, in Fischer 344 rats, both the pyridyloxobutylation and methylation pathways are critical in the lung tumorigenesis of NNK. The relative importance of these pathways in human lung carcinogenesis is not known. If pyridyloxobutylation is critical, as in the rat, a higher percentage of G→T transversions than that observed in mice would be expected as a result of exposure to NNK. In the absence of additional information, it is difficult to assign mutations in human genes to particular carcinogen adducts for an exposure that is as complex as that to tobacco smoke. Numerous compounds that damage DNA are present in tobacco smoke and many of these cause G→T transversion mutations: examples, in addition to nitrosamines and polycyclic aromatic hydrocarbons, include aromatic amines, oxygen radicals and α,β -unsaturated aldehydes (Singer & Essigmann, 1991; Moriya, 1993; Moriya *et al.*, 1994; Nesnow *et al.*, 1995). With respect to the *p53* gene, which is commonly mutated in tobacco-related cancers, mutations at G are frequently observed, which is consistent with the multiple carcinogens in tobacco products that bind to G. The spectrum of mutations in the *p53* gene from lung tumours has been attributed in part to reactions with polycyclic aromatic hydrocarbon diol epoxides, subject to the limitations discussed above; at present, no evidence has been found that NNK produces a similar mutational spectrum (Pfeifer *et al.*, 2002; Ziegel *et al.*, 2004).

(b) *Other mechanisms*

NNK is a high-affinity agonist for both the β_1 - and β_2 -adrenergic receptors in human pulmonary adenocarcinoma cell lines and in Chinese hamster ovary cell lines that have been transfected with the human β_1 - or β_2 -adrenergic-receptor gene (Schuller, 2002). NNK and other β -adrenergic receptor agonists stimulate the release of arachidonic acid from cell membrane phospholipids, which results in stimulated DNA synthesis and proliferation of human pulmonary adenocarcinoma cells. The mitogenic response to NNK is reduced upon treatment with β -adrenergic receptor antagonists, such as propranolol, and with cyclooxygenase and lipoxygenase inhibitors. Similar results have been obtained in pancreatic cells. In cell lines derived from human pancreatic adenocarcinomas, NNK

stimulated the release of arachidonic acid, which led to DNA synthesis and cell proliferation. In a model of pancreatic carcinogenesis that was induced transplacentally by treatment of pregnant hamsters with NNK and ethanol, treatment of the offspring with ibuprofen and the 5-lipoxygenase-activating protein inhibitor MK886 began 4 weeks after the birth and inhibited pancreatic tumorigenesis (Schuller *et al.*, 2002). These results indicate that receptor binding of NNK could play a role in human lung and pancreatic carcinogenesis (Schuller, 2002).

NNK binds to the α_7 nicotinic acetylcholine receptor (α_7 nAChR) in small-cell lung carcinoma and pulmonary neuroendocrine cells, which results in the influx of Ca^{2+} , release of 5-hydroxytryptamine (serotonin) and activation of a mitogenic pathway mediated by protein kinase C, Raf-1, mitogen-activated protein kinase and c-Myc. Unstimulated small-cell lung carcinoma cells from smokers demonstrated high base levels of 5-hydroxytryptamine release and individual downstream signalling components in comparison with pulmonary neuroendocrine cells. Subchronic exposure of the latter cells to NNK up-regulated the α_7 nAChR and its associated mitogenic pathways (Schuller *et al.*, 2003). NNK at 0.1 nM simultaneously stimulates phosphorylation of the oncogenic proteins Bcl2 and c-Myc through the α_7 nAChR in association with increased proliferation of human small-cell lung carcinoma cells, which suggests that NNK facilitates a functional cooperation between Bcl2 and c-Myc in a mechanism that involves phosphorylation of both regulators (Jin *et al.*, 2004).

The $p16^{\text{INK4a}}$ ($p16$) tumour-suppressor gene can be inactivated by hypermethylation of its promoter region. In Fischer 344 rats, 94% of adenocarcinomas induced by NNK were hypermethylated at the $p16$ gene promoter and this change was frequently detected in precursor lesions of the tumours such as adenomas and hyperplasias. This timing of $p16$ hypermethylation was reproduced in human squamous-cell carcinomas in which the $p16$ gene was coordinately methylated in 75% of carcinoma *in situ* lesions adjacent to squamous-cell carcinomas that harboured this change. The frequency of $p16$ hypermethylation increased during disease progression from basal-cell hyperplasia to squamous metaplasia to carcinoma *in situ* (Belinsky *et al.*, 1998). Hypermethylation of $p16$ was also detected in 45% of rat liver tumours induced by NNK, and is a common event in human hepatocellular carcinoma (Pulling *et al.*, 2001). The death-associated protein kinase ($DAPK$) gene is methylated in 23–44% of human non-small-cell lung cancers and in 52% of mouse lung tumours induced by NNK (Pulling *et al.*, 2004). $DAPK$ methylation was observed at a similar prevalence in NNK-induced hyperplasias and adenocarcinomas, which suggests that inactivation of this gene is one pathway for tumour development in the mouse lung (Pulling *et al.*, 2004). The retinoic acid receptor gene β ($RAR-\beta$), which encodes one of the primary receptors for retinoic acid, is down-regulated by methylation in human lung cancer (Vuillemenot *et al.*, 2004). Methylated alleles of this gene were detected in virtually all primary lung tumours induced in mice by NNK and in 54% of preneoplastic hyperplasias induced by NNK (Vuillemenot *et al.*, 2004).

The serine/threonine kinase Akt (or protein kinase B) is activated in non-small-cell lung cancer cells and promotes cellular survival and resistance to chemotherapy or radiation

(Brognaard *et al.*, 2001). NNK activates Akt in non-immortalized human airway epithelial cells. Activation of Akt by NNK occurred dose dependently within minutes and depended upon α_7 nAChR. Activated Akt increased phosphorylation of certain downstream substrates that control the cellular cell cycle and protein translation, and partially induced a transformed phenotype. Active Akt was detected in airway epithelial cells and lung tumours from NNK-treated A/J mice and in human lung cancers from smokers (West *et al.*, 2003). These studies were extended by examining Akt activation at intermediate steps in carcinogenesis. The phosphatidylinositol 3'-kinase/Akt pathway was analysed in isogenic, immortalized or tumorigenic human lung bronchial epithelial cells *in vitro* and in a spectrum of NNK-induced mouse lung lesions *in vivo*. Progressive activation of the phosphatidylinositol 3'-kinase/Akt pathway correlated with phenotypic progression of lung epithelial cells, which strengthens the hypothesis that Akt activity plays a role in lung tumorigenesis (West *et al.*, 2004).

4.5.2 N'-Nitrosornicotine (NNN)

A convincing body of data demonstrates that NNN requires metabolic activation to form DNA adducts that drive the mutagenic and carcinogenic processes. Metabolic activation of NNN occurs by 2'-hydroxylation and 5'-hydroxylation and leads to the formation of diazohydroxides that bind to DNA and are mutagenic. This process is observed in both rodent and human tissues. Metabolic activation of NNN is catalysed by CYP enzymes and, among these, CYP2A enzymes are outstanding catalysts in both rodents and humans. The formation of HPB-releasing DNA adducts of NNN has been clearly demonstrated in the rat nasal mucosa and oesophagus, which are target tissues of NNN carcinogenesis. HPB-releasing haemoglobin adducts of NNN are also produced in rats. As discussed above, HPB-releasing DNA and haemoglobin adducts have been detected in humans exposed to tobacco products, and their sources could be either NNK or NNN or both. Thus, there are clear parallels between the mechanisms of metabolic activation of NNN in rodents and humans.